A CALORIMETRIC STUDY OF

β-SULTAMS

AND

β-LACTAMS

By Summia Naz

Thesis submitted to the University of Huddersfield in partial fulfilment of the requirements for the degree of Doctor of Philosophy

January 2009

In The Loving

Memory of My Amazing

and Beautiful Father Haji

Mohammed Akram

Abstract

The hydrolytic degradation of a series of β-sultams and β-lactams was investigated using isothermal microcalorimetry (IMC), to determine kinetic and enthalpic data. The importance of these studies was to model the process of hydrolysis as this was a simplification of the mechanism by which β-lactams and β-sultams function as serine protease inhibitors.

Calorimetric studies were conducted using a Thermal Activity Monitor (TAM 2277). Three categories of experiments were conducted: in the solid state, varying relative humidity (R/H) and in aqueous solution. Hydrolytic rate constants and enthalpies were determined for the solid state studies and these were related to substituent effects. However, for the experiments relating to the R/H studies no conclusive results were obtained. As expected, for solution state studies the hydrolytic rate constant in all cases changed with temperature (298K, 310K and 323K).

Theoretical predictions were then made for a novel β-sultam based on these results with an excellent correlation observed between theoretical calculations and experimental results.

Finally, calorimetric experiments were conducted on a series of β-lactams. This was for two reasons firstly; to determine if calorimetry can monitor low reaction rates and secondly; to compare rates of hydrolysis with the β-sultams. For a series of β-lactams, solution state hydrolytic rate constants and enthalpies were determined. An overall comparison of β-lactams and β-sultams appeared to indicate that in all cases β-lactams reacted slower than β-sultams.

Contents page

Chapter 1: Introduction

Contents page

Chapter 2: Organic synthesis

Synthesis of 2-aroyl-β-sultams

Synthesis of 1-aroyl-β-lactams

Chapter 3: Calorimetric studies of β-sultams

Results and Discussion

Contents page

Solid state studies

Solution state studies

Chapter 4: Calorimetric studies of β-lactams

Chapter 5: Conclusions and future work

Abbreviations

Asp	Asparginine
BC II	*Bacillus cereus β-Lactamase II*
CDCl₃	Deuterated chloroform
CHCl₃	Trichloromethane/chloroform
Cl₂	Chlorine
DSC	Differential Scanning Calorimetry
β-Lactam	Azetidin-2-one
β-Sultam	1,2-Thiazetidine-1,1-dioxide
d	Doublet
dd	Doublet of doublets
DCM	Dichloromethane
DVM	Digital Volt Meter
DMAP	4,4-Dimethylaminopyridine
Et₃N	Triethylamine
EtOAc	Ethyl acetate
EtOH	Ethanol
Gly	Glycine
His	Histadine
HPLC	High performance liquid chromatography
IMC	Isothermal Microcalorimetry
IR	Infra-Red spectroscopy
mg	Milligram
mL	Millilitre
mmol	millimole
m.p.	Melting point
Na₂CO₃	Sodium carbonate
NAG	*N*-acetyl-glucosamine
NAM	*N*-acetyl-muramic acid
NMR	Nuclear Magnetic Resonance spectroscopy
NO₂	Nitro
OH	Hydroxy
OMe	Methoxy

P99	*Enterobacter cloacae* P99-β-Lactamase
PPE	Porcine Pancreatic Elastase
PPM	Parts per million
R61	Transpeptidase enzyme
R/H	Relative humidity
Ser	Serine
SO$_2$	Sulfur dioxide
TAM	Thermal Activity Monitor
TLC	Thin layer chromatography
TSA	Transition State Analogue
XRPD	X-ray powder diffraction

Publication

L.J. Waters, S. Naz, K. Hemming, Calorimetric investigations of the hydrolytic degradation for a series of *β*-sultams, *Journal of Thermal Analysis and Calorimetry*, 93, 2, **2008**, 339-342.

1. Introduction

1.0 General introduction to a calorimetric study of *β*-sultams and *β*-lactams

The basis of this thesis is a calorimetric study of *β*-sultams and *β*-lactams, shown in **Figure 1**. To understand why this research is of scientific interest firstly requires an understanding of the role bacterium play in disease.
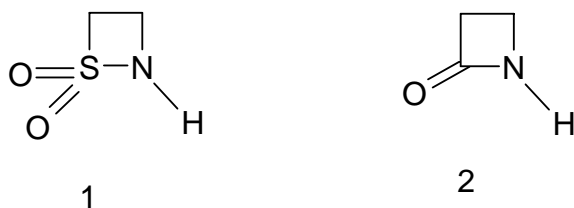
Figure 1: *β*-sultam (1) and *β*-lactam (2)

Bacteria are micro-organisms that can be responsible for disease; there are two different types, Gram positive and Gram negative. Bacterial cells, unlike animal cells, exhibit a cell wall that is made up of peptidoglycan, *N*-acetyl-glucosamine (NAG) and *N*-acetyl-muramic acid (NAM).[1] Antibacterial agents work to prevent cell wall synthesis and therefore prevent the spread of disease. For example, *β*-lactams are a group of antibacterial agents that work by inhibiting bacterial cell wall synthesis by binding to the transpeptidase enzyme. However the efficacy of *β*-lactam antibiotics is quickly being eroded, with *β*-lactamase enzymes primarily responsible for the increased resistance. *β*-lactamases bind to the *β*-lactam allowing the transpeptidase enzyme to continue bacterial cell wall formation. One solution to this problem is that *β*-lactam antibiotics can be administered with serine protease inhibitors, which can inhibit the *β*-lactamase from binding to the *β*-lactam antibiotic.

β-sultams are potential serine protease inhibitors.[2] *β*-sultams are highly strained, highly reactive cyclic sulfonyl analogues of *β*-lactams. *β*-sultams and *β*-lactams differ from each other in that the sulfonyl chemical moiety in *β*-sultams is replaced by carbonyl in the *β*-lactams. *β*-sultams act as sulfonylating agents of serine enzymes, inactivating the enzyme by forming a stable adduct.[3]

The hydrolysis of *β*-sultams compared with *β*-lactams is of great interest

because the function of the transpeptidase enzyme and the β-lactamase enzyme is the same. Previous studies have shown β-sultams hydrolyse via S-N bond fission and β-lactams via endocyclic and exocyclic C-N fission.[4] Further investigation into the rates of hydrolysis of β-sultams compared with β-lactams is required together with further analysis at different temperatures. A potential serine protease inhibitor should bind to the serine protease enzyme, in the case of β-sultams they react only by S-N fission. Therefore if β-sultams are to be successful serine protease inhibitors, the study of the rate at which the β-sultam ring opens is of great importance.

To fully investigate β-sultams as potential serine protease inhibitors, synthesis followed by analytical measurements must be conducted. Previous spectrophotometric kinetic studies have shown that there is a relationship between the different substituted β-sultams and their rates of hydrolysis. Calorimetric studies of β-sultams have not been conducted prior to this thesis. Further analytical and thermodynamic investigations are to be conducted using isothermal microcalorimetry to understand fully the hydrolytic reaction of β-sultams compared with β-lactams, but also amongst the β-sultams and β-lactams with respect to different substituent effects.

Isothermal microcalorimetry requires no prior sample preparation yet yields a variety of parameters, for example reaction order, rate constant and enthalpies, can be determined. This technique is not limited to compounds in solution, for example samples can be in the solid state under atmospheric conditions or hygrostats can be used to determine thermodynamic parameters at different relative humidities. In addition, isothermal microcalorimetry is not limited to compounds with a chromophore, whereas many analytical experiments are. Thus, calorimetry may provide a far more versatile analytical technique than those traditionally used. Solid state isothermal microcalorimetry is of particular importance in the pharmaceutical industry, allowing the determination of stability which is crucial in the final stages of drug development. The stability and degradation of solid samples can be investigated at different relative humidities using isothermal microcalorimetry.[5] The amorphicity content within

a sample of single or mixed formulations can be studied as well as compounds in solution under varying controlled conditions to observe hydrolysis.[6] The technique can also effectively be combined with other analytical techniques, for example NMR, IR and Raman spectroscopy. Therefore synthetic chemistry followed by analytical measurements can provide useful information. To fully understand the theory behind the compounds that were chosen for study in this research firstly requires a thorough discussion of the role of bacteria and its role in decreased drug efficacy.

1.1 Bacteria

Bacteria were first discovered in the 1670s by Van Leeuwenhoek, although it was not until the nineteenth century that the French scientist Pasteur discovered that these micro-organisms might be responsible for disease.[7] There are two different types of bacteria that exist, Gram positive and Gram negative. The Danish physician Christian Gram invented the Gram staining technique in 1884 which was used to classify bacteria. The bacteria are treated with a violet dye, iodine, and rinsed with alcohol. Gram positive bacteria remain purple and Gram negative bacteria stain pink. The difference between the two cells is caused by the amount of peptidoglycan in the cell wall. Gram positive are richer in peptidoglycan than Gram negative.[8]

The cell wall maintains the structural integrity, temperature, pH and osmotic pressure of the bacteria. The polysaccharide part of the peptidoglycan is made up of a repeating disaccharide unit of *N*-acetyl-glucosamine (NAG) and *N*-acetyl-muramic acid (NAM). A unique bacterial pentapeptide is attached to the D-lactyl moiety of NAM; the peptides from two separate strands are cross linked by DD-transpeptidase to give the rigid cell wall.[9]

Cell wall synthesis is a well researched mechanism, the prevention of cell wall synthesis leads to bacterial death. Many antibiotics work by inhibiting cell wall synthesis for example, penicillins, cephalosporins and carbapenems. These antibacterial agents kill or prevent the growth of bacteria and it is therefore important to understand their structure and mode of action.[10]

1.2 Antibacterial agents

Antibacterial agents in the *β*-lactam class such as penicillin consist of a four membered amide ring (**Figure 2**). Antibacterials are selective in their action against bacterial cells. Different mechanisms exist: inhibition of cell metabolism, inhibition of bacterial cell wall synthesis, interactions with the plasma membrane, disruption of protein synthesis and inhibition of nucleic acid transcription and replication. Antibacterials which inhibit cell wall synthesis prevent bacterial replication and are therefore of great interest.

Of those antibacterials which inhibit cell wall synthesis, there are two major classes of interest, penicillins and cephalosporins. Sir Alexander Fleming first discovered penicillin in 1928; he recognised the death of bacterial colonies by a rare species of penicillium. It was not until 1938 (Florey) that penicillin was isolated, 16 years later it was used as an antibacterial.[11]

ß-lactam ring   Penicillin
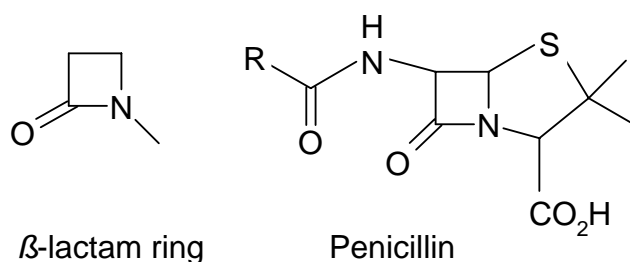
Figure 2: Structure of a *β*-lactam ring and penicillin.

Penicillins inhibit cell wall synthesis, this leads to bacterial cell lysis which in turn is followed by cell death. Cell wall synthesis involves a transpeptidase enzyme, which facilitates the incorporation of glycan crosslinks into the cell wall. The crosslinks increase the rigidity of the cell membrane. At this point energy is generated during amino acid hydrolysis (loss of D-ala) which is used in the formation of the crosslink (peptide bond) as shown in **Figure 3**. Penicillins work by mimicking the original D-ala-D-ala amino acid sequence and are thus recognised by the transpeptidase enzyme which disrupts cell wall synthesis.
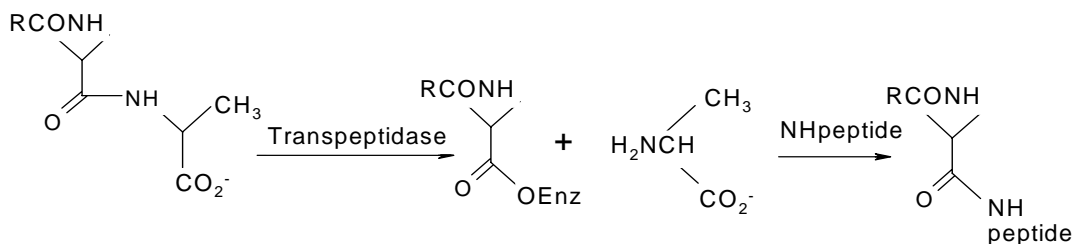
Figure 3: The transpeptidase enzyme incorporates glycan crosslinks into the cell membrane.

Penicillin is not the only β-lactam antibacterial agent that exists; other classes do exist and are similar in structure and mechanism. Some of these related β-lactam antibacterial agents are discussed in the following section.

1.3 β-Lactam based antibiotics

Nearly eighty years after Sir Alexander Fleming's discovery of penicillin,[12] β-lactams continue to be one of the most important classes of antibacterial agents.[13] β-Lactams are active acylating agents, acylating nucleophilic residues in a diverse range of bacterial and mammalian serine active enzymes, hence displaying a wide range of biological activities.[14, 15] The origin of this biological activity originates with the chemical reactivity of the small ring system (β-lactam ring).[16] Antibiotics, which comprise of the β-lactam ring, are: penicillins, cephalosporins, carbapenems and monobactams as shown in **Figure 4**.

Penicillin

Cephalosporin

Monobactam

Ca rbapenem
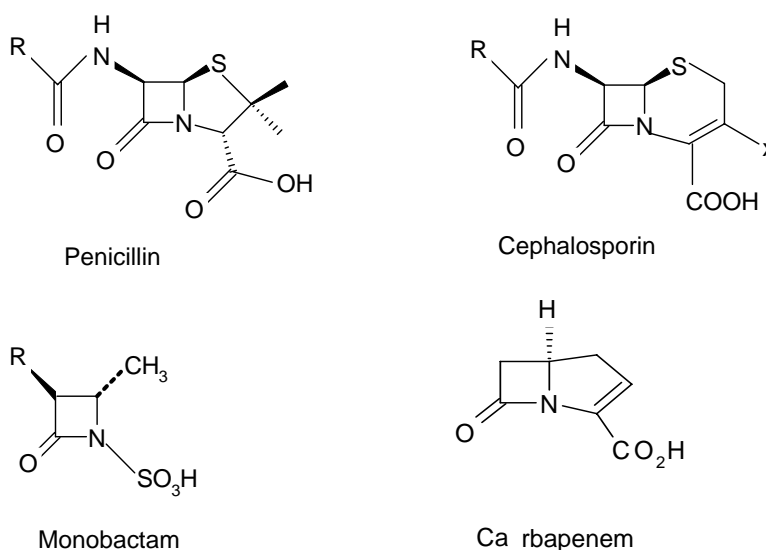
Figure 4: Antibiotics which contain β-lactam rings.

β-Lactam antibiotics prevent cell wall synthesis in bacteria, for example penicillin covalently binds to the transpeptidase enzyme (**Figure 5**) forming a stable acyl-enzyme adduct.
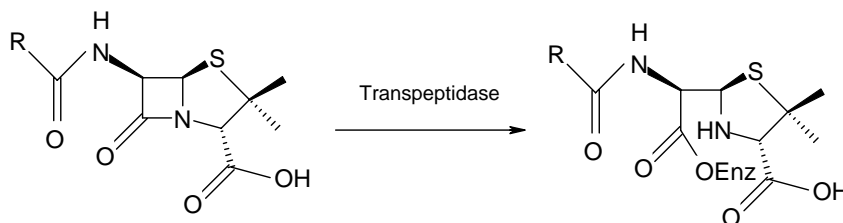
Figure 5: Inhibition of bacterial cell wall synthesis.

Unfortunately, antibacterial therapy and the efficacy of β-lactam antibiotics are quickly being eroded as bacterial resistance to β-lactam antibiotics increases. [17,18] Bacterial resistance to all clinically used antibiotics is being identified in hospitals all around the world, and now there is an urgent need to develop new antibiotics.[19]

When first discovered the β-lactam antibiotic penicillin was effective against all types of Gram-positive bacteria, for example; pneumonia, wound and skin infections. However, some bacteria are now resistant to most types of antibiotics. Resistance to β-lactam antibiotics occurs by four major mechanisms: [20] alterations in penicillin binding proteins,[21] efflux via specific drug pumps,[22] impaired entry into the bacterial cell and production of inactivating enzymes, for example β-lactamases. The inhibition of β-lactams will now be discussed in more detail.

1.3.1   Inhibition of β-lactams

As previously discussed, resistance to β-lactam antibiotics occurs via four different mechanisms; the mechanism of particular interest for this work is the production of inactivating enzymes, for example, β-lactamases. There are 470 β-lactamases known to date.[23] These are divided into four classes: A, B, C and D. Classes A, C and D have similar mechanisms. The Class B β-lactamases are metalloenzymes which require one or two zinc ions to carry out hydrolysis of the β-lactam.[24] Classes **A and C** are of great concern for the resistance of

antibiotics.[25, 26, 27]

The β-lactamase enzyme is primarily responsible for resistance by catalysing the hydrolysis of the β-lactam (**Figure 6**), where the ring opens to form a bacterially inert β-amino acid.[28]
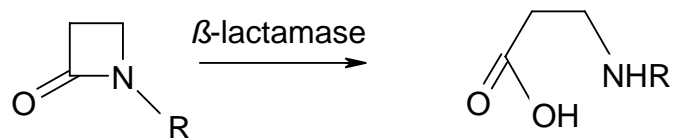
Figure 6: *β*-lactam ring opening.

One way to overcome resistance of some bacteria to β-lactam antibiotics is to administer mechanism based inactivators with penicillin, for example sulbactam, tazobactam and clavulanate. These inactivators inhibit β-lactamase and preserve antibacterial activity. Further research is being carried out to develop novel β-lactam compounds, which are more stable towards the β-lactamase.[29, 30] The University of Huddersfield have also been investigating β-sultams as potential serine protease inhibitors of the transpeptidase and β-lactamase enzymes. To understand serine protease inhibition it is important to understand the structure and mechanism of serine protease enzymes.

1.3.2   Serine protease enzymes

Serine proteases are a class of enzymes that cleave peptide bonds in proteins. They are characterised by the presence of a serine residue in the active site of the enzyme. There are a wide range of serine proteases that exist; participating in a wide range of functions in the body, for example, trypsin and subtilisin are involved in digestion and thrombin in blood coagulation.[31] The three most studied serine protease enzymes are chymotrypsin, trypsin and elastase. They are synthesised by the pancreatic cells and secreted in the small intestine. All three are very similar in structure, as shown in **Figure 7.**
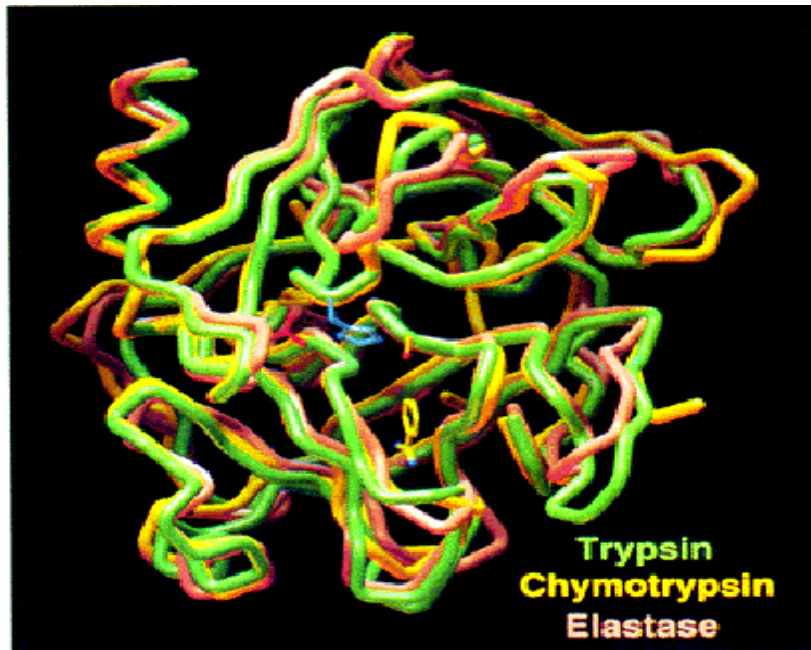
Figure 7: Comparison of 3-D structures of trypsin, chymotrypsin and elastase.[32]

Serine proteases are involved in a catalytic mechanism. The active site of serine proteases are characterised by a catalytic triad and an oxyanion hole. There are three groups in the catalytic triad, Ser-195 which acts as the nucleophile, His-57 and Asp-102 which behave as a general base and a H-bond acceptor. The oxyanion hole consists of a backbone of amide NHs of Ser-195 and Gly-193 [33]. A summary of the catalytic mechanism is shown in **Figure 8**.
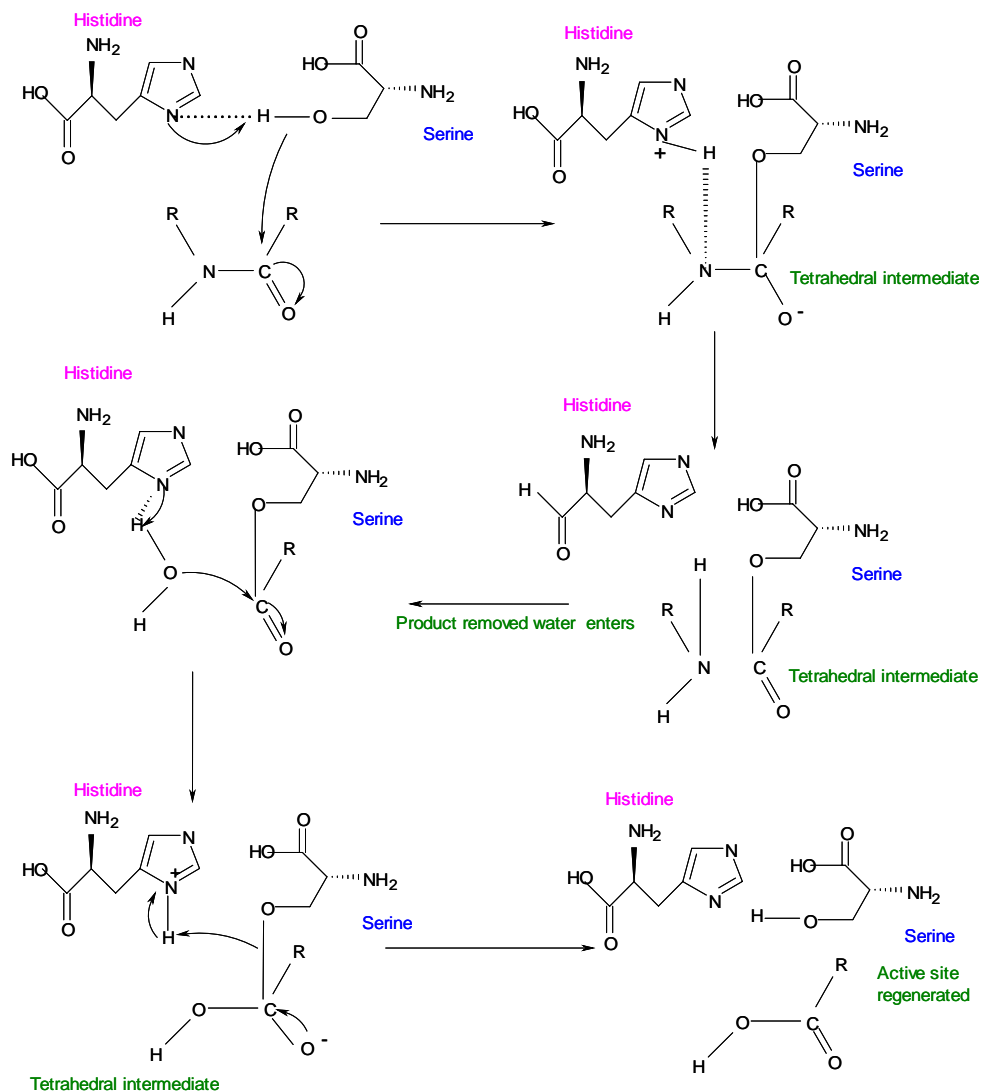
Figure 8: Serine protease catalytic mechanism.[31, 32]

A polypeptide substrate binds to the surface of the serine protease enzyme; the carbonyl carbon of this bond is positioned near the nucleophilic serine.

Serine -OH attacks the carbonyl carbon, nitrogen of the histidine accepts the hydrogen from the -OH of the serine. A pair of electrons from the double bond of the carbonyl oxygen moves to the oxygen. A tetrahedral intermediate is generated.

The nitrogen carbon bond in the peptide is broken. The covalent electrons attack the hydrogen of the histidine, breaking a bond. The electrons that

previously moved from the carbonyl oxygen double bond move back from the negative oxygen to recreate the bond, generating an acyl-enzyme intermediate.

Water replaces the N-terminus of the cleaved peptide, and attacks the carbonyl carbon. Nitrogen from the histidine accepts a proton from the water. Electrons from the double bond move to the oxygen making it negative. A bond between the oxygen of the water and the carbon is formed. Generating a tetrahedral intermediate.

The bond formed in the first step between the serine and the carbonyl carbon moves to attack the hydrogen that the histidine just acquired. The electron-deficient carbonyl carbon re-forms the double bond with the oxygen. As a result, the C-terminus of the peptide is now ejected.

An important part of this mechanism is the generation of tetrahedral intermediates. The serine proteases preferentially bind to the transition state; preferential binding is responsible for much of the catalytic efficiency of the enzyme. Serine proteases therefore make good targets for transition state analogue inhibitors (TSA). TSA inhibitors resemble the substrate's structure in the transition state; they are stable, similar in geometry and charge. It is for this reason that *β*-sultams are potential inhibitors of serine proteases; they are structurally similar to *β*-lactams. In addition the chemical properties and behaviour are important if they are to be considered as potential inhibitors. For example, synthetic difficulty, chemical stability and more importantly their mechanism of action must all be known.

1.4 *β*-Sultams

β-Sultams (1, 2-thiazetidine 1, 1-dioxides) **(1)** are highly strained, highly reactive sulfonyl analogues of *β*-lactams **(2)**[34] shown in **Figure 9**. They contain three different heteroatom bonds: N-S, S-C, and N-C.[35]
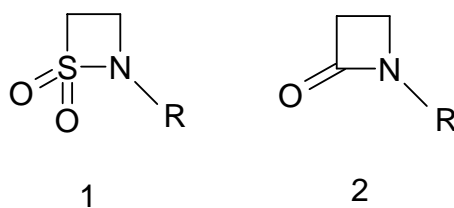
Figure 9: The basic structure of a *β*-sultam (1) and a *β*-lactam (2).

It is already known that the *β*-sultam ring is less stable in comparison with the *β*-lactam ring; this is a result of increased distortion within the *β*-sultam ring.[36] The increased distortion is created by the difference in the C-S and N-S bond length. The C-S and N-S bonds are longer than the corresponding C-C and C-N bonds of the *β*-lactam ring. *β*-sultams act as sulfonylating agents of serine enzymes, inactivating the enzyme by forming a stable adduct shown in **Figure 10**.
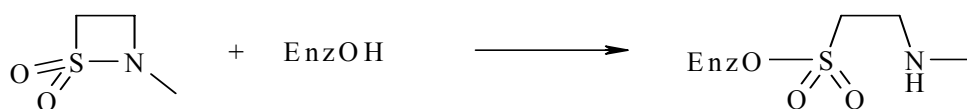
Figure 10: Serine enzyme inactivation of a *β*-sultam.

β-Sultams react with nucleophilic centres and can also behave as peptide mimics, where the sulfonyl group replaces the carbonyl to mimic the peptide. They also mimic tetrahedral intermediates by acting as transition state analogue inhibitors.[37]

There are 4 distinct routes of synthesis for *β*-sultams, these are:
1) Cyclisation by S-N bond formation.
2) Cyclisation by C-N bond formation.
3) [2 + 2] cycloadditions of sulfonimines and alkenes (C-N and C-S bond formation).
4) [2 + 2] cycloadditions of sulfenes and imines (C-C and N-S bond formation).

An example of C-N bond formation is the cyclisation of *β*-hydroxysulfonamide mesylates (**Figure 11**); this method was first described by Thompson in 1984.[38]
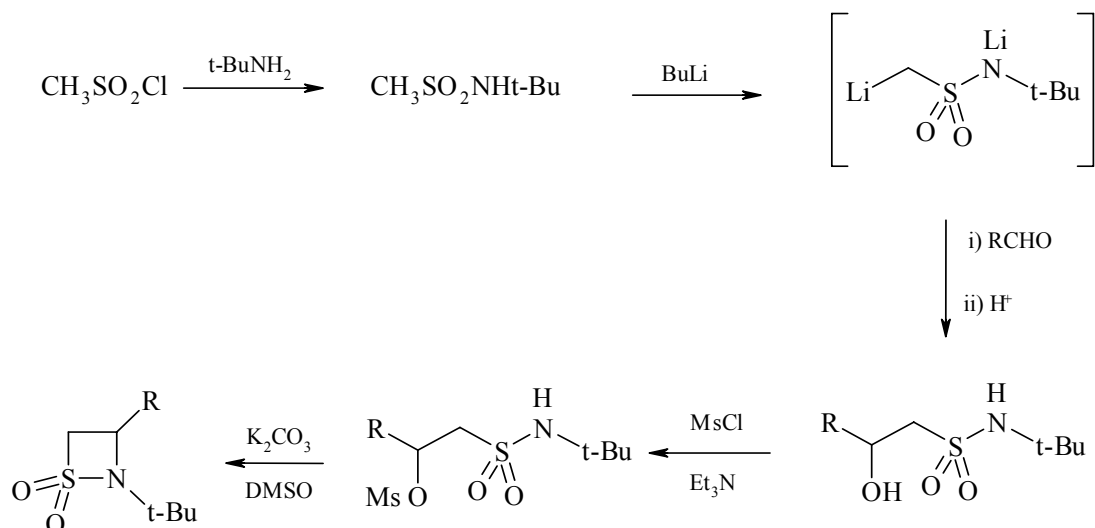
Figure 11: Synthesis of a *β*-sultam via C-N bond formation.

Baganz synthesised the first *β*-sultam in the 1960s by the oxidative chlorination of cystine diethyl ester which gives a *β*-amino sulfonyl chloride. Intramolecular cyclisation with dehydrochlorination follows to give the *β*-sultam shown in **Figure 12**.[39]
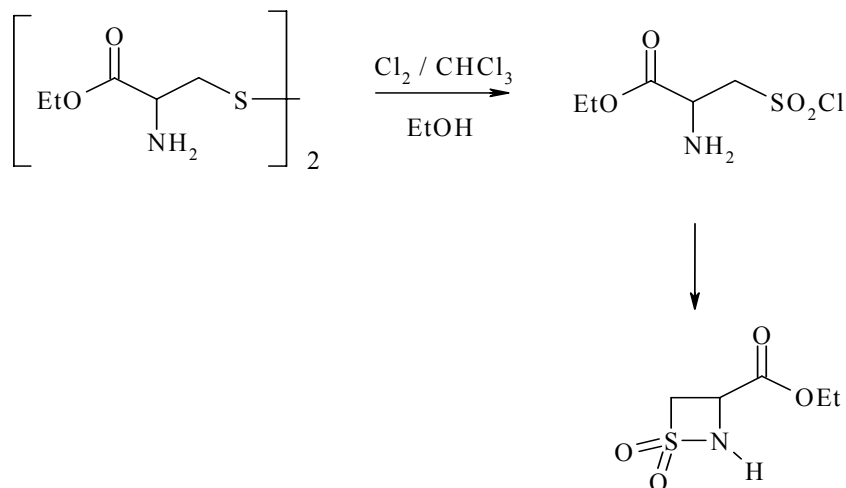
Figure 12: Synthesis of *β*-sultam by Baganz.

Investigations are still ongoing for novel compounds and the development of new serine protease inhibitors. There are many factors to be considered when developing a new drug (inhibitor). The first being the identification of candidates, followed by the characterisation of these candidates by such techniques such as NMR (Nuclear Magnetic Resonance), IR (Infra Red) and

Raman spectroscopy, mass spectrometry and biological testing. Further analytical tests can then be conducted, for example, HPLC (High Performance Liquid Chromatography), thermal measurements using DSC (Differential Scanning Calorimetry), IMC (Isothermal microcalorimetry) and enzyme binding studies. Molecular modelling also plays an important role as many predictions and calculations contribute to drug discovery. Once all these factors have been considered drug development follows which includes toxicity, pharmacokinetics, metabolism, physicochemical properties, formulations and *in vitro* studies, followed by clinical trials. This process of drug discovery can take many years. This particular research project is part of an ongoing research programme where potential medicinal compounds (*β*-sultams), have been synthesised and partially characterised. This project is to carry on this work by employing calorimetric techniques to study *β*-sultams.

1.4.1 *β*-Sultams and *β*-Lactams: kinetic and organic synthetic studies.

The chemical reactivity of *β*-sultams is of great interest. Sulfonation is not a well studied process and sulfonyl derivatives are much less reactive than their acyl counterparts.[40] *β*-sultams are the sulfonyl analogues of *β*-lactams and have been studied to determine the difference in chemical and physical properties between these two groups. *β*-sultams are potential serine protease inhibitors and can therefore stop the *β*-lactamase enzyme from binding to the pencillin, which prevents bacterial cell wall synthesis. The serine enzymes transpeptidase and *β*-lactamase enzyme have an OH group.[41] Hydrolysis studies using water and alcohols can mimic the OH group in these enzymes. This allows simple, cost effective studies to initially be carried out. The hydrolysis can then be further looked into using these enzymes.

Many hydrolysis and organic synthetic studies have been conducted at the University of Huddersfield, and many of these have a focus of comparison between the *β*-lactams and *β*-sultams. Some of these studies will now be reviewed.

The aminolysis reactions of *N*-aroyl *β*-lactams have been studied. In water the *β*

-lactam ring of β-lactam antibiotics undergoes attack by nucleophilic reagents such as amines and alcohols in competition with hydroxide ions.

Nucleophilic substitution at the carbonyl centre of the β-lactams is an acyl transfer process involving covalent bond formation between the carbonyl carbon and the nucleophile as well as C-N bond fission of the β-lactam.

As shown in **Figure 13**, the reaction of amines with penicillins gives the corresponding penicilloyl amide via cleavage of the amide bond: the amine is acylated.[42]
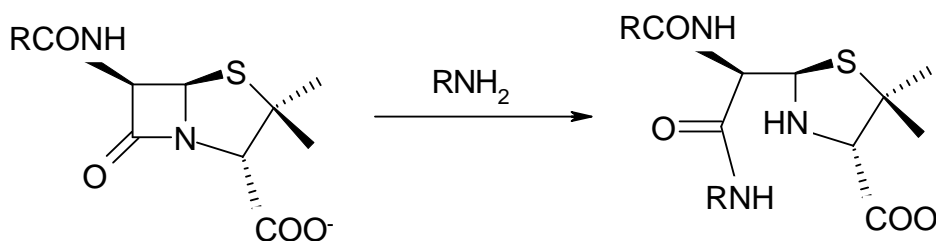
Figure 13: Pencillin hydrolysis.

Incorporating a benzamide as a potential leaving group into a simple azetidin-2-one gives the imide N-benzoyl-β-lactam (**Figure 14**), which is of interest as it contains an endocyclic and exocyclic centre both of which are potential sites for nucleophilic attack. When hydrolysis with hydroxide was studied, there was competition between the two sites for hydroxide ion attack as a function of substituents in the aroyl group.
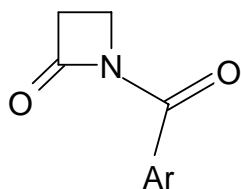
Figure 14: N-benzoyl-β-lactam.

N-aroyl β-lactams were investigated further by determining the effect on the rate of reaction, where the basicity of amine nucelophiles was varied and

studying the effect of varying the substituents in the aryl residue of the amide leaving group. The environment the subtituents are exposed to effects the rate of hydrolysis.

The rates of the aminolysis of the *N*-aroyl β-lactams were studied by UV-spectrophotometry in 1% acetonitrile-water (v/v) at 30°C with 1.0 M ionic strength maintained by KCL. The amine behaved as a nucleophile and a buffer.

The site of nucleophilic attack was determined by a product analysis of the reaction, using NMR and ESI-MS (electrospray ionisation mass spectrometry). Results showed at least 90% of the attack occurs via the β-lactam carbonyl. The kinetics of aminolysis were studied by spectrophotometrically measuring the change in absorbance due to product formation using the amine as both buffer and reactant with excess amine over *N*-aroyl β-lactam. Simple first order kinetics were observed.[43]

The aminolysis of *N*-aroyl β-lactams showed a high sensitivity to both the basicity of the attacking amine and that of the amide leaving group. The aminolysis of *N*-aroyl β-lactams appears to occur by a concerted pathway in which bond formation and fission occur simultaneously.

The structure of individual β-sultams and β-lactams play a key role in their reactivity. Structure-reactivity relationships in the inactivation of elastase in a series of β-sultams has been studied.[44]

Human neutrophil elastase (HNE) is a serine enzyme which is a destructive proteolytic enzyme which is able to catalyse the hydrolysis of the components of connective tissue. As previously mentioned the development of serine enzyme inhibitors are of great interest.

HNE is released in response to inflammatory stimuli and has a major role in protein digestion. It has been implicated in the development of diseases such as emphysema, cystic fibrosis and rheumatoid arthritis. HNE belongs to the

trypsin class and the structure has been determined by X-ray crystallography.[45] There have been numerous studies to find small molecule inhibitors of HNE.[46] However, structural and inhibition studies have been conducted on the related but readily available Porcine Pancreatic Elastase (PPE), due to the difficulty in obtaining HNE.[47]

Many inhibitors are acylating agents of the active site serine residue of serine proteases.[48] The mechanism of inhibition involves the displacement of a leaving group from the acylating agent to generate a stable acyl enzyme which only reacts slowly with nucleophiles such as water to regenerate the enzyme and so this process leads to effective inhibition.

Serine enzymes react with acyl substrates, but they are also known to react with other electrophilic centres such as phosphonyl derivatives.[49] The main reason why sulfonation of serine enzymes is not a well studied process is because sulfonyl derivatives are much less reactive than their acyl counterparts. *β*-sultams are excellent candidates to explore the mechanism of sulfonation and possible inhibition of serine protease enzymes. *β*-Sultams are unique amongst the sultams and sulfonamides, in that they are more reactive than their amide or lactam counterparts.[50]

The following *β*-sultams were studied and synthesised at the University of Huddersfield in order to study their enzyme inhibitory properties.
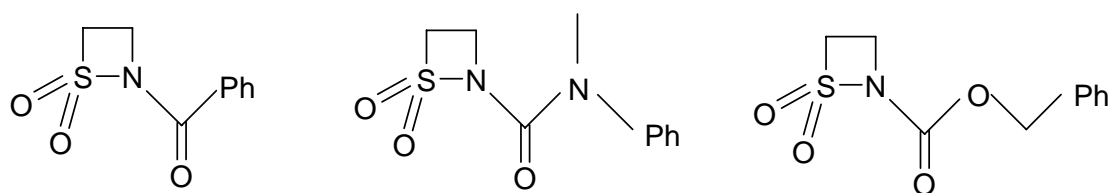
Figure 15: Substituted *β*-sultams synthesised at the University of Huddersfield

In order to test the inhibitory properties, *N*-acyl-*β*-sultams were incubated together with PPE in a buffered solution. Aliquots of the incubation solution

containing enzyme and potential inhibitor were then removed from the incubation cell after an incubation time and assayed for PPE activity against an anilide substrate that was introduced for the enzyme to hydrolyse.

It was found that *N*-substituents not only influence the rate of S-N bond fission and reaction through inductive effects altering the electrophilicity of the sulfonyl centre, but also change binding energies through molecular recognition effects such as interactions between the substituent and a binding pocket in the enzyme.

The rates of enzyme inactivation could be increased if recognition elements were built into the structure of the *β*-sultams. Alkyl chains can therefore be added to the simple *β*-sultam ring at the 4-position with the intention of improving binding at the active site of PPE as shown in **Figure 16**.

Variation in the *N*-substituted *β*-sultams causes differences in the rates of inactivation by 4 orders of magnitude. It is hoped that in the future, improved enzyme binding will allow the application of more stable and more selective enzyme inhibitors.[51]
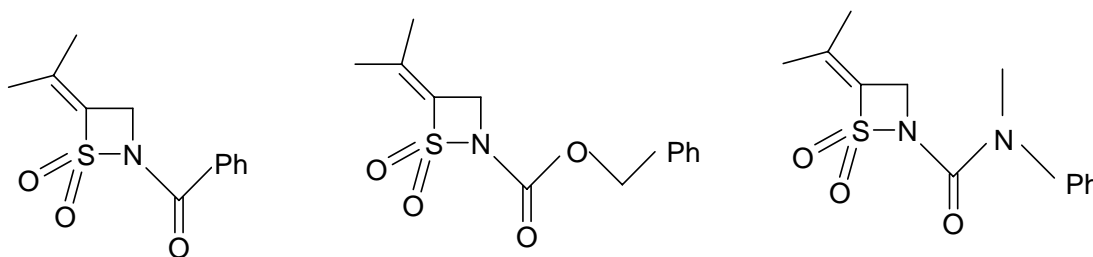
Figure 16: Substituted *β*-sultams synthesised at the University of Huddersfield

N-acyl substituted *β*-sultams and *N*-aroyl substituted *β*-sultams showed that rates of hydrolysis are affected by the different substituents within each group.

To further understand the hydrolysis of *β*-sultams the reactivity and selectivity in the inhibition of elastase by 3-oxo-*β*-sultams was looked at. Hydrolysis

occurs via S-N fission and C-N fission (**Figure 17**). These compounds are extremely interesting as they are both β-lactams and β-sultams. The compounds used in this study were synthesised at the University of Huddersfield by Naveed Ahmed and the hydrolysis studies were conducted by Wing Tsang.

3-Oxo-β-sultams were found to be a novel class of time-dependent inhibitors of elastase. The enzyme hydrolysed the amide bond by acylation. The hydrolysis of 3-oxo-β-sultams with hydroxide occurs at the sulfonyl centre with S-N fission and expulsion of the amide leaving group.[52]

Increasing the selectivity between these two reactive centres was explored by examining the effect of substituents on the reactivity of 3-oxo-β-sultams towards hydrolysis and enzyme inhibition. [53, 54]

The 3-oxo-β-sultams were found to be a new class of acylating agent for the enzymes, but the structure is chemically too reactive for further studies towards therapeutic application as sulfonylation in water was too fast - the half life of the *N*-benzyl derivative at pH6 in water is only 6 minutes.[55]
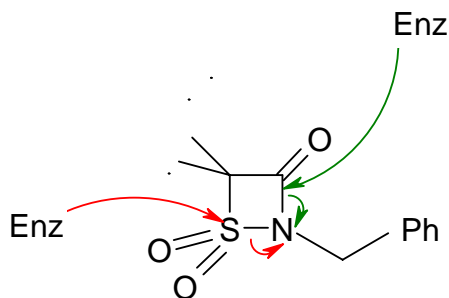
Figure 17: 3-oxo-β-sultams, hydrolysis can occur via S-N and C-N fission.

The 3-oxo-β-sultams are unusual in that the enzyme reacts at the acyl centre whereas the hydrolysis reaction occurs at the sulfonyl centre. Variation of the structure by simple substituents leads to differences in rates of inactivation. There is a large differential effect of substituents on the relative reactivities of hydrolysis and enzyme reaction.

For this reason, second order rate constants for alkaline hydrolysis (k_{OH}) at the enzyme inhibition (k_i) of PPE at pH6 (0.1 M MES buffer) by 3-oxo-β-sultams in 1% acetonitrile, 1.0 M ionic strength at 30°C, were studied and the results are shown below.[56]
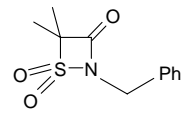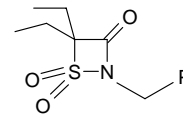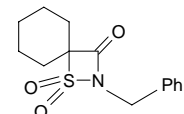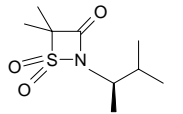
$k_{OH}\,M^{-1}\,s^{-1}$	1.83 x 10^{-5}	1.86 x 10^{-4}	5.99 x 10^{-3}	3.89 x 10^{-4}

Table 1: Shows rates of hydrolysis for 3-oxo-β-sultams.
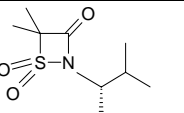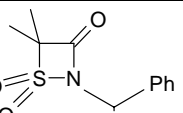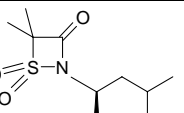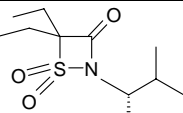
$k_{OH}\,M^{-1}\,s^{-1}$	Not determined	2.42 x 10^{-4}	3.27 x 10^{-4}	1.74 x 10^{-3}

Table 2: Shows rates of hydrolysis for 3-oxo-β-sultams.

β-Sultams themselves have been the study of further investigation and the reactivity and the mechanisms of reaction of a series of β-sultams with nucleophiles were studied. Reactions were studied by stop flow UV spectrophotometry, stock solutions were prepared at twice the standard UV concentration in 1 M KCl. The substrate solution and the reaction mixture were placed in separate syringes at a thermostatted temperature of 30°C before pneumatic injection into the reaction cell.

Pseudo first-order rate constants from exponential plots of absorbance against time were obtained using the commercial fitting software (Applied Photophysics). The pH of the reaction was measured before and after each kinetic run. The solubility of compounds was maintained by working within the

linear range of absorbance in corresponding Beer-Lambert plots. Pseudo first order rate constants from exponential plots of absorbance against time or gradients of initial slopes were obtained.

Results for the reactivity of N-unsubstituted β-sultams in aqueous sodium hydroxide solution gave first order rate constants. The observed pH independent reaction and absorbance changes are consistent with the hydrolysis pathway shown in **Figure 18**.
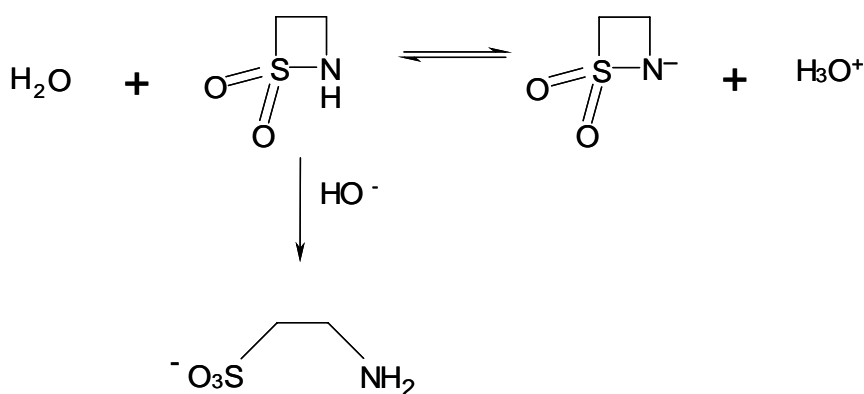
Figure 18: β-sultam hydrolysis.

Exploring the possibility of neighbouring group participation by a carboxy group on the β-sultam nitrogen in the hydrolysis of β-sultams was also studied and an example structure is shown below. The rates of hydrolysis were determined spectrophotometrically at a wide range of aqueous solution pHs.
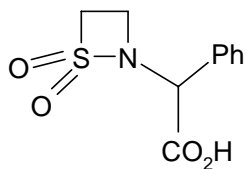
Figure 19: Carboxy group incorporated on the β-sultam.

Second order rates of hydrolysis were observed. Rates of hydrolysis were typically 20 fold lower that that for the N-benzyl β-sultam shown in **Figure 20**.
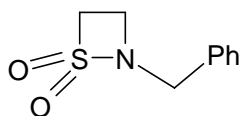
Figure 20: *N*-benzyl β-sultam.

Similar rates of hydroxide ion hydrolysis have been observed for benzyl penicillin and its methyl ester. Interestingly, *N*-(m-chlorophenyl) β-sultam, shown **Figure 21**, has a low reactivity towards nucleophiles.[57]
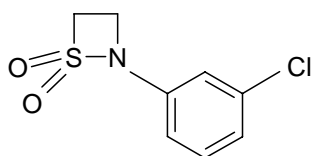
Figure 21: *N*-(m-chlorophenyl) β-sultam.

N-Benzoyl β-sultam **Figure 22** have also been studied and the parent compound is an extremely reactive β-sultam and undergoes alkaline hydrolysis with S-N fission and expulsion of an amide leaving group. It reacts with O-nucleophiles in aqueous solution but does not readily react with other nucleophiles.[58]
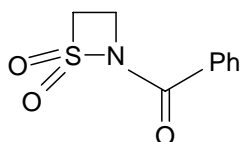
Figure 22: *N*-benzoyl β-sultam.

In general amides and lactams are more reactive than the corresponding sulfonamides.[59] However, β-sultams are 10^2 to 10^3 fold more reactive than their corresponding acyl analogues the β-lactams. This is believed to be due to the extra strain relief that is available to β-sultams over β-lactams and due to the increased bond and angle distortion that is present in the β-sultams compared to β-lactams.[60, 61]

This research project is concerned with *N*-aroyl-β-sultams and isothermal microcalorimetry which has fewer limitations. For example, extensive studies

can be conducted in the solid and solution state and any compound with or without a chromophore can be investigated. For example, **Figure 23** shows a *β*-sultam without a chromophore. Isothermal microcalorimetry can observe rates of hydrolysis for *β*-sultams without a chromophore (see Chapter 3).
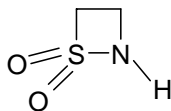
Figure 23: *β*-sultam without a chromophore.

An introduction to calorimetry, solid state and solution phase systems and an introduction to the Thermal Activity Monitor (TAM) used to conduct experimental research will be now be discussed.

1.5 Introduction to calorimetry.

Calorimetry is an analytical technique where there is an exchange in heat energy. Thermodynamic and kinetic parameters can be derived from the thermal calorimetric data obtained.[62] Calorimeters can be divided in to three groups: adiabatic, heat conduction and power compensation calorimeters.[63, 64] The principle difference between all three calorimeters is their mode of heat measurement, which is discussed as follows:

Adiabatic calorimeters – there is no heat change between the reaction vessel and calorimeter. The heat output during the experiment is equal to the product between the measured temperature change and the heat capacity of the vessel and its content. Isoperibolic calorimeters also exist and are sometimes called semi adiabatic, the heat exchange with the surrounding is important and significant, and a corrected value for the temperature change is used.

Heat conduction calorimeters – this is the most common type of calorimeter and is used for solution chemistry and biology. Heat conduction calorimeters produce heat at the reaction vessel which flows to a heat sink and the amount of heat evolved is recorded by allowing it to pass through a thermopile wall. The heat flow is directly proportional to the thermopile potential. One particular

type of heat conduction calorimetry is isothermal microcalorimetry.

Power compensation calorimeters – use the idea of combining both adiabatic and heat conduction. The adiabatic calorimeter is used to monitor exothermic processes also heat conduction calorimeters can cause a temporary increase in temperature. In both these cases a cooling power can be applied to the reaction vessel to compensate for the temperature increase. This can be achieved when an electrical current is allowed to pass through a thermopile plate (an electrical device that converts thermal energy into electrical energy), where there is a cooling power on one side of the plate and a heating power on the other side of the plate.

Heat conduction calorimetry is commonly used; the type that is used in this thesis is isothermal microcalorimetry.

1.5.1 Isothermal microcalorimetry.

Isothermal microcalorimetry is an analytical method allowing the determination of minute amounts of evolved or absorbed heat.[65] Calorimetric observations can be made where compounds in the solid state are used which is not normally feasible using other analytical techniques,[66, 67] for example, HPLC. In addition thermodynamic parameters obtained can give mechanistic information, rate constants, enthalpies and reaction order. From these parameters activation energy, change in entropy, Gibbs energy and heat capacity can be determined.

The isothermal heat conduction calorimeter comprises of two main chambers, the sample and reference chambers, which are manufactured with an inert material. They are identical in geometry and have the same physical properties with respect to heat capacity and thermal conductance. Both chambers are kept in isothermal conditions, heat that is released or absorbed in the reaction vessel flows to or from a surrounding heat sink. Thermopiles detect the heat change in the sample cell relative to the reference cell.

Sample preparation is minimal and non-invasive, and this technique is therefore

suited to a wide range of systems, such as solids and simple solution phase systems to complex heterogeneous pharmaceutical formulations. One example of a solution phase reaction is the oxidation of ascorbic acid.[68] Data output observed after 1.5 hours showed there was a mechanistic change, initially assuming a first order process, after 1.5 hours the rate constant changed by almost two orders of magnitude. The rate change was observed over a small period of time, which undoubtedly would have been missed when using conventional analytical methods. Isothermal microcalorimetry is also widely applied to pharmaceuticals to assess changes in crystallinity induced during the processing of powders by determining the heat of crystallisation, [69, 70, 71] and to characterise drug powders by measuring the heat of solution or the heat of water adsorption.[72, 73, 74] An example is a solid state experiment into the stability of benzoyl peroxide, which is a non-toxic, colourless, odourless and tasteless crystalline solid, used in the treatment of acne. Rate constants were determined at a range of temperatures appropriate for storage and the observed degradation rate of benzoyl peroxide showed that it is suitable for medicinal use.[75]

Isothermal calorimeters, for example, the Thermal Activity Monitor (TAM, Thermometric, AB, Jarfalla, Sweden) are also fitted with an isothermal titration calorimetric unit (ITC), which is suitable for studying biological reactions. For example, in the pharmaceutical industry ITC could facilitate the prediction of the affinities of potential drug compounds for particular enzymes, avoiding expensive synthesis and analysis.[76]

The type of isothermal microcalorimetry used to conduct experimental work in this thesis is isothermal batch calorimetry.

1.5.2   Isothermal batch calorimetry.

Isothermal calorimetry (batch mode), isothermal titration calorimetry and DSC are the most common types of calorimetry used today. Literature supports the use for combining the different types of calorimeters to obtain thermodynamic and kinetic information. For example, the physical stability of amorphous nifedipine and phenobarbital was studied by melting and subsequent cooling in

a differential scanning calorimeter (DSC), followed by their heats of crystallisation monitored by isothermal microcalorimetry.[77]

Isothermal batch calorimetry can also be used to predict shelf lives, calculate rates and enthalpies. This is achieved by direct measurement, in real time and by conducting experiments at different temperatures. The main advantage of using isothermal microcalorimetry is that solid and solution phase systems can be studied.

1.5.3   Solid and solution phase systems

Isothermal microcalorimetry (IMC) is a useful tool within the pharmaceutical industry. Solid and solution state systems can be studied to determine stability, compatibility, amorphicity, shelf life, drug-drug interactions, enzyme based kinetic and drug screening studies. The technique is non-invasive and non-destructive and the quality of data is better than that of traditional techniques. A traditional technique that is used to study stability is HPLC (High Performance Liquid Chromotography), where sample preparation is often extensive and destructive. In addition the technique is not sensitive to small changes in concentration, where small amounts of compound can be used in a calorimetric experiment and significant outputs can be achieved.[78]

Microcalorimetry is often preferred over traditional methods, in some cases more information is provided on the reaction mechanism, kinetics and thermodynamics associated with the process.[79] There have been a number of studies conducted throughout the years involving solid state material and solution phase systems and in some cases solid state material with the addition of water to observe various phenomena. The reason being some drugs/compounds are hygroscopic and once a tablet is in solution how long it takes to dissolve and its bioavailability is important. In particular within the pharmaceutical industry solid drug compounds present a number of challenging analysis problems to pharmaceutical scientists. Initial problems arise within the early stages when a potential medicinal compound has been identified. Characterisation techniques must identify the most stable form and how much

of it is crystalline and how much is not (amorphicity).

In addition the drug must be formulated so it can be packed and stored correctly. Also the rate at which the drug dissolves i.e. bioavailability.[80] A number of stability studies have been conducted, some of which are discussed below.

An example of stability studies, were those conducted by Pikal and Dellerman, where they studied the solution and solid state stability of several cephalosporins. Within the solid state, the stability of various physical forms of the cephalosporins were investigated, reaction enthalpies were calculated and correlated to the concentration of water present. The study proved that reaction rates as low as 1% per year can readily be observed using isothermal microcalorimetry.[81]

Further stability tests have been conducted to determine the drug stability in tablets using isothermal heat conduction calorimetry. The decomposition of a drug usually constitutes an exothermic process accompanied by an evolution of heat which is low and at present only microcalorimetry has the ability to detect such low signals. In one example, a variety of drug mixtures were compressed to 300 mg in weight and 10 mm in diameter. Placebo and non compressed mixtures were examined by microcalorimetry at 80°C. Emcompress® which is a pharmaceutical excipient was tested on its own and Emcompress® containing tablets were tested, the calorimetric outputs were compared. Decomposition of a drug usually constitutes an exothermic process accompanied by an evolution of heat which is low and at present only microcalorimetry has the ability to detect such low signals. The study showed Emcompress® (a pharmaceutical excipient) exhibited a high exothermic value because of a change in crystallinaty and for Emcompress® containing tablets the same signal interfered in such a way that the calorimetric output did not directly reflect the drug decomposition with sufficient accuracy. However, if the heat flow signal detects other processes including drug decomposition, the calorimetric outputs can provide information about interactions in dosage forms that can influence

the quality of a final drug product.[82]

It is important to note that in the pharmaceutical industry, variation can occur in the extent of crystallinity in a medicinal product. The ability to detect and quantify the amount of amorphous material within a highly crystalline drug is important when considering a solid dosage form. Processing operations such as milling, [83] spray drying, [84, 85] mixing and lyophilisation[86] can cause disruption or activation to the crystal structure, leading to various degrees of disorder. Briggner *et al.*[62] used isothermal microcalorimetry to study changes in the crystallinity of spray dried and micronized lactose monohydrate. This study used a humidity chamber, where the sample was placed in an ampoule under conditions that allowed the transition to the thermodynamically stable crystalline state to occur. Saturated salt solutions were used to generate different relative humidities between 53% and 85% RH. The hygrostat method was used, where a small glass insert is filled with the desired saturated salt solution and placed into an ampoule. The absorbed water behaved as a plasticizer to lower the glass transition temperature of the amorphous lactose below the experimental temperature (298K), at which point recrystallisation occurred. The calorimetric output is shown in **Figure 24**.
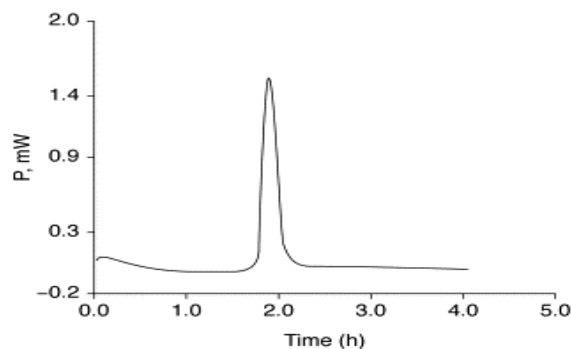
Figure 24: Typical microcalorimetric output for spray-dried lactose (20 mg powder, 85% RH, 298K).[87]

The initial response is thought to be caused by a slight imbalance in the generation of water vapour or the amorphous material undergoing structural collapse followed by absorption of water (endothermic). This is followed by a sharp response from the recrystallisation process or sorption of water vapour onto the powder (exothermic).[88] The results discussed show how isothermal

microcalorimetry is not limited to compounds in the solid state or solution. Various phenomena were detected and analysed and the data presented in this study showed complex isothermal microcalorimetric outputs that may not have been detected using traditional methods.

The studies discussed so far are within the pharmaceutical industry; however isothermal microcalorimetry has also proved to be useful within the biosciences field. For example, IMC has been used to predict storage stability of pellets of implantable bone void filler formulated with and without the antibiotic tobramycin. The experiment was conducted using batch calorimetry. Two different pellets were used made up of fully hydrated calcium sulfate, which were defined in the study as CaS (calcium sulfate) and CaS-tobra (calcium sulfate with antibiotic tobramycin). The mass used was 12.5 g corresponding to 100 pellets at 27% RH. The calorimetric outputs were analysed and compared. At each temperature, heat flow was more exothermic for CaS-tobra than for CaS. At temperatures 313K and 323K there was an apparent decrease in heat flow rate at over 25 hours. The exothermic differences observed between the two pellets were due to degradative changes in tobramycin.[89]

IMC has also been used to compare the dynamic stability of ultra-high molecular weight polyethylene (UHMWPE). UHMWPE is a thermoplastic and can be used medicinally, for example in spine replacement or as a biomaterial in knees or hips. The experiment was conducted at 298K, 30% RH. Four different methods of sterilisation were used to sterilise the UHMWPE: gamma ray irradiation in air (γAir) and in nitrogen (γN$_2$), ethylene oxide gas (EtO), and gas plasma (GP). The exothermic activity observed was the oxidation of various chemical bonds. The GP and EtO showed no significant rate increase compared with unsterilised. The γAir and γN$_2$ showed a seven fold increase rate of reaction. This initial work suggests that IMC is a promising and sensitive technique for evaluating and predicting the dynamic chemical stability of biomaterials, and for measuring *in vitro* metabolic responses of living cells to various biomaterials in solid and particulate form.[90]

IMC is not only limited to the pharmaceutical and bioscience field it can be used in many other fields such as in the food, dental and cosmetics industries. For example, a detailed study was conducted assessing the stability of spray-congealed solid dispersions with carnauba wax. The study was conducted to observe the change in the thermodynamic state of spray-congealed carnauba wax during storage. The wax showed instability and slow aging during storage to a stable form. The objective was to accelerate stabilisation, in order to accelerate the thermodynamic change in the spray congealed wax; three annealing procedures were developed and compared using isothermal microcalorimetry. Results showed carnauba wax had different stable states at different temperatures; the stabilisation process was delayed at room temperature and accelerated by an annealing procedure. IMC was used to observe the effect of annealing on the stabilisation of spray congealed carnauba wax, showing that it can be a useful tool in determining stability within different formulations of the same compound.[91]

As previously mentioned IMC can be combined with other analytical techniques to determine various physical phenomena. For example, IMC was used to study the thermo-oxidative stability of polyamide 6 films III between the temperature range of 373K-403K and sample weight of 0.5 g in 3 mL ampoules. The calorimetric output observed showed a continuous decrease in heat flow due to the depletion of oxygen. The heat flow output was characterised by an initial peak and a sigmoidal increase. Altering the temperature changed the position of the peak. Isothermal microcalorimetry heat flow curves provided information relating to exothermic and endothermic processes created by oxidation to determine the stability.[92]

IMC stability studies have provided useful information whether IMC is used on its own or in combination with other techniques. Amorphicity studies have also been conducted using isothermal microcalorimetry, for example assessing the degree of solid-state disorder (amorphicity) of lyophilised formulations of proteins. Two formulations of growth hormone were prepared by lyophilization and studied using a calorimeter at different relative humidities at 298K.

Microcalorimetric outputs showed recrystallisation events occurred in the different formulations.[93]

IMC was found to be useful over traditional techniques such as differential scanning calorimetry (DSC) and X-ray powder diffraction (XRPD) as these techniques are unable to detect solid-state disorder at levels < 10%. To assess the amorphous content of mixed or single formulations the analytical method used must be sensitive enough. For example, the amorphous content of mixed systems, trehalose with lactose, has been looked at using IMC. Calorimetric results detected and quantified the amorphous trehalose that was mixed with lactose.[94]

Amorphous raffinose has also been studied calorimetrically and combined with near IR (Infra Red) to investigate water sorption and desorption of crystalline amorphous raffinose. The importance of calorimetry in this investigation was to monitor water vapour interaction with amorphous raffinose under controlled RH (relative humidity) to see the effect of sample mass. Calorimetric outputs showed that crystallisation of amorphous raffinose is a prolonged process. Different hydrates and hydrate mixes are formed depending on the amount of water available and these differences contributed to different enthalpies of crystallisation.[95]

The amorphicity of lactose which is a pharmaceutical excipient has also been studied.[96] An excipient is an inactive substance used as a carrier for the active ingredients of a medication. Experiments were conducted at 298K, sample weights of 25–500 mg in the solid state. The powder sample was placed in the sample vessel together with a small tube filled with a saturated salt solution. Potassium bromide (81% RH) was used for samples with an amorphous content of 20% or more and sodium bromide (57% RH) was used for samples with lower concentrations of amorphous material.[97] Deionised water was used in the reference vessel. The calorimetric results showed typical heat curves and were similar to those reported by Sebhatu et al., 1994[98] Briggner et al., 1994[99] and Buckton et al., 1995.[100] These heat curves showed complexities where many

different events occurred simultaneously during the crystallisation of amorphous lactose. The three different processes creating these distinct heat profiles were possibly absorption of water vapour followed by crystallisation of amorphous lactose ending with a probable recrystallisation of anhydrous β-lactose to the α-monohydrate-form.

As previously mentioned IMC can be used in combination with other analytical techniques. A variety of thermal techniques have been used to assess the impact of feed concentration on the amorphous content and polymorphic forms present in spray dried lactose. Isothermal microcalorimetry was used to assess the heats of crystallisation of the amorphous materials, which enabled the determination of the % amorphous content. Experiments were conducted using batch calorimetry, 20 mg samples and 75% RH. The study showed isothermal microcalorimetry combined with other analytical techniques, which allowed the determination of appropriate feed concentrations of spray dried lactose, which can be manufactured with various polymorphic proportions which suit the desired tabletting properties.[101]

IMC has also been used to quantify low levels (<10%) of amorphous content in micronised (reducing the average diameter of a solid materials diameter) active batches, using dynamic vapour sorption.[102] Micronisation is a pharmaceutical process where the average diameter of solid materials is reduced. During the processing of pharmaceutical solids (e.g. milling, spray drying, tablet compaction, wet granulation and lyophilisation), various degrees of disorder in the form of crystal defects and/or amorphous regions were generated. Samples (500±5 mg) were prepared by weighing known quantities of amorphous and crystalline BED (a development candidate for Pharmacia, a benzyl ether derivative) directly into the vapour perfusion ampoules. The samples were then exposed to the following method: 0% RH for 3 h, 30% relative pressure acetone for 3 h, 90% relative pressure acetone for 4 h, 0% RH for 3 h then finally 30% relative pressure acetone for 3 h. The isothermal microcalorimetry and dynamic vapour sorption data showed agreement (±0.2% amorphous content) and indicated that the amount of amorphous material generated is extremely sensitive to small changes in the operating conditions of the microniser.

Shelf life predictions can also be made using solid state IMC. A study was conducted to show the stability and excipient compatibility of a solid drug (S)-(3-(2-(4-(S)-(4-(amino-imino-methyl)-phenyl)-4-methyl-2,5-dioxo-imidazolidin-1-yl)-acetylamino))-3-phenyl-propionic acid ethyl ester, acetate in the solid state) through the use of IMC combined with HPLC. Results showed chemical decomposition after 3-4 days at temperatures 333K – 353K. The evolved heat versus the amount of degraded drug showed a linear relationship. Larger calorimetric outputs were observed for the binary mixtures and granules (microcrystalline cellulose, potato starch and lactose), indicating decreased stability. Other formulations gave similar calorimetric outputs as that for the pure solid drug. Calorimetric analysis combined with HPLC allowed prediction of shelf life at room temperature.[103]

The solid state oxidation of L-ascorbic acid (Vitamin C) has also been studied using the TAM.[104] Dry un-sieved samples (0.5 g) with the addition of 0, 10, 20, 30, 50, 100 and 200 μL of water were used, the experiment lasted 50 hours. Kinetic and thermodynamic parameters were calculated using the Origin graphics package. The experimental results showed that the rate constant and change in enthalpy for the oxidation process were independent of the quantity of water in the reaction sample. The power time curves showed that the rate of reaction increased with increasing amounts of water. The initial calorimetric output is possibly due to the oxygen dissolved in the water phase, reacting at the ascorbic acid crystal surface. It can be noted that the rate of reaction was dependent on the quantity of water, and hence the available oxygen concentration. (The rate constant for the reaction remained the same) and will only change if there is a change in the reaction mechanism or temperature.[105]

It has been reported that IMC can be used to characterise a model solid-state interaction, for example, the browning reaction. The degradation of the HIV protease inhibitor with DMP 450, a primary amine, in a binary mixture with hydrous lactose was followed in the presence of 5% (w/w) additional water. Brown discoloration was observed in the post experiment mixtures and the associated activation energy was determined. This experiment demonstrated that the utilisation of microcalorimetry for rapid screening of drug and excipient

interactions can provide the same information in one week, where traditional methods can take 8–12 weeks.[106]

As mentioned previously, IMC is not limited to the physical state of a compound. Solid state and solution IMC plays an important part in drug candidate screening, in the development of new pharmaceutical products and in testing the stability and amorphicity of biochemical and industrial candidates. The data for complex and simple systems allows the determination of thermodynamic and kinetic parameters. Calorimetric studies are still ongoing to understand complex systems further, particularly solid state systems.

The basis of this thesis is a batch isothermal microcalorimetric study of solid and solution phase systems using β-sultams and β-lactams. The calorimeter used to conduct these experiments is the thermal activity monitor (TAM 2277-201).

1.5.4 Thermal Activity Monitor (TAM)

The calorimeter used for this research was the Thermal Activity Monitor (TAM). Two different types of calorimeters exist, single calorimeters and twin. Single calorimeters consists of a sample holder surrounded by an aluminium block (heat sink) maintained at a constant temperature, which is achieved by close contact with a surrounding thermostat. The TAM 2277-201 is a twin calorimeter; four separate twin calorimeters are built into the TAM.

The Thermal Activity Monitor (TAM, 2277-201) is a non invasive, non-destructive technique in which the rate of a reaction can be measured continuously as a function of time. The calorimeter has no influence on the reaction and prior to analysis no sample preparation is required. The sample can be in any physical state, solid, liquid, gas or any combination; it can be of any form e.g. wood shavings, biological tissue or even live animals and is therefore versatile.[107 - 110] The technique is highly sensitive, the sensitivity is such that the reaction environment can be controlled (humidity, temperature, partial pressure and pH). It has been reported that the TAM has sufficient sensitivity to monitor

slow reactions with lifetimes of up to 10,000 years, and that only 50 hours of data is required to discriminate between a reaction that has a first order rate constant of 1 x 10^{-11} s^{-1} and a reaction with a first order rate constant[111] of 2 x 10^{-11} s^{-1}. The calorimetric outputs observed are endothermic (heat absorbed by the reaction) and exothermic (heat produced by the reaction) providing information related to rate, basic chemical reactions, change of phase, changes of structure and metabolism of living systems.

The TAM system can be seen in **Figure 25** it comprises of a precisely thermostatted water bath, amplifier, digital calibration unit, a control and digital display unit.[112]
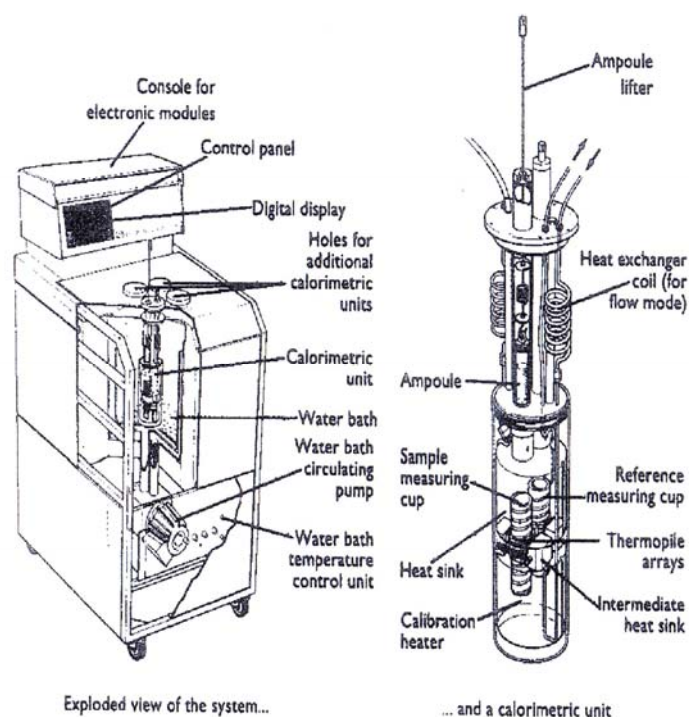
Figure 25: The TAM system and calorimetric unit.[113]

Temperatures are maintained via a heat flow system which is achieved by utilising the thermostat which surrounds the reaction measuring vessels and acts as a heat sink, the thermostat is responsible for isothermal conditions. The water thermostat comprises of a heat sink which surrounds the measuring cylinders, water is continuously pumped upwards into a cylindrical stainless steel tank. The complex system described maintains the water at a constant temperature

which is monitored by two thermistors situated in the connecting tube. One thermistor operates upto 323K and the other above 323K, the temperature can be set by the operator using the appropriate method supplied. A pre-heater and fine heater work continuously with the water thermostat and thermistors to maintain the desired temperature. The amplifier is another control that is set prior to experimentation; there are a range of settings 3, 10, 30, 100, 300 or 1000 μW. The TAM is linked to a PC via a RS232 serial port, controlling and capturing data through a software package, Digitam[TM]. This calorimetric unit consists of four channels operating in the microwatt range;[114] all four channels are contained within the accurately controlled water bath. The temperature of the water bath is regulated by the thermostat with an operating range of 5 to 90°C.[115] Each of the four channels consists of two identical chambers; sample and reference, permitting four separate experiments to be conducted simultaneously, all computer controlled. Conducting experiments in batch mode requires reference and sample ampoules to be closely matched, for example if a solution phase reaction is under study, consisting of 2 mL solvent and 1 mL deionised water then the reference material might also be 2 mL solvent and 1mL deionised water. The reference material should always be inert to ensure the thermal power observed is not a result of external factors. When performing batch mode experiments the ampoules are initially lowered just above the thermopiles (equilibrium position). The thermopiles are situated around the reaction vessel and are used to quantify and detect the temperature difference. This system works by measuring heat flow, for example the rate of thermal energy produced or absorbed by the sample, which accompanies all physical, chemical and biological processes. The ampoules (**Figure 26**)[115] are left at the equilibrium position for approximately 40 minutes, minimising any thermal shock when lowering into the measuring position. It should be noted that, with respect to ampoule fill volume, there is a significant effect on the derived rate constant and enthalpy.[116] A fill volume below 50% for 3, 4 and 20 mL glass ampoules has a significant negative effect on accuracy.

Figure 26: Diagram to show 3 mL ampoules used for TAM calorimetric studies.[115]

The channels that hold 3 mL and 4 mL ampoules are designed in such a way that the thermopiles only cover a fraction of the ampoule surface; experiments conducted should involve ampoule fill volumes above 75%.

1.5.5 Calibration unit.

The TAM must be calibrated prior to any experiment change or use for the first time or if the TAM is switched off. The digital calibration unit is responsible for accurately supplying known power levels to the calibration resistors in the sample side A and reference side B, calibration is static or dynamic. The calibration resistors are situated close to the position of the reaction ensuring the calibration and measurement results are accurate. The power values required are supplied by the calibration unit and an external computer provides the overall control of the calibration, via the RS232 interface and the input/output sockets.

The TAM operates in two modes which are the ampoule mode and the flow mode. The following steps must be followed to carry out the ampoule mode static calibration, which is the method used throughout the research presented in this thesis. The first step is to select the range in μW using the appropriate channel amplifier 3, 10, 30, 100, 300, 1,000, or 3,000. The Digital Voltmeter (DVM), computer amplifier, electrical calibration and calorimeter signal setting are also switched to the same output. The experiment is switched on and left until a stable baseline is achieved. If the baseline is off scale, adjustments are

made via the amplifier zero control until the DVM reads zero. The zero base line is left to plateau; once plateau is achieved the electrical calibration is switched on and again left to stabilise. If the output is not correct the amplifier control is adjusted and left to plateau. Once achieved electrical calibration is switched off and left to return to zero.

Calorimetry can be used alone or combined with other analytical techniques, such as Raman spectroscopy. When combined they are used to determine various chemical, physical and structural properties. Structural properties play an important role in enzyme inhibition and drug activity.

In summary, the aim of this research is to characterise and conduct calorimetric experiments on a range of unsubstituted and substituted β-sultams and β-lactams. The primary reason for conducting this research is to contribute towards the development of an inhibitor to enhance the efficacy of β-lactam antibiotics.

1.6 Research objectives

The overall aim for this research is to synthesise a series of β-sultams and β-lactams and carry out calorimetric hydrolysis and degradation studies using a Thermal Activity Monitor (TAM). There are seven individual objectives associated with this work:

1. **To synthesise a series of β-sultams and β-lactams using conventional synthetic techniques.**

2. **To conduct solid state calorimetric experiments to determine the stability of four β-sultams (A-D).**

3. **To conduct calorimetric relative humidity experiments on the four β-sultams investigated in objective 2.**

4. **To conduct solution state calorimetric experiments using the same four β-sultams investigated in objective 2 at both pH4 and pH8 at 298K, 310K and 323K.**

5. **Using the information obtained from objectives 2-4 to predict and test the calorimetric method on a β-sultam without a chromophore (F).**

6. **To conduct solution state calorimetric experiments for a series of four β-lactams at both pH4 and pH8 at 298K and 323K.**

7. **To compare and contrast β-sultam and β-lactam data with respect to hydrolysis and substituent effect based on the data obtained in objectives 2-6.**

References

1. D. Hesek, M. Lee, K. Morio, S. Mobashery, Synthesis of a fragment of bacterial cell wall, *The Journal of Organic Chemistry,* 69, **2004**, 2137-2146.

2. M.I. Page, *β*-sultams mechanism of reactions and use as inhibitors of serine proteases. *Accounts of Chemical Research*, 37, (5), **2004**, 297 303.

3. M.I. Page, P.S. Hinchliffe, J.M. Wood, L.P. Harding, A.P. Laws Novel mechanism of inhibiting *β*-lactamases by sulfonylation using *β*-sultams., *Bioorganic and Medicinal Chemistry Letters*, 13, (24), **2003**, 4489-92.

4. W. Tsang, PhD Thesis, University of Huddersfield, **2005**.

5. S.Gaisford, G.Buckton, Potential applications microcalorimetry for the study of physical processes in pharmaceuticals, *Thermochimica Acta*, 380, (2), **2001**, 185-198

6. D. Al-Hadithi, G. Buckton, S. Brocchini, Quantification of amorphous content in mixed systems: amorphous treahalose with lactose, *Thermochimica Acta*, 417, (2), **2004**, 193-199.

7. G.L. Patrick, *An introduction to medicinal chemistry*, Oxford University press, **2001**, 375.

8. C.K. Mathews, K.E.V. Holde, *Biochemistry*, The Benjamin/Cummings publishing company, Redwood City California, **1990**, 288-299.

9. C. Goffin, J-M. Ghuysen, Biochemistry and comparative genomics of SxxK superfamily acyltransferases offer a clue to the mycobacterial paradox: presence of penicillin-susceptible target proteins versus lack of efficiency of penicillin as therapeutic agent, *Microbiology and Molecular Biology,* 66, (4), **2002**, 702-738.

10. JV. Heijenoort, Formation of the glycan chains in the synthesis of bacterial peptidoglycan, *Glycobiology*, 11, (3), **2001**.

11. G.L. Patrick, *An introduction to medicinal chemistry*, Oxford University press, **2001**, 375.

12. D. Freitag, P. Schwab, P. Metz, A concise synthesis of *β*-lactam–sulfonamide hybrids, *Tetrahedron Letters*, 45, **2004**, 3589–3592.

13. R.B. Morin, M. Gorman, *Chemistry and biology of β-lactam antibiotics*, Academic press, New York, 1-3, **1982**.

14. M.I. Page, *The chemistry of β-lactams*, Blackie academic and professional, New York, **1992**, 148 - 197.

15. R.A. Firestone, P.L. Barker, J.M. Pisano, B.M. Ashe, M.E. Dahlgren, Monocyclic *β*-lactam inhibitors of human leukocyte elastase, *Tetrahedron*, 46, (7), **1990**, 2255 – 2262.

16. M.I. Page, A.P. Laws, The chemical reactivity of *β*-lactams, *β*-sultams and *β*-phospholactams, *Tetrahedron*, 56, (31), **2000**, 5631-5638.

17. H.C. Neu, The crisis in antibiotic resistance, *Science*, 257, (5073), **1992**, 1064-1073.

18. K. Bush, G.A. Jacoby, A.A. Medeiros, A functional classification scheme for *β*-lactamases and its correlation with molecular structure, *Antimicrobial Agents and Chemotherapy*, 39, (6), **1995**, 1211-1233.

19. A.P. Johnson, Intermediate vancomycin resistance in Staphylococcus aureus: a major threat or a minor inconvenience? *Journal of Antimicrobial Chemotherapy*, 42, (3), **1998**, 289-291.

20. M.S. Helfand, R.A Bonomo, *β*-lactamase: A survey of protein diversity, *Current Drug Targets-Infectious Disorders*, 3, (1), **2003**, 9-23.

21. Y. Tsurusako, K. Fukushima, K. Nishizaki, T. Takata, T. Ogawa, T. Nakashima, K. Sugata, S. Yorizane, T. Ogawara, Y. Masuda, The alteration of penicillin-binding proteins (PBPs) in drug-resistant streptococcus pneumoniae isolated from acute otitis media, *Acta Oto-laryngologica Supplementum*, 540, **1999**, 67-71.

22. M.H. Saier, Jr.,I.T. Paulsen, M.K. Sliwinski, S.S. Pao, R.A. Skurray, H. Nikaido, Evolutionary origins of multidrug and drug-specific efflux pumps in bacteria, *The FASEB Journal,* 12, **1998**, 265-274.

23. J.F. Fisher, S.O. Meroueh, S. Mobashery, Bacterial resistance to *β*-Lactam antibiotics: compelling opportunism, compelling opportunity, *Chemical Reviews*, 105, (2), **2005**, 395-424.

24. K. Bush, Metallo- *β*-lactamases: a class apart, *Clinical Infectious Diseases*, 27, **1998**, 48-53.

25. A. Bulychev, I. Massova, S.A. Lerner, S. Mobashery, Penem BRL 42715: An effective inactivator of *β*-lactamases, *Journal of the American Chemical Society*, 117, (17), **1995**, 4797-4801.

26. M.S. Wilke, A.L. Lovering, N.C.J. Strynadka, *β*-lactam antibiotic resistance: a current structural perspective, *Current Opinion in Microbiology*, 8, (5), **2005**, 525-533.

27. E. Lobkovsky, P.C. Moews, H. Liu, H. Zhao, J-M. Frere, J.R. Knox, Evolution of an enzyme activity: crystallographic structure at 2-Å resolution of cephalosporinase from the *ampC* gene of *enterobacter cloacae* P99 and comparison with a class A penicillinase, *National Academy of Sciences of the United States of America*, 90, (23), **1993**, 11257-11261.

28. M.I. Page, P.S. Hinchliffe, J.M. Wood, L.P. Harding, A.P. Laws, Novel mechanism of inhibiting *β*-lactamases by sulfonylation using *β*-sultams, *Bioorganic & Medicinal Chemistry Letters*, 13, (24), **2003**, 4489-4492.

29. C. Yoakim, W.W. Ogilvie, D.R. Cameron, C. Chabot, C. Grande-Maître, I. Guse, B. Haché, S. Kawai, J. Naud, J.A. O'Meara, R. Plante, R. Déziel, Potent *β*-lactam inhibitors of human cytomegalovirus protease, *Antiviral Chemistry and Chemotherapy*, 9, **1998**, 379-387.

30. R. Déziel, E. Malenfant, Inhibition of human cytomegalovirus protease N_o with monocyclic *β*-lactams, *Bioorganic and Medicinal Chemistry Letters*, 8, (11), **1998**, 1437-1442.

31. C. Walsh, *Enzymatic reaction mechanisms*, W.H. Freeman and company, San Francisco, **1979**, 55.

32. G.L. Zubay, W.W. Parson, D.E. Vance, *Principles of biochemistry*, W.C.Brown, Iowa, **1995**.

33. N. Ahmed, PhD Thesis, University of Huddersfield, April **2005**.

34. D. Glasl, G. Ribs, H-H. Otto, Properties and reactions of substituted 1,2-thiazetidine 1,1-dioxides: synthesis of *N*-substituted 4,4-dimethyl-1,2-thiazetidine-3-one 1,1-dioxides, and a new base-catalysed rearrangement to thiazolidin-4-one 1,1-dioxides, *Helvetica Chimica Acta*, 80, **1997**, 671-683.

35. D. Enders, S. Wallert, Efficient asymmetric synthesis of 3-substituted *β*-sultams, *Tetrahedron Letters*, 43, (29), **2002**, 5109-5111.

36. M.I. Page, A.P. Laws, The chemical reactivity of *β*-sultams, *β*-lactams and *β*-phospholactams. *Tetrahedron,* 56, (31), **2000**, 5631-5638.

37. M.I. Page, *In: Comprehensive medicinal chemistry*, P.G. Sammes, Pergamon, Oxford, 2, **1990**, 61-67.

38. M.E. Thompson, α,*N*-Alkanesulfonamide dianions: formation and chemoselective C-alkylation, *The Journal of Organic Chemistry*, 49, (10), **1984**, 1700-1703.

39. H. Baganz, G. Dransch, Synthesis of *β*-sultams, *Chemische Berichte*, 93, (4), **1960**, 784.

40. J.M. Wood, M. I. Page, *Trends In Heterocyclic Chemistry*, 8, **2002**, 19.

41. M.I. Page, A.P. Laws, The mechanism of catalysis and the inhibition of *β*-lactamases, *Chemical Communications*, **1998**, 1609-1617.

42. J.M. Frere, M. Nguyen-Disteche, J. Coyette, B. Joris, In *The chemistry of beta-lactams*, Edited M.I. Page, Glasgow: Chapman and Hall, **1992**, 148–195.

43. W.Y. Tsang, N. Ahmed, M.I. Page, The aminolysis of *N*-aroyl *β*-lactams occurs by a concerted mechanism, *Organic and Biomolecular Chemistry*, **2007**, 5, 485-493

44. P.S. Hinchliffe, J.M. Wood, A.M. Davis, R.P. Austin, R.P. Beckett, M.I. Page, Structure-reactivity relationships in the inactivation of elastase by *β*-sultams, *Organic and Biomolecular Chemistry*, 1, **2003**, 67-80.

45. M.A. Navia, B.M. McKeever, J.P. Springer, T.Y. Lin, H.R. Williams, E.M. Fluder, C.P. Dorn, K. Hoogsteen, Structure of human neutrophil elastase in complex with a peptide chloromethyl ketone inhibitor at 1.84-A resolution. *Proceedings of the National Academy of Sciences of the United States of America*, 86, (1) **1989**, 7-11.

46. W. A. Metz and N. P. Peet, *Prog. Inflammation Res.*, **1999**, 9, 853–868.

47. W.Bode, E. Meyer Jr, J.C. Powers, Human leukocyte and porcine pancreatic elastase: X-ray crystal structures, mechanism, substrate specificity, and mechanism-based inhibitors *Biochemistry*, 28, **1989**, 1951–1962.

48. C.W. Wharton, *The serine proteinases in Comprehensive Biological catalysis*, Edited M. Sinnott, London Academic press, 1, (11), **1997**, 345–379.

49. M.I. Page, *In: Comprehensive medicinal chemistry*, P.G. Sammes, Pergamon, Oxford, 2, **1990**, 61-67.

50. M.I. Page, *β*-sultams-mechanism of reactions and use as inhibitors of serine proteases. *Accounts of Chemical Research*, 37, (5), **2004**, 297-303.

51. P.S. Hinchliffe, J.M. Wood, A.M. Davis, R.P. Austin, R.P. Beckett, M.I. Page, Structure-reactivity relationships in the inactivation of elastase by *β*-sultams, *Organic and Biomolecular Chemistry*, 1, **2003**, 67-80.

52. N. Ahmed, W. Y. Tsang, M. I. Page, Acyl vs Sulfonyl Transfer in *N*-Acyl *β*-Sultams and 3-Oxo *β*-sultams, *Organic Letters.*, 6, (2), **2004**, 201–203.

53. M. I. Page, *β*-Sultams-Mechanism of Reactions and Use as Inhibitors of Serine Proteases, *Accounts of Chemical Research,* 37, (5), **2004**, 297–303.

54. M.I. Page, P.S. Hinchliffe, J.M. Wood, L.P. Harding, A.P. Laws, Novel mechanism of inhibiting *β*-lactamases by sulfonylation using *β*-sultams, *Bioorganic & Medicinal Chemistry Letters*, 13, (24), **2003**, 4489-4492.

55. W.Y. Tsang, N. Ahmed, L.P. Harding, K. Hemming, A.P. Laws, M.I. Page, Acylation versus Sulfonylation in the Inhibition of Elastase by 3-Oxo-*β*-Sultams, *Journal of the American Chemical Society*, 127, (25), **2005**, 8946-8947.

56. W-Y Tsang, N.Ahmed, K. Hemming, M.I. Page, Reactivity and selectivity in the inhibition of elastase by 3-oxo-*β*-sultams and in their hydrolysis, *Organic and Biomolecular Chemistry*, 5, **2007**, 3993-4000.

57. P. Proctor, N.P. Gensmantel, M.I. Page, The chemical reactivity of penicllins and other *β*-lactam antibiotics, *Journal of the Chemical Society, Perkin Transactions 2*, 9, **1982**, 1185.

58. J.M. Wood, P.S. Hinchliffe, A.P. Laws, M.I. Page, Reactivity and the mechanisms of reaction of *β*-sultams with nucelophiles, *Journal of the Chemical Society, Perkin Transactions 2*, (5), **2002**, 938-946.

59. J.M. Wood, M.I. Page, The Mechanism of sulfonyl transfer in strained cyclic sulfonamides, *Trends in Heterocyclic Chemistry*, 8, **2002**, 19-34.

60. M.I. Page, *β*-sultams-mechanism of reactions and use as inhibitors of serine proteases. *Accounts of Chemical Research*, 37 (5), **2004**, 297-303.

61. N.J. Baxter, A.P. Laws, L.J.M. Rigoreau, M.I. Page, The hydrolytic reactivity of *β*-sultams, *Journal of the Chemical Society, Perkin Transactions, 2*, (11), **1996**, 2245-2246.

62. M. Stödeman, I. Wadsö, Scope of microcalorimetry in the area of macrocyclic chemistry, *Pure and Applied Chemistry*, 67, (7), **1995**, 1059-1068.

63. I. Wädso, Thermal and energetic studies of cellular systems, Wright Bristol, **1987**, 34.

64. I. Wädso, *Solution calorimetry*, Blackwell, Oxford, **1994**, 161.

65. T. Selzer, M. Radau, J. Kreuter, The use of isothermal heat conduction microcalorimetry to evaluate drug stability in tablets, *International Journal of Pharmaceutics*, 184, (2), **1999**, 199-206.

66. A. Constantinescu, D. Han, L. Packer, Vitamin E recycling in human erythrocyte membranes, *The Journal of Biological Chemistry*, 268, (15), **1993**, 10906-10913.

67. G. Buckton, A.E. Beezer, The applications of microcalorimetry in the field of physical pharmacy, *International Journal of Pharmaceutics*, 72, (3), **1991**, 181-191.

68. R.J. Willson, A.E. Beezer, J.C. Mitchell, W. Loh, Determination of thermodynamic and kinetic parameters from isothermal heat conduction microcalorimetry: applications to long-term-reaction studies, *The Journal of Physical Chemistry*, 99, (18), **1995**, 7108-7113.

69. L-E. Briggner, G. Buckton, K. Bystrom, P. Darcy, The use of isothermal microcalorimetry in the study of changes in crystallinity induced during the processing of powders, *International Journal of Pharmaceutics*, 105, (2), **1994**, 125-135.

70. G.H. Ward, R.K. Schultz, Process-induced crystallinity changes in albuterol sulphate and its effect on powder physical stability. *Pharmaceutical Research*, 12, **1995**, 773-779.

71. G. Buckton, P. Darcy, Assessment of disorder in crystalline powders—a review of analytical techniques and their application, *International Journal of Pharmaceutics*, 179, (2), **1999**, 141-158.

72. E. Yonemochi, Y. Ueno, T. Ohmae, T. Oguchi, S. Nakajima, K. Yamamoto, Evaluation of amorphous ursodeoxycholic acid by thermal methods, *Pharmaceutical Research*, 14, (6), **1997**, 798-803.

73. Y. Ueno, E. Yonemochi, T. Tozuka, S. Yamamura, T. Oguchi, K. Yamamoto, Characterisation of ursodeoxycholic acid amorphous prepared by spray-drying method, *Journal of Pharmacy and Pharmacology*, 50, **1998**, 1213-1219.

74. M. Pudipeddi, T.D. Sokoloski, S.P. Duddu, J.T. Carstensen, Quantitative characterization of adsorption isotherms using isothermal microcalorimetry, *Journal of pharmaceutical Sciences*, 85, (4), **1996**, 381.

75. F. Zaman, A.E. Beezer, J.C. Mitchell, Q. Clarkson, J. Elliot, A.F. Davis, R.J. Willson. The stability of benzoyl peroxide by isothermal microcalorimetry, *International Journal of Pharmaceutics*, 227, (1-2), **2001**, 133-137.

76. J.E. Ladbury, B.Z. Chowdhry, *Biocalorimetry: applications of calorimetry in the biological sciences*, John Wiley and Sons, New York, **1998**, 103-111.

77. Y. Aso, S. Yoshioka, S. Kojima, Feasibility of using isothermal microcalorimetry to evaluate the physical stability of amorphous nifedipine and phenobarbital, *Thermochimica Acta*, 380, (2), **2001**, 199-204.

78. M. A. Phipps, L.A Mackin, Application of isothermal microcalorimetry in solid state drug development, *Pharmaceutical Science and Technology Today*, 3, (1), **2000**, 9-17.

79. A.E. Beezer, An outline of new calculation methods for the determination of both thermodynamic and kinetic parameters from isothermal heat conduction microcalorimetry, *Thermochimica Acta,* 380, (2), **2001**, 205-208.

80. L.B. Gilman, M.A. Phipps, Article: Pharmaceutical isothermal microcalorimetry, **2005**.

81. M.J. Pikal, K.M. Dellerman, Stability testing of pharmaceuticals by high-sensitivity isothermal calorimetry at 25°C: cephalosporins in the solid and aqueous solution states, *International Journal of Pharmaceutics,* 50, (3), **1989**, 233–252.

82. T. Selzer, M. Radau, J. Kreuter, The use of isothermal heat conduction microcalorimetry to evaluate drug stability in tablets, *International Journal of Pharmaceutics*, 184, (2), **1999**, 199–206.

83. J. Waltersson, P. Lundgren, The effect of mechanical communition on drug stability, *Acta Pharmaceutica Suecica*, 22, **1985**, 291–300.

84. M. Mumenthaler, H. Leuenberger, Atmospheric spray-freeze drying: a suitable alternative in freeze-drying technology, *International Journal of Pharmaceutics,* 72, (2), **1991**, 97–110.

85. T. Konno, Physical and chemical changes of medicinals in mixtures with adsorbents in the solid state IV. Reduced-pressure mixing for practical use of amorphous mixtures of flufenamic acid, *Chemical and Pharmaceutical Bulletin,* 38, (7), **1990**, 2003.

86. M.J. Pikal, A.L. Lukes, J.E. Lang, K. Gaines, Quantitative crystallinity determinations of β-lactam antibiotics by solution calorimetry : correlations with stability, *Journal of Pharmaceutical Sciences,* 67, **1978**, 767–772.

87. L-E. Briggner, G.Buckton, K. Bystrom, P. Darcy, The use of isothermal microcalorimetry in the study of changes in crystallinity induced during the processing of powders, *International Journal of Pharmaceutics*, 105, (2), **1994**, 125–135.

88. G. Buckton and P. Darcy, Water mobility in amorphous lactose below and close to the glass transition temperature, *International Journal of Pharmaceutics,* 136, (1-2), **1996**, 141–146.

89. M.J. Koenigbauer, S.H. Brooks, G. Rullo, R.A. Couch, Solid-state stability testing of drugs by isothermal microcalorimetry, *Pharmaceutical Research*, 9, **1992**, 939–944.

90. A.U. Daniels, S.J. Charlebois, E.A. Lewis, Isothermal microcalorimetry: a new tool for biomaterials research, *Medical plastics and Biomaterials Magazine*, K.Quinn, USA, **1998**.

91. M. Emas, H. Nyqvist, Methods of studying aging and stabilization of spray-congealed solid dispersions with carnauba wax. 1. Microcalorimetric investigation, *International Journal of Pharmaceutics*, 197, (1-2), **2000**, 117–127.

92. D. Forsström, L-G. Svensson, B. Terselius, Thermo-oxidative stability of polyamide 6 films III. Isothermal microcalorimetry *Polymer Degradation and Stability*, 67, **2000**, 263-269.

93. M. Mosharraf, Assessment of degree of disorder (amorphicity) of lyophilized formulations of growth hormone using isothermal microcalorimetry, *Drug Development and Industrial Pharmacy*, 30, (5), **2004**, 461-472.

94. D. Al-Hadithi, G. Buckton, S. Brocchini, Quantification of amorphous content in mixed systems: amorphous trehalose with lactose, *Thermochimica Acta*, 417, (2), **2004**, 193–199.

95. S.E. Hogan, G. Buckton, Water sorption/desorption near IR and calorimetric study of crystalline and amorphous raffinose, *International Journal of Pharmaceutics*, 227, (1-2), **2001**, 57–69.

96. C. Gustafsson, H. Lennholm, T. Iversen, C. Nyström, Comparison of solid-state NMR and isothermal microcalorimetry in the assessment of the amorphous component of lactose, *International Journal of Pharmaceutics*, 174, (1-2), **1998**, 243-252.

97. H. Nyqvist, Saturated salt solutions for maintaining specified relative humidities, *International Journal of Pharmaceutical Technology and Product Manufacturing*, 4, (2), **1983**, 47–48.

98. T. Sebhatu, M. Angberg, C. Ahlneck, Assessment of the degree of disorder in crystalline solids by isothermal microcalorimetry, *International Journal of Pharmaceutics*, 104, (2), **1994**, 135–144.

99. L.-E. Briggner, G. Buckton, K. Bystrom and P. Darcy, The use of isothermal microcalorimetry in the study of changes in crystallinity induced during the processing of powders, *International Journal of Pharmaceutics*, 105, (2), **1994**, 125–135.

100. G. Buckton, P. Darcy, A.J. Mackellar, The use of isothermal microcalorimetry in the study of small degrees of amorphous content of powders, *International Journal of Pharmaceutics*, 117, (2), **1995**, 253–256.

101. O.C. Chidavaenzi, G. Buckton, F. Koosha, R. Pathak, The use of thermal techniques to assess the impact of feed concentration on the amorphous content and polymorphic forms present in spray dried lactose, *International Journal of Pharmaceutics*, 159, (1), **1997**, 67-74.

102. L. Mackin, R. Zanon, J.M. Park, K. Foster, H. Opalenik, M. Demonte, Quantification of low levels (<10%) of amorphous content in micronised

active batches using dynamic vapour sorption and isothermal microcalorimetry, *International Journal of Pharmaceutics*, 231, (2), **2002**, 227-236.

103. T. Selzer, M. Radau, J. Kreuter, Use of isothermal heat conduction microcalorimetry to evaluate stability and excipient compatibility of a solid drug, *International Journal of Pharmaceutics*, 171, (2), **1998**, 227–241.

104. J. Suurkuusk, I. Wadso, A multi channel microcalorimetry system. *Chemica Scripta,* 20, **1982**, 155-163.

105. R.J. Willson, A.E. Beezer, J.C. Mitchell, Solid state reactions studied by isothermal microcalorimetry; the solid state oxidation of ascorbic acid, *International Journal of Pharmaceutics*, 132, (1-2), **1996**, 45-51.

106. R.D. Vickery, M.B. Maurin, Utility of microcalorimetry in the characterization of the browning reaction, *Journal of Pharmaceutical and Biomedical Analysis*, 20, (1-2), **1999**, 385–388.

107. A.E Beezer, Biological microcalorimetry, Academic press, London, **1980**.

108. A.M. James, Thermal and energetic studies of cellular biological systems, Institute of physics, Bristol, **1987**.

109. G. Buckton, A.E. Beezer, A microcalorimetric study of powder surface energetics, *International Journal of Pharmaceutics*, 41, (1-2), **1988**, 139-145.

110. A.K. Hills, PhD Thesis, University of Kent, **2001**.

111. R.J. Willson, PhD Thesis, University of Kent, **1995**.

112. M.A.A. O'Neill, PhD Thesis, University Of Greenwich, **2002**.

113. L.J. Waters, PhD Thesis, University of Greenwich, **2003**.

114. TAM – Thermal Activity Monitor for highly sensitive thermal analyses, Promotional brochure, Thermometric AB, **2001**.

115. Thermometric Technical Specifications, supplied with TAM.

116. M.A.A. O'Neill, A.E. Beezer, R.M. Deal, A.C. Morris, J.C. Mitchell, J.A.Orchard, J.A. Connor, Survey of the effect of fill volume on the values for the enthalpy and rate constant derived from isothermal microcalorimetry: applications of a newly developed test reaction*, Thermochimica Acta*, 397, (1-2), **2003**, 163-169.

2. Organic synthesis

2.0 Introduction

The β-sultams and β-lactams were synthesised at the University of Huddersfield. All reagents were obtained from Aldrich.

In order to conduct successful calorimetric experiments pure compounds were required, in particular β-sultams as they are reactive, temperature and moisture sensitive. To determine purity after synthesis and before calorimetric experiments, TLC, IR and ^{1}H NMR experiments were conducted.

Chromatography was performed on silica gel 60 (0.063-0.200 mm). TLC was carried out using fluorescent (254nm) aluminium backed TLC plates. Melting points were determined using a Gallenkamp melting point apparatus. IR spectroscopy was carried out on the Perkin Elmer 1600 and NMR spectra were recorded on a Bruker Avance DPX400 NMR Spectrometer.

2.1 Synthesis of taurine sulfonyl chloride
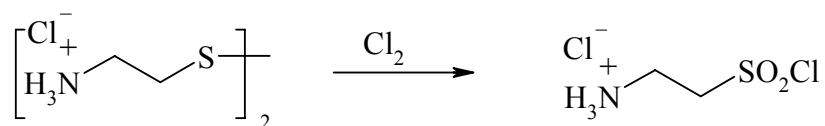
Step 1: Chlorine was passed into a -10ºC solution of cystamine dihydrochloride (Aldrich) (20.2 g, 89.8 mmol) in dry chloroform (400 mL) and absolute ethanol (200 mL) under nitrogen until saturation, noted by a permanent pale green colour. The system was purged with nitrogen followed by the addition of dry ether (100 mL) and stirred for one hour. The reaction mixture was stored at 4ºC overnight. A white crystalline precipitate was formed and filtered (vacuum filtration) and washed with dry ether, to yield (30.4 g, 96 %) of white solid.

IR: υ_{max} (cm^{-1}) (nujol) 3421, 1654, 1457, 1380, 1400, 1161, 774 identical to that reported in the literature.[1]

2.1.1 Synthesis of 1,2-thiazetidine 1,1-dioxide (ethane *β*-sultam) (A)
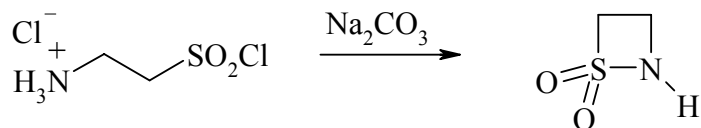
Step 2: Taurine sulfonyl chloride (30.4 g, 169 mmol) was added to finely ground sodium carbonate (35.9 g, 339 mmol) in dry ethyl acetate (950 mL) and stirred at ambient temperature for 48 hours. The reaction mixture was filtered (vacuum filtration) through Celite and the solvent removed by reduced pressure rotary evaporation at 30°C, which gave a fine white powder, (11.27 g, 62 %), m.p. 50 - 51 °C. (Literature value 51 – 52 °C).[2]

IR: υ_{max} (cm^{-1}) (nujol) 3305, 3046, 1336, 1300, 1172, 1151, 760.

^{1}H NMR: δ (CDCl$_3$) 3.40 (2H, dt *J* 3.9 and 6.9 Hz C*H$_2$*SO$_2$); 4.30 (2H, dt *J* 1.6 and 7.0 Hz C*H$_2$*N); 5.7 (1H, s, N*H*).

^{13}C NMR: δ (CDCl$_3$) 28.1 (*C*H$_2$SO$_2$) 60.9 (*C*H$_2$NH).

Synthesis of 2-aroyl-*β*-sultams

2.2 Synthesis of 2-benzoyl-1,2-thiazetidine 1,1-dioxide (B)
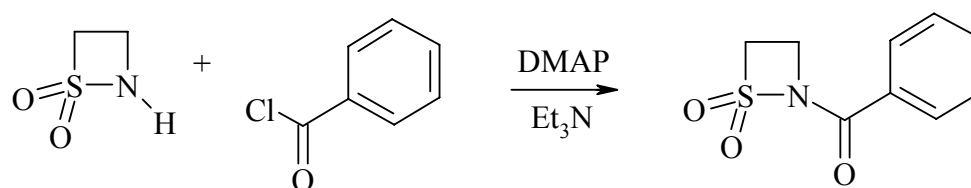
Benzoyl chloride (2.6 g, 18.5 mmol) was added dropwise to a solution 1,2-thiazetidine-1,1-dioxide (2.0 g, 18.6 mmol) and DMAP (0.15 g, 1.23 mmol) in anhydrous dichloromethane (50 mL) at −78 °C. The reaction mixture was stirred for 30 minutes at −78 °C and 15 minutes at room temperature. Triethylamine (1.9 mL, 18.78 mmol) was added dropwise over 12 minutes at −78 °C forming a white precipitate. The mixture was allowed to stir at room temperature for 24 hours before the reaction mixture was filtered (gravity filtration) and the solvent removed by reduced pressure rotary evaporation at 30

^{o}C. The pale yellow oil was purified by column chromatography using silica (75 g) (3:1 ether : DCM) to give a white solid. (0.99 g, 25 %), m.p. 95-96 ^{o}C.[1]

The numbering scheme for the *N*-aroyl substituted *β*-sultams used for NMR analysis is as follows:
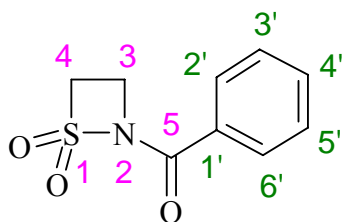
IR υ_{max} (cm^{-1}) (nujol) 3150, 2923, 1667, 1461, 1376, 1344, 1200, 1156, 718

^{1}H NMR: δ (CDCl$_3$) 8.00 (2*H*, Ph 2'/6'), 7.63 (1*H*, Ph 4'), 7.52 (2*H*, Ph3'/5'), 4.30 (2H, t, *J* 7.4 Hz, C*H$_2$*-NR), 3.92 (2H, t, *J* 7.4 Hz, C*H$_2$*-SO$_2$).

^{13}C NMR: δ (CDCl$_3$) 167.4 (*C*5), 133.5 (*C*1'), 133.6 (*C*H-Ph 2'/6'), 132.1 (*C*H-Ph 3'/5'), 128.9 (*C*4'), 56.9 (*C*H$_2$-NR) 30.9 (*C*H$_2$-SO$_2$).

2.3 Synthesis of 2-(4-chlorobenzoyl)-1,2-thiazetidine 1,1-dioxide (C)
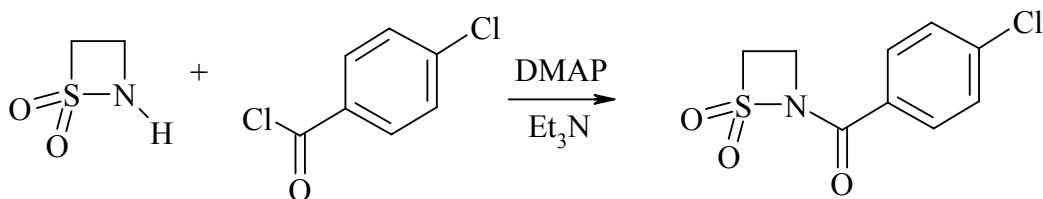
4-Chlorobenzoyl chloride (1.63 g, 9.31 mmol) was added dropwise to a solution of 1,2-thiazetidine-1,1-dioxide (1 g, 9.33 mmol) and DMAP (0.2 g, 1.63 mmol) in anhydrous dichloromethane (50 mL) at –78 ^{o}C. The reaction mixture was stirred for 30 minutes at –78 ^{o}C and 15 minutes at room temperature. Triethylamine (1.2 mL, 9.31 mmol) was added dropwise over 12 minutes at –78 ^{o}C forming a white precipitate. The mixture was allowed to stir at room temperature for 24 hours before the reaction mixture was filtered (gravity filtration) and the solvent removed by rotary evaporation 30 ^{o}C. The pale

yellow oil was purified by column chromatography (silica 75 g) (3:1 ether: DCM) to give a white solid. (1.35 g, 59 %), m.p. 84-86 °C.[1]
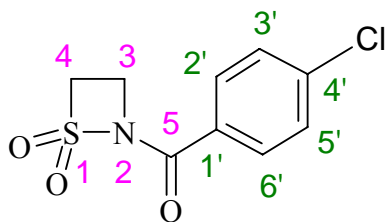
IR υ$_{max}$ (cm^{-1}) (nujol) 1649, 1591, 1461, 1377, 1331, 1159, 1092, 1013.

^{1}H NMR: δ (CDCl$_3$) 7.96 (2H, d, *J* 8.5 Hz, *H*2' / *H*6'), 7.52 (2H, d, *J* 8.5 Hz, *H*3' / *H*5'), 4.33 (2H, t, *J* 7.4 Hz, C*H$_2$*NR), 3.93 (2H, t, *J* 7.4 Hz, C*H$_2$*SO$_2$).

^{13}C NMR 166.4 (*C*5), 140.2 (*C*1'), 130.4 (*C*4'), 129.8 (*C*H 2'/6'), 129.3 (*C*H 3'/5'), 57.0 (*C*H$_2$NR), 30.9 (*C*H$_2$SO$_2$).

2.4 Synthesis of 2-(4-methoxybenzoyl)-1,2-thiazetidine 1,1-dioxide (D)
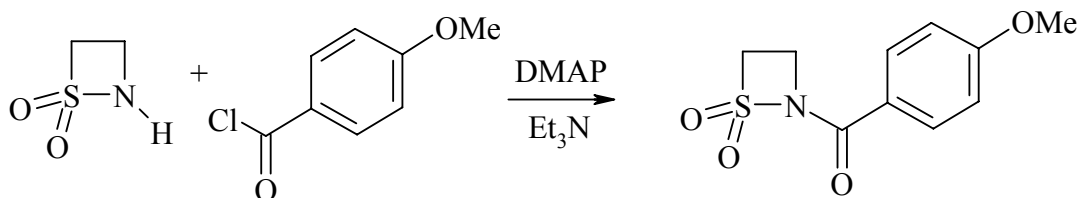
4-Methoxybenzoyl chloride (1.59 g, 9.32 mmol) in 10 mL DCM was added dropwise to a solution of 1,2-thiazetidine-1,1-dioxide (1 g, 9.33 mmol) and DMAP (0.2 g, 1.63 mmol) in anhydrous dichloromethane (50 mL) at −78 °C. The reaction mixture was stirred for 30 minutes at −78 °C and for 15 minutes at room temperature. Triethylamine (0.94 g, 9.29 mmol) was added dropwise over 12 minutes at −78 °C forming a white precipitate. The mixture was stirred at room temperature for 24 hours and then filtered (gravity filtration) and the solvent removed by rotary evaporation at 30 °C. The colourless oil was purified by column chromatography (silica 75 g) (3:1 ether: DCM) to give a white solid. (1.01 g, 45.08 %), m.p. 98-99 °C.[1]
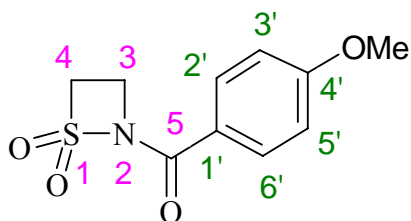
IR υ_{max} (cm^{-1}) (nujol) 2284, 1663, 1603, 1512, 1376, 1264, 1202, 1155, 1028.

**^{1}H NMR:** δ (CDCl$_3$) 8.01 (2H, d, *J* 8.7, *H*2' / *H*6'), 7.01 (2H, d, *J* 8.7, *H*3' / *H*5'), 4.29 (2H, t, *J* 7.3, C*H*$_2$NR), 3.91 (2H, t, *J* 7.4, C*H*$_2$SO$_2$), 3.89 (3H, s, C*H*$_3$).

^{13}C NMR 166.7 (*C*5), 163.9 (C1'), 130.7 (*CH* 2'/6'), 124.2 (C4'), 114.2 (*CH* 3'/5'), 56.5 (*CH*$_2$NR), 55.5 (*CH*$_2$SO$_2$), 30.7 (*CH*$_3$).

2.5 Attempted synthesis of 2-(4-nitrobenzoyl)-1,2-thiazetidine 1,1-dioxide (E)
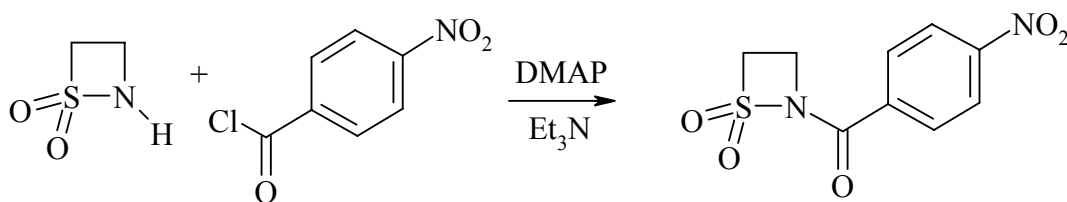
4-Nitrobenzoyl chloride (1.73 g, 9.32 mmol) was added dropwise to a solution of 1,2-thiazetidine-1,1-dioxide (1 g, 9.33 mmol) and DMAP (0.2 g, 1.63 mmol) in dry dichloromethane (50 ml) at −78 °C. The reaction mixture was stirred for 30 minutes at −78 °C and 15 minutes at room temperature. Triethylamine (1.3 ml, 9.29 mmol) was added dropwise over 12 minutes at −78 °C forming a dark brown precipitate. The mixture was stirred at room temperature for 24 hours before the reaction mixture was filtered and the solvent removed by rotary evaporation at 30 °C. The dark oil obtained yielded none of the desired product upon attempted chromatographic purification.

Synthesis of 1-aroyl-*β*-lactams

2.6 Synthesis of 1–benzoyl-1-azetidin-2-one
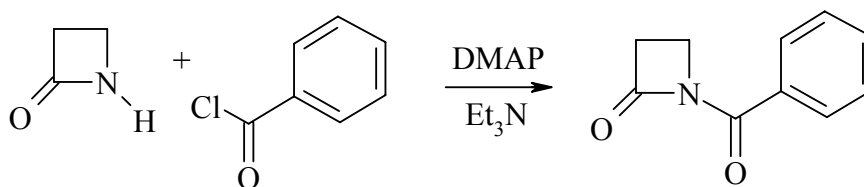
Benzoyl chloride (0.99 g, 7.07 mmol) was added dropwise over 12 minutes to a stirred solution of 2-azetidinone (Aldrich) (0.5 g 7.04 mmol) and DMAP (0.1 g, 0.82 mmol) in dry dichloromethane (20 mL) at -78 ^{o}C. The reaction mixture was left to stir at -10 ^{o}C for 40 minutes. Triethylamine (0.98 mL, 7.02 mmol) was added dropwise over 12 minutes forming a white precipitate at -78 ^{o}C and the mixture left to stir for 15 minutes at the same temperature, then left to stir for 24 hours at ambient temperature. The pale yellow reaction mixture was filtered (gravity filtration) and solvent was removed by reduced pressure rotary evaporation at 30 ^{o}C to yield a pale yellow oil, which was purified by column chromatography (silica 75 g) (3:1 ether:DCM). The solvent was removed by reduced pressure rotary evaporation, and the flask was washed again with DCM. The solvent was removed and the flask was left to stand at -10 ^{o}C in an ice bath under nitrogen to yield a white solid. (0.59 g, 48 %), m.p. 125-127 ^{o}C.
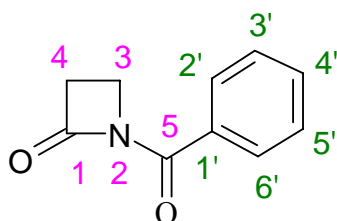
IR υ_{max} (cm^{-1}) (solid) 1671, 1330, 1316, 1195, 1448, 1295, 958.

^{1}H NMR: δ (CDCl$_3$) 7.98 (2H, 2' / 6'), 7.58 (1H, 4'), 7.47 (2H, 3'/ 5'), 3.79 (2H, t, J 4.3 Hz, CH_2-NR), 3.12 (2H, t, J 5.5 Hz, CH_2-CO).

^{13}C NMR: δ (CDCl$_3$) 166.2 (*C*1), 163.9 (*C*5), 133.2 (*C*1'), 131.9. (H2'/ H6', *Ph*), 129.7, 130.0 (*C*4') 128.1 (H3' / H5', *Ph*), 36.8 (CH_2-NR) 35.1 (CH_2-CO).

2.7 Synthesis of 1-(4-chlorobenzoyl)-1-azetidin-2-one
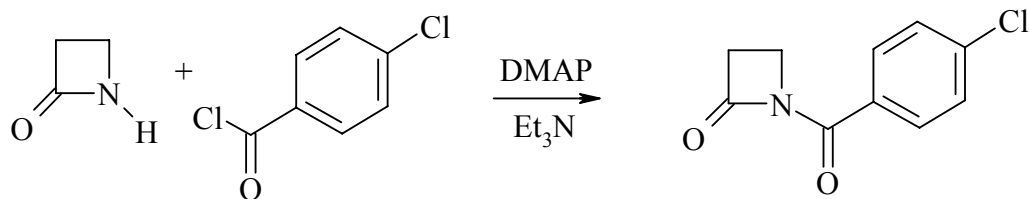
4-Chlorobenzoyl chloride (1.48 g, 8.45 mmol) was added dropwise to a solution of 2-azetidinone (Aldrich) (0.5 g, 7.04 mmol) and DMAP (0.1 g, 0.82 mmol) in dry dichloromethane (25 mL) at -78 °C. The reaction mixture was stirred for 15 minutes at -78 °C and for 30 minutes at room temperature. Triethylamine (0.98 mL, 7.02 mmol) was added dropwise over 12 minutes at -78 °C (forming a white precipitate) and the mixture was left to stir at ambient temperature for 24 hours. The reaction mixture was filtered (gravity filtration) and the solvent removed by reduced pressure rotary evaporation at 30 °C. The pale yellow oil was purified using column chromatography (silica 75 g) (3:1 ether:DCM) and gave a white solid, (0.51 g, 30 %), m.p 127-128°C.[1]
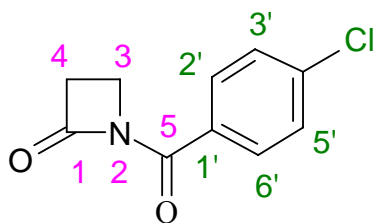
IR υ_{max} (cm^{-1}) (solid) 1779, 1662, 1587, 1403, 1294, 1283, 1037, 641.

^{1}H NMR: δ (CDCl$_3$) 7.95 (2*H*, d, *J* 9.0 Hz 2'/6'), 7.30 (2*H*, d, *J* 9.0 Hz, 3'/5'), 3.76 (2*H*, t, *J* 5.5 Hz, C*H*$_2$N), 3.12 (2*H*, t, *J* 5.5 Hz, C*H*$_2$CO).

^{13}C NMR: δ (CDCl$_3$) 164.9 (*C*1), 163.8 (*C*5), 139.4 (*C*1') 131.1 (*C*H a/c), 130.1 (*C*-Cl) 128.4 (*C*H b/d), 36.7 (*C*H$_2$N), 34.9 (*C*H$_2$CO).

2.8 Synthesis of 1-(4-methoxybenzoyl)-1-azetidin-2-one
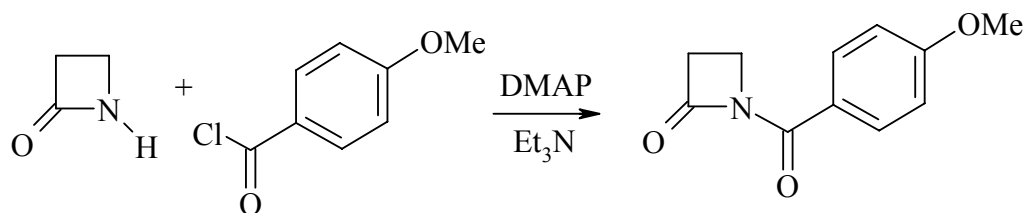
4-Methoxybenzoyl chloride (1.44 g, 8.44 mmol) in 10 mL dichloromethane was added dropwise over 12 minutes to a stirred solution of 2-azetidinone (0.5 g, 7.03 mmol) (Aldrich) and DMAP (0.1 g, 0.82 mmol) in dry dichloromethane (20 mL) at -78 °C and left to stir for 15 minutes at -78 °C and 30 minutes room temperature. Triethylamine (0.98 mL, 7.02 mmol) was added dropwise over 12 minutes forming a white precipitate. The reaction mixture was left to stir for 1 hour at -10 °C and for a further 24 hours at ambient temperature. The reaction mixture was filtered (gravity filtration) and the solvent was removed by reduced pressure rotary evaporation at 30 °C to yield a pale yellow oil, which was purified by column chromatography (silica 75 g) (3:1 ether:DCM) and gave a white solid, (0.18 g, 10.4 % m.p), 125-127 °C.[1]
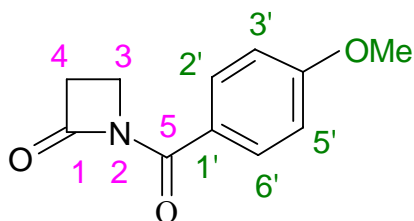
IR υ_{max} (cm^{-1}) (solid) 1789, 1659, 1311, 1283, 1254, 1191, 1175, 1099, 1017, 766.

^{1}H NMR: δ **(CDCl$_3$)** 8.03 (2*H*, d, *J* 9.5 Hz 2' / 6'), 6.96 (2*H*, d, *J*, 9.5.Hz 3' / 5'), 3.87 (3H, s, C*H$_3$*), 3.76 (2H, t, *J* 5.5, C*H$_2$*N), 3.09 (2H, t, *J* 5.5, C*H$_2$*CO).

^{13}C NMR: δ **(CDCl$_3$)** 165.5 (*C*1), 164.1 (*C*5), 163.7 (*C*1'), 132.2 (*C*2'/6') 123.9 (*C*OMe), 113.5 (*C*3'/5'), 55.4 (*C*H$_3$) 36.6 (*C*H$_2$N), 34.7 (*C*H$_2$CO).

2.9 Discussion

The β-sultams synthesised are potential serine enzyme inhibitors, which function via attack of the serine OH group at the sulfonyl. Small differences between each β-sultam may contribute towards enzyme recognition increasing the reactivity of the β-sultam. These small differences include changing the substituent in the aryl ring of the *N*-aroylated β-sultams.

During hydrolysis the amide-leaving group plays an essential role and its ability to stabilise any intermediate negative charge onto the amide nitrogen will depend upon the benzene ring substituents. The *N*-aroylated β-sultams in particular are synthetic targets because of their potential enhanced reactivity towards hydrolysis and possible inactivation of serine enzymes.

Ethane β-sultam, which is initially synthesised from taurine sulfonyl chloride and is used as a precursor to synthesise *N*-aroylated β-sultams. It is important to note taurine present in mammals shows various biological properties. The mechanism of action is still not well understood therefore investigating derivatives of taurine such as β-sultams is of interest, furthermore they are convenient synthons in heteroatom chemistry.[3]

The synthesis of ethane β-sultam (**Figure 27**) requires specific experimental conditions to ensure a high yield. The yields for all β-sultams discussed depends upon experimental conditions including column chromatography which was used for separation. The synthesis and mechanisms of these reactions will be discussed followed by an analysis of previous hydrolysis and kinetic studies carried out by Page *et al*.

Synthesis of ethane-β-sultam
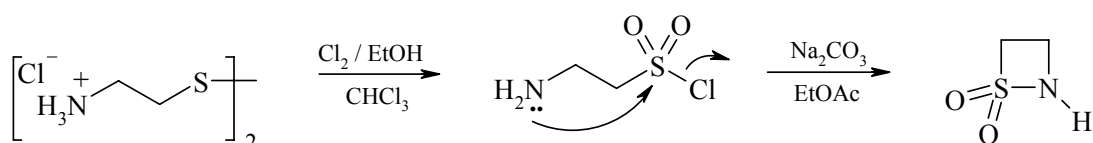
Figure 27: Synthesis of ethane-β-sultam (A).

Cystamine dihydrochloride is a disulfide compound and was oxidised to taurine sulfonyl chloride using chlorine gas. **Figure 28** shows the possible routes through to the taurine sulfonyl chloride, shown as R-SO$_2$Cl.

$$R-S-\underset{\underset{O}{\|}}{\overset{\overset{O}{\|}}{S}}-R \quad \xrightarrow{\text{HOCl}} \quad [\ RSOH\ ] \quad + \quad RSO_2Cl$$

$$R-\underset{\underset{O}{\|}}{S}-S-R \quad \xrightarrow{\text{HOCl}} \quad R-\underset{\underset{O}{\|}}{\overset{\overset{O}{\|}}{S}}-S-R \quad + \quad HCl$$

$$R-\underset{\underset{O}{\|}}{\overset{\overset{O}{\|}}{S}}-S-R \quad \xrightarrow{\text{HOCl}} \quad R-\underset{\underset{O}{\|}}{\overset{\overset{O}{\|}}{S}}-\overset{\overset{O}{\|}}{S}-R \quad + \quad HCl$$

$$RSCl \ + \ R-\underset{\underset{O}{\|}}{\overset{\overset{O}{\|}}{S}}-\overset{\overset{O}{\|}}{S}-R \quad \xrightarrow{\text{HOCl}} \quad R-SO_2Cl \ + \ R-S-\underset{\underset{O}{\|}}{\overset{\overset{O}{\|}}{S}}-R \ + \ HCl$$
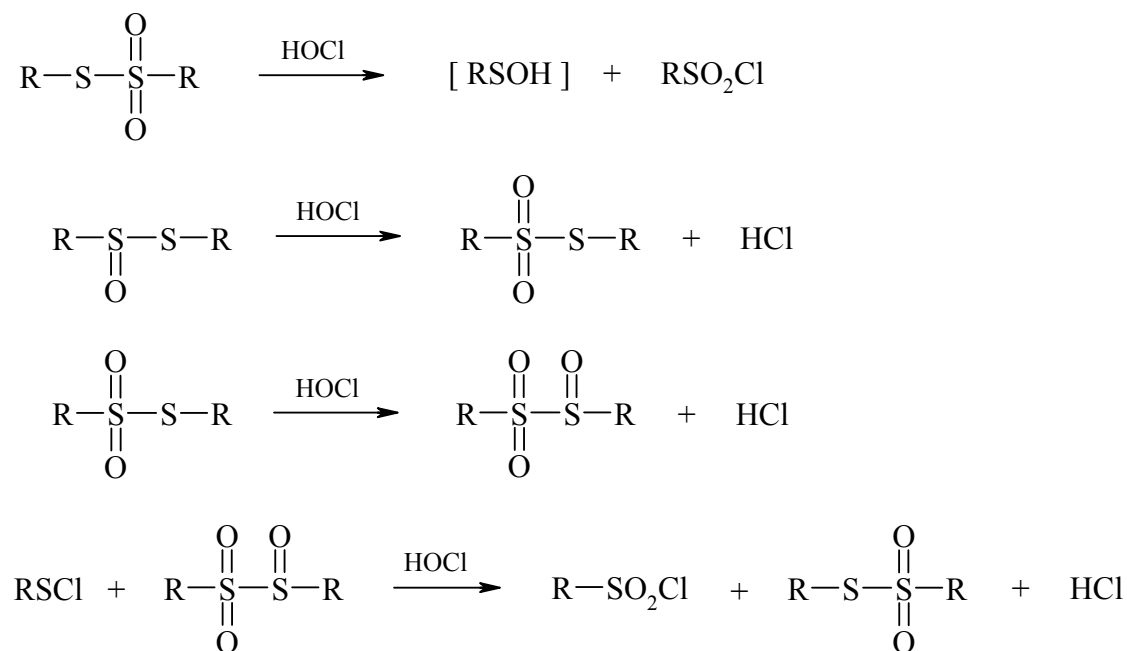
Figure 28: Possible mechanistic routes for the formation of taurine sulfonyl chloride.

These mechanisms require the generation of hyperchlorous acid (HOCl) together with an oxidised sulfur precursor. The chlorination is carried out in ethanol. The ethanol reacts with chlorine generating *in situ* hyperchlorous acid (1), which is an oxidative species. This step is still unclear and reports only suggest it.[4]

$$EtOH \quad \xrightarrow{\text{Cl}_2} \quad EtCl \ + \ HOCl \qquad \text{(equation 1)}$$
$$\text{(1)}$$
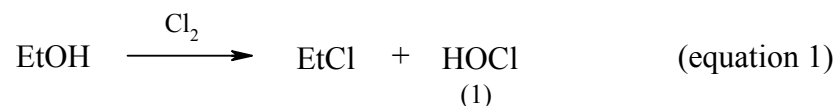
Hyperchlorous acid then reacts with the disulfide cystamine to form sulfenic acid (2) and sulfenyl chloride (3) (equation 2).

$$RS-SR \quad \xrightarrow{\text{HOCl}} \quad [\ RSOH\ ] \ + \ RSCl \qquad \text{(equation 2)}$$
$$\qquad\qquad\qquad \text{(2)} \qquad\quad \text{(3)}$$
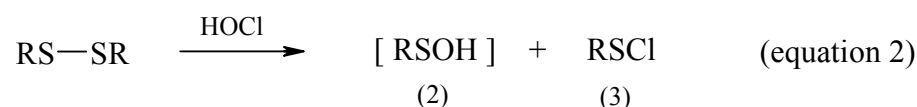
Another possibility is that chlorine interacts with the disulfide cystamine to give sulfenyl chloride (equation 3). However, this mechanism is unclear.[5]

$$RS-SR \xrightarrow{Cl_2} 2RSCl \qquad \text{(equation 3)}$$

Sulfenic acid (2) has never been isolated and could possibly react with the sulfenyl chloride (3) to form a thiosulfinate (4).[6] (equation 4).

$$[RSOH] + RSCl \longrightarrow R-\underset{\underset{O}{\|}}{S}-S-R + HCl \qquad \text{(equation 4)}$$
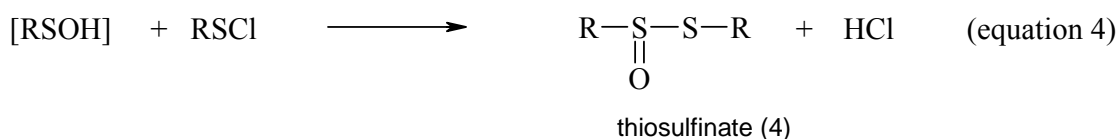
thiosulfinate (4)

Disproportionation of sulfenic acid has also been suggested as a possible route for the formation of the thiosulfinates (equation 5).[7]

$$[RSOH] \longrightarrow R-\underset{\underset{O}{\|}}{S}-S-R + H_2O \qquad \text{(equation 5)}$$

(4)
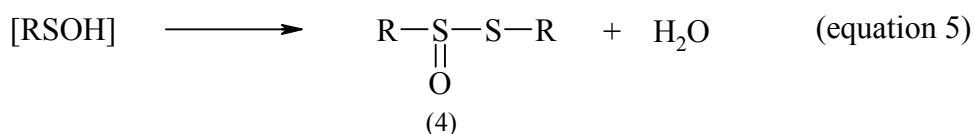
Thiosulfinate (4) could also disproportionate to form a thiolsulfonate and disulfide (equation 6).[8]

$$2\ R-\underset{\underset{O}{\|}}{S}-S-R \longrightarrow R-S-S-R + R-S-\underset{\underset{O}{\overset{O}{\|}}}{\overset{\|}{S}}-R \qquad \text{(equation 6)}$$

(4)
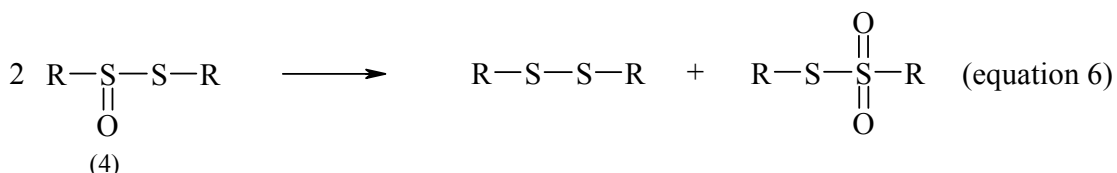
The thiosulfinate (4) or thiosulfonate could then form the sulfonyl chloride as already shown in **Figure 28**.

The final step involves the cyclisation of taurine sulfonyl chloride using Na_2CO_3 in EtOAc. The cyclisation step involves nucleophilic displacement of chloride. This intramolecular reaction is favourable and no polymerisation is observed.

The method used to synthesise *N*-aroylated-*β*-sultams was developed by Naveed Ahmed from a method originally described by Otto *et al.*[9] **Figure 29** shows a general mechanism where ethane *β*-sultam is used as a precursor to synthesise *N*-aroylated-*β*-sultams.

Synthesis of 2-aroyl-*β*-sultams
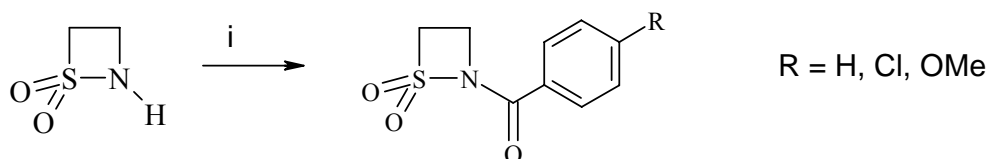
i. R-C$_6$H$_4$-COCl, DMAP, DCM, Et$_3$N, -78 °C - ambient 24 hours

Figure 29: Figure to show unsubstituted *β*-sultam converted to 2-aroyl-*β*-sultam.

Synthesis by this method involves the dissolving of the *β*-sultams in DCM at −78°C, followed by the dropwise addition of an acid chloride in the presence of DMAP, concluding with the dropwise addition of triethylamine to give the *N*-aroyl-*β*-sultam. The general mechanism using DMAP as the catalyst for the *N*-aroyl-*β*-sultams is shown in **Figure 30**. The DMAP speeds up the acylation step by several orders of magnitude.[10]
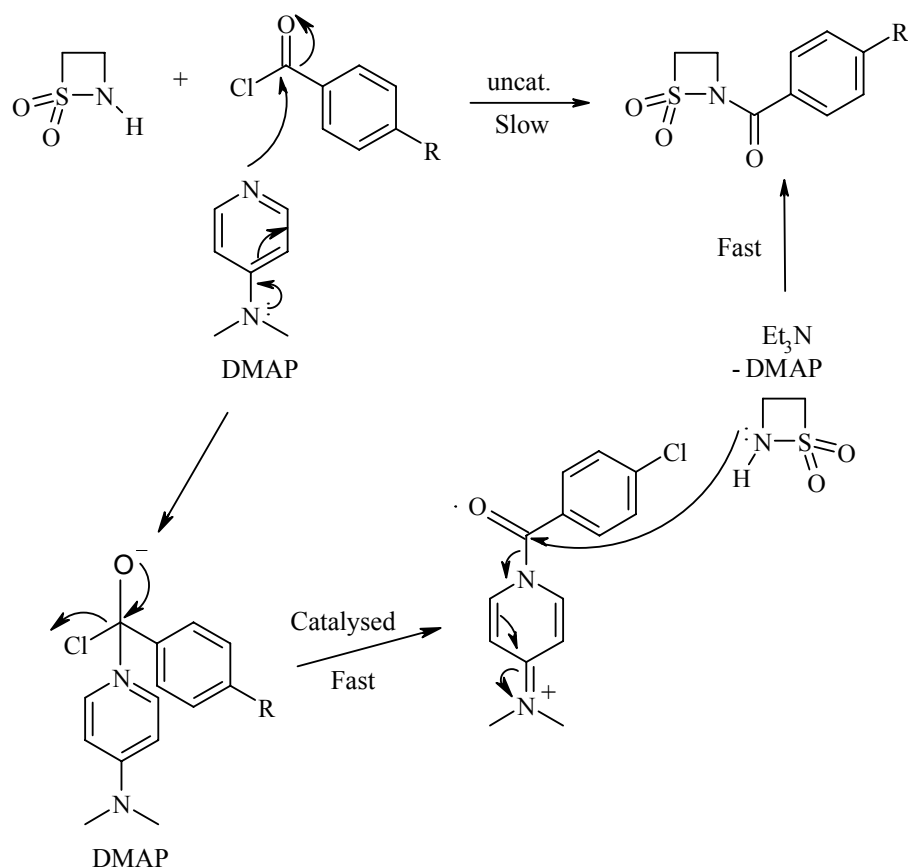
Figure 30: A general mechanism using DMAP as the catalyst for the *N*-acyl-*β*-sultams.

The *N*-aroylated-*β*-sultams have different substituents on the benzene ring. Although only three have been looked at in detail, synthesis of other *N*-aroyl and *N*-acylated-*β*-sultams is possible.

When considering the unsubstituted benzene ring all carbons are equivalent. However the addition of a new group onto the carbon changes the reactivity. Different substituents have mesomeric and resonance effects. The mesomeric effect is an electron redistribution that occurs via a pi-orbital. The mesomeric effect is M- negative for electron withdrawing substituents and M+ for electron releasing substituents. Chlorine and the NO_2 substituent are electron withdrawing. The methoxy and benzyl substituent are electron releasing.

The lone pair on the oxygen of the methoxy group can be incorporated into the ring making the phenyl ring electron rich. Conversely, chlorine withdraws charge from the ring leaving it electron deficient. These factors are to be considered when attempting to synthesise *N*-aroylated-*β*-sultams which contain a phenyl ring and more importantly need to be considered when looking at hydrolysis and hence reactivity.

As previously discussed, kinetic studies carried out at the University of Huddersfield have shown a structure–activity relationship between the enzyme and inhibitor (P99, R61 or PPE with the *N*-aroyl-*β*-sultam).[11] From the results obtained *N*-benzoyl-*β*-sultam appears to be the most potent inhibitor of porcine pancreatic elastase (PPE). X-ray crystal structures of PPE showed that the active site serine is sulfonylated.[12] *N*-benzoyl-*β*-sultam also inactivates the transpeptidase enzyme R61, via reaction at sulfur as shown in **Figure 31**.[12]
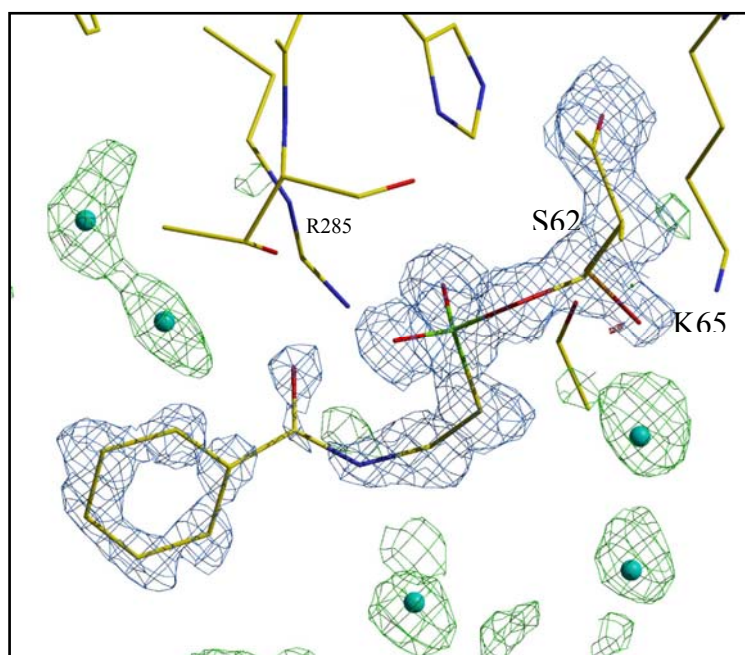
Figure 31: shows the serine residue (S62) covalently attached to the *N*-benzoyl-*β*-sultam at the sulphur and that the ring has opened via S-N fission.[12]

The hydrolysis studies carried out by Wing Tsang distinguished between S-N fission and (O=) C-N fission. ^{1}H-NMR studies showed that the alkaline

hydrolysis of the *N*-benzoyl-β-sultam occurred via S-N fission as a result of attack on the sulfur of the β-sultam ring. Thus previous studies can be seen to indicate that *N*-aroyl-β-sultams react with nucleophiles at sulfur (SO$_2$) and not at the exocyclic carbonyl, shown in **Figure 32**.
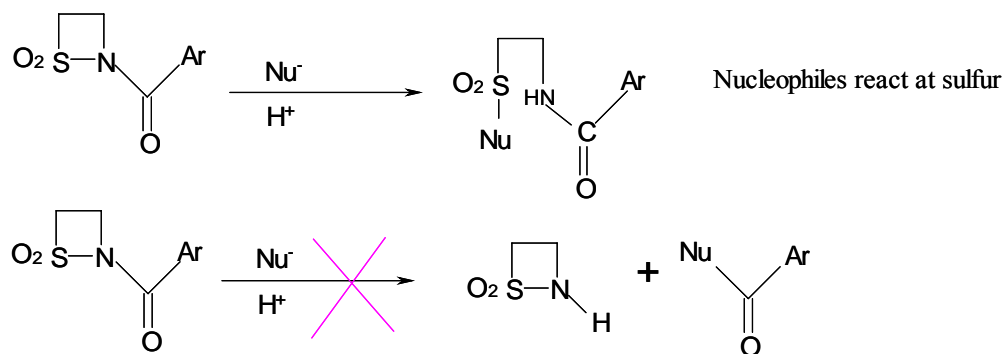
Figure 32: *N*-Aroyl-β-sultams react with nucleophiles at sulfur.

To further understand the stability, reactivity and mechanistic nature of the β-sultam and β-lactams in detail, calorimetric studies can be conducted to determine rates and enthalpies. In addition the unsubstituted β-sultam and β-lactam do not have chromophores, therefore traditional techniques for example, HPLC used at the University of Huddersfield, could not be used for previous studies. Calorimetry however, is not limited by the physical state or if the compound has a chromophore.

Calorimetry when combined with previous studies will provide useful data which can lead to potential medicinal compounds that can be used within the pharmaceutical industry. β-Sultams are good candidates to explore because of their possible inhibition of serine protease enzymes. Compounds containing sulfonamides are also well known for their wide range of biological activities as antibacterials[13] and peptidomimetic properties.[14, 15, 16]

When considering a successful inhibitor chemical reactivity is usually considered in terms of the electrophilic nature of the acyl centre and the leaving group ability of the group displaced. Increased chemical reactivity may lead to

a faster rate of reaction with the target enzyme but may also lead to greater hydrolytic and metabolic instability.[17] For this reason a study of chemical reactivity is also important.

A calorimetric study will follow. Where hydrolysis experiments were conducted under varying conditions in the solid state, varying RH, water/solvent mixtures and buffer controlled conditions. The calorimetric data will help to understand the stability, hydrolytic and mechanistic nature of these molecules. Some β-lactams have been studied previously by calorimetry, however there is no comparative study to date involving β-lactams and their sulfonyl analogues β-sultams. To understand the chemical reactivity and see how these compounds that are very similar in structure vary with regards to hydrolysis, ^{1}H-NMR can be used in conjunction with calorimetry. This will allow a detailed comparison to further understand and clarify what processes are occurring on a molecular level and to determine hydrolysis.

Calorimetric experimental methods and results will now be discussed in the following chapter.

References

1. N. Ahmed, PhD Thesis, University of Huddersfield, April, **2005**, 79.

2. A. Champseix, J. Chanet-Ray, A. Ettienne, A. Le Berre, J. Masson, C. Napierale, R. Vessiere, Syntheses de *β*-sultames (thiazetidines-1,2-dioxyde-1,1), *Bulletin de la Societe Chimique de France*, **1985**, 463-472.

3. G. Mielniczak, A. Łopusiński, Synthesis of 2-phosphoro-1,2-thiazetidine 1,1-dioxide, *Heteroatom Chemistry*, 10, (1), **1999**, 61-67.

4. G. Capozzi, G. Modena, In the chemistry of the thiol group, Edited S. Patai, John Wiley & Sons, New York, Part 2, **1974**.

5. L. Bateman, C.G. Moore, M. Porter, The reaction of sulphur and sulphur compounds with olefinic substances. Part XI. The mechanism of interaction of sulphur with mono-olefins and 1:5-dienes, *Journal of the Chemical Society,* **1958**, 2866-2879.

6. L. Di. Nunno, G. Modena, G. Scorrano, *Ricerca Scientifica*, 35, **1965**, 1423.

7. N. Kharasch, C.Y Meyers, The chemistry of organic sulfur compounds, Pergamon Press, Oxford; New York, **1961**, Chapter 32.

8. J.L. Kice, *Progress in Inorganic Chemistry*, 17, **1972**, 147.

9. D. Glasl, G. Rihs, H.H. Otto, Properties and reactions of substituted 1,2-thiazetidine 1,1-dioxides: synthesis of *N*-substituted 4,4-dimethyl-1,2-thiazetidin-3-one 1,1-dioxides, and a new base-catalyzed rearrangement to thiazolidin-4-one 1,1-dioxides, *Helvetica Chimica Acta*, 80, (3), **1997**, 671-683.

10. C.F. Gregory, Enantioselective nucleophilic catalysis with planar-chiral heterocycles, *Accounts of Chemical Research,* 33, (6), **2000**, 412-420.

11. M. Beardsell, P. S. Hinchliffe, J.M. Wood, R.C. Wilmouth, C.J. Schofield, M.I. Page, *β*-Sultams – A novel class of serine protease inhibitors, *Chemical Communications*, 5, **2001**, 497-498.

12. J. M. Wood, PhD Thesis, University of Huddersfield, **2001**, 70.

13. T.B. Vree, Y.A. Hekster Clinical pharmacokinetics of sulfonamides and their metabolites: an encyclopedia, *Antibiotics and Chemotherapy*, Basel; New York: Karger, 37, **1987**, 1-214.

14. C. Gennari, B. Salom, D. Potenza, A. Williams, Synthesis of sulfonamido-pseudopeptides: new chiral unnatural oligomers, *Angewandte Chemie. International Edited in English*, 33, (20), **1994**, 2067.

15. C. Gennari, H.P. Nestler, B. Salom, W.C. Still, Solid-phase synthesis of vinylogous sulfonyl peptides, *Angewandte Chemie. International Edited in English*, 34, (16), **1995**, 1763.

16. K.F. Ho, D.C.W. Fung, W.Y. Wong, W.H. Chan, A.W.M. Lee, Synthesis and Diels–Alder reactions of *α,β*-unsaturated-*γ*-sultams, *Tetrahedron Letters*, 42, (17), **2001**, 3121–3124.

17. N.O. Sykes, S.J.F. Macdonald, M.I. Page, Acylating agents as enzyme inhibitors and understanding their reactivity for drug design, *Journal of Medicinal Chemistry*, 45, (13), **2002**, 2850-2856.

3. Calorimetric studies of β-sultams

3.0 Calorimetry introduction

Calorimeters can observe all processes, chemical and physical which involve an exchange in heat energy to or from their surroundings.[1] Calorimetry is a non-specific technique, which will monitor and record all reactions that occur. There are many advantages that are associated with isothermal microcalorimetry, for example, compounds without a chromophore can be studied, and only small amounts of compound are required to observe a significant output.

All experimental data obtained must be validated and it is therefore important to initially discuss the imidazole catalysed hydrolysis of triacetin which is a universal test reaction system for the validation of isothermal heat conduction calorimeters.[2] This reaction is suitable for the following reasons: it is simple to perform, robust in operation, it requires readily available cheap materials and it is applicable to a range of commercially available calorimeters. The experiment is conducted at 298K, 0.267 g triacetin is added to 5 mL deionised water. Triacetin is not readily soluble so thorough mixing is required. A buffer solution is made up consisting of 1.6 g acetic acid, 2.72 g imidazole and 10 mL deionised water. 3 mL glass ampoules supplied from Thermometric are used to conduct the experiment. The time is noted at the time of addition of buffer to triacetin, time = 0. The values obtained for the reaction rate, k_R, and the enthalpy of reaction, $\Delta_R H$, are: $k_R = 2.80 \pm 0.10 \times 10^{-6}$ dm^3 mol^{-1} s^{-1}, $\Delta_R H = -91.7 \pm 3.0$ kJmol^{-1}. These values are used to validate reaction systems for any given calorimeter, and such a test reaction will be discussed later.

Previous calorimetric research using the Thermal Activity Monitor (TAM) has been conducted within the pharmaceutical, chemical and life science industries. [3] [4, 5] Examples in the pharmaceutical industry include degradation,[6] drug excipient compatibility[7] and dissolution studies.[8]

Within the biosciences field the TAM system has been used to measure complex metabolic processes, as well as the effects of pollutants on ecological systems.[9] The TAM has been used extensively in this work to study the

hydrolysis of β-sultams and β-lactams. Experimental procedures will now follow.

3.1 TAM experimental

(All reagents were supplied from Aldrich and were used without further purification. Solution state sample spectra were obtained using a Jeol ECA, 500 MHz FT-NMR spectrometer. The Mettler Toledo pH Meter was used to monitor the pH before and after solutions were made up. The isothermal microcalorimeter TAM 2277 was used to conduct all calorimetric experiments).

Initial experiments were conducted on compounds A, B, C and D (**Figure 33**) in the solid state at 298K, 310K and 313K. Further experiments were conducted at different relative humidities, in solution using water and acetonitrile, controlling pH and ionic strength. A fifth compound (F) was also investigated in later studies. For all calorimetric experiments 3 mL glass ampoules were used and supplied from Thermometric Ltd. Each separate experimental protocol will now be detailed. The concentration used in the following experiments was the concentration of β-sultam and acetonitrile and not the final concentration.

A   B   C

D
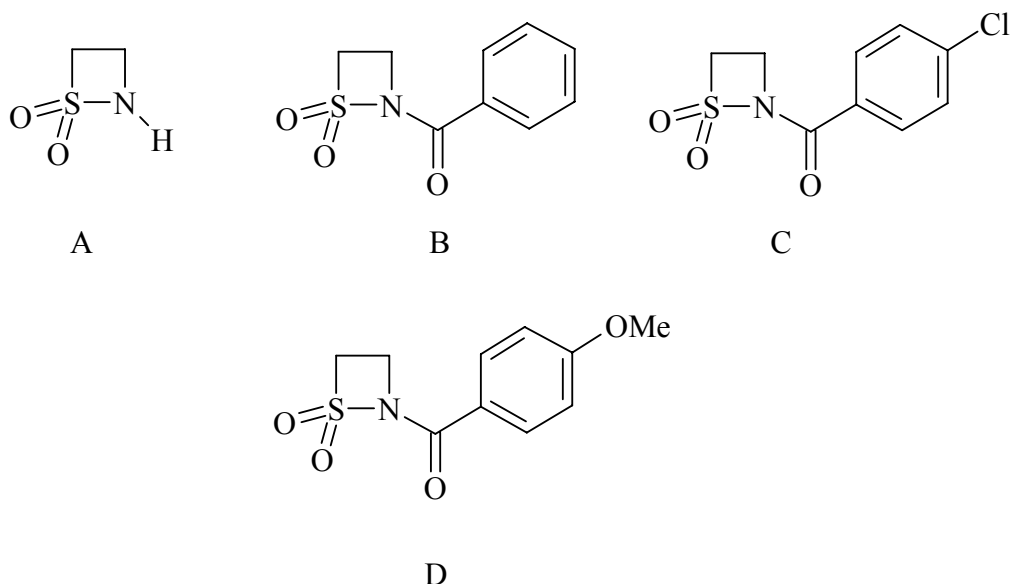
Figure 33: β-sultams used to conduct hydrolysis experiments.

3.1.1 Calibration of a calorimetric unit.

Prior to experimentation, calibration of the calorimetric unit was routinely undertaken. Calibration of a calorimetric unit required two glass ampoules containing identical material i.e. water, solvent or empty. The ampoules were loaded onto the calorimeter at the equilibrium position and left to equilibrate for approximately 40 minutes. The ampoules were then lowered further into the sample and reference chambers, during which a slight disruption was observed to the data which was a direct result of frictional heat. The ampoules were left for a further 50-60 minutes to achieve a stable baseline. The base line should have read 0.00, in those cases where the base line did not; it was adjusted via the amplifier. Once a stable base line was achieved the electrical calibration was switched on. The calibration signal was then adjusted to the required thermal power. Once the calibration signal was corrected and plateau was observed, the calibration was switched off. The signal was left to decay back to zero until a stable baseline was observed again. A typical calorimetric calibration curve is shown in **Figure 34**.

Figure 34: A typical calorimetric output from an electrical calibration.

3.1.2 Test and reference reaction: Imidazole catalysed hydrolysis of triacetin.

The reaction was conducted in a pH 7 buffer solution. Buffer solution: 1.6 g acetic acid was added to 2.72 g of imidazole and made up to 10.0 mL with

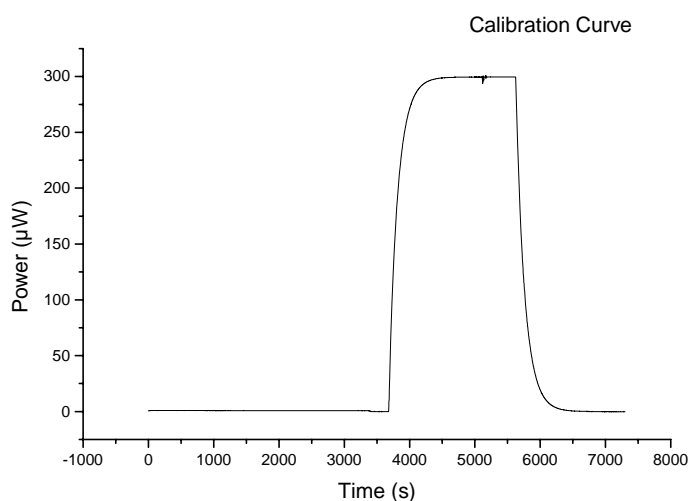deionised water. The reaction solution consisting of 0.267 g triacetin was made up to 5.0 mL with buffer solution, which was shaken to obtain a homogeneous mixture. Addition of buffer (2 mL) to triacetin (1mL) was monitored using a stopwatch. This is the time zero (t=0) for the reaction. The reference ampoule was filled with 3.0 mL of buffer. Both ampoules were lowered carefully at 298K and left to thermally equilibrate for 45 minutes -1 hour. They were then lowered carefully to minimise any thermal shock. Once lowered, data was collected via Digitam^{TM}.

3.1.3   Solid state hydrolysis of β-sultams A, B, C and D at 298K, 310K, 323K.

For solid state experiments at 298K, 310K and 313K, an empty glass ampoule was hermetically crimp-sealed to be used as the reference. β-sultam A, B, C or D (20.0 mg) was transferred to a 3 mL glass ampoule and the sample ampoule was hermetically crimp-sealed. The reference and sample ampoules were then placed into the calorimeter and left to thermally equilibrate for 40 minutes in the load position prior to being lowered over a one minute period to the measurement position, at this point data was collected. These experiments were repeated several times to ensure accuracy, validity and reliability was achieved.

3.1.4   Solid state study of β-sultams A, B, C and D, varying relative humidity (RH) at 310K.

Two different RH experiments were conducted at 310K, 7% RH (NaOH) and 75% RH (NaCl), using β-sultams A, B, C, and D. An empty glass ampoule containing a small vial with the desired saturated salt solution in it was hermetically crimp-sealed to be used as the reference. The reaction ampoule contained a small vial of the same saturated salt solution together with β-sultam A, B, C or D (10 mg). Experiments were also attempted with 20 mg. The reference and sample ampoules were then placed into the calorimeter and left to thermally equilibrate for 40 minutes in the load position prior to being lowered over a one minute period to the measurement position, at this point data was

collected. These experiments were repeated several times to ensure accuracy, validity and reliability was achieved.

3.1.5 Hydrolysis of β-sultams A, B, C and D at 298K in aqueous solution, pH 7 (water and acetonitrile).

For hydrolysis experiments at pH 7 (sodium hydroxide or hydrochloric acid was added to obtain pH 7) and at 298K a variation of sample weight (40 mg or 20 mg) and solution volumes were used to determine the feasibility of the experiments. The various volumes used for the reference were 2.0 mL or 2.5 mL acetonitrile and 1.0 mL or 0.5 mL water at pH 7. For example, 2.0 mL acetonitrile was used with 1.0 mL water to make 3.0 mL. The desired volumes were transferred to a 3.0 mL glass ampoule and hermetically crimp-sealed to be used as a reference.

The point of solvent/compound mixing with water was recorded as the start time of the reaction. The sample ampoule was hermetically crimp-sealed. The reference and sample ampoules were placed into the calorimeter and left to thermally equilibrate for 40 minutes in the load position prior to being lowered over a one minute period to the measurement position, at which point data recording began. These experiments were repeated several times to ensure accuracy, validity and reliability was achieved.

3.1.6 Hydrolysis of β-sultams A, B, C and D at 298K in aqueous solution (controlled ionic strength, pH 4 at 0.02M).

The reaction was conducted at 298K and pH 4.0. The buffer solution consisted of 0.49 g potassium acetate and 3.35 g potassium chloride, which was added to 50.0 mL distilled water and shaken vigorously 60 times to ensure thorough mixing. HCl was added to obtain pH 4.0 using a pH meter. The β-sultam was mixed with acetonitrile to make a 0.02M solution. The reference ampoule was filled with 2.0 mL of buffer and 1.0 mL solvent. The reaction ampoule was filled with 2.0 mL buffer, 1.0 mL of the desired β-sultam solution and

hermetically crimp-sealed. Both ampoules were lowered into the calorimeter and left to thermally equilibrate for 40 minutes in the load position prior to being lowered over a one minute period to the measurement position, at which point data recording began. These experiments were repeated several times to ensure accuracy, validity and reliability was achieved.

3.1.7 Hydrolysis of β-sultams A, B, C and D at 298K, 310K, 323K in aqueous solution (controlled ionic strength, pH 4 at 0.008M).

The same method was used for the next set of experiments which were conducted at temperatures 298K, 310K and 323K at 0.008M. The buffer solution consisted of 0.49 g potassium acetate and 3.35 g potassium chloride, which was added to 50.0 mL distilled water and shaken vigorously 60 times to ensure thorough mixing. HCl was added to obtain pH 4.0 using a pH meter. The β-sultam was mixed with acetonitrile to make a 0.008M solution. The reference ampoule was filled with 2.0 mL of buffer and 1.0 mL solvent. The reaction ampoule was filled with 2.0 mL buffer and 1.0 mL of the desired β-sultam solution and hermetically crimp-sealed. Both ampoules were lowered into the calorimeter and left to thermally equilibrate for 40 minutes in the load position prior to being lowered over a one minute period to the measurement position, at which point data recording began. These experiments were repeated several times to ensure accuracy, validity and reliability was achieved.

3.1.8 Hydrolysis of β-sultams A, B, C and D at 298K in aqueous solution (controlled ionic strength, pH 8 at 0.008M).

The reaction was conducted at pH 8.0. The buffer solution consisted of 0.6 g sodium dihydrogen phosphate and 2.26 g potassium chloride which was added to 50.0 mL distilled water and shaken vigorously to ensure thorough mixing. HCl was added to obtain pH 8.0 using a pH meter. The β-sultam was mixed with acetonitrile to make a 0.008M solution. The reference ampoule was filled with 2.0 mL of buffer and 1.0 mL solvent and hermetically crimp-sealed. The reaction ampoule was filled with 2.0 mL buffer, 1.0 mL of the β-sultam

solution and hermetically crimp-sealed. Both ampoules were lowered into the calorimeter and left to thermally equilibrate for 40 minutes in the load position prior to being lowered over a one minute period to the measurement position, at which point data recording began. These experiments were repeated several times to ensure accuracy, validity and reliability was achieved.

3.1.9 Hydrolysis of β-sultam F at 298K in aqueous solution (controlled ionic strength, pH 8 and pH 4 at 0.008M).

Experiments were conducted at pH 4.0 and pH 8.0. The buffer solution for pH 8.0 consisted of 0.6 g sodium dihydrogen phosphate and 2.26 g potassium chloride which was added to 50.0 mL distilled water and shaken vigorously to ensure thorough mixing. HCl was added to obtain pH 8.0 using a pH meter. The buffer solution for pH 4.0 consisted of 0.49 g potassium acetate and 3.35 g potassium chloride which was added to 50.0 mL distilled water and shaken vigorously to ensure thorough mixing. HCl was added to obtain pH 4.0 using a pH meter. A 0.008M solution of β-sultam in acetonitrile was used for all experiments. The reference ampoule was filled with 2.0 mL of buffer and 1.0 mL solvent and hermetically crimp-sealed. The reaction ampoule was filled with 2.0 mL buffer and 1.0 mL of the β-sultam solution and hermetically crimp-sealed, both ampoules were lowered into the calorimeter and left to thermally equilibrate for 40 minutes in the load position prior to being lowered over a one minute period to the measurement position, at which point data recording began.

3.2 Data Analysis

Kinetic and thermodynamic parameters can be determined from calorimetric outputs. Kinetics is the study of the rates of chemical processes. The relationship between rate and concentration which can be expressed mathematically in the form of an equation called a rate law, rate varies with time and concentration.

Reactions are found to have rate laws of the form;

$$r = k\,[A]^a\,[B]^b \qquad\qquad \textbf{Equation 7}$$

Where k is a constant, the power a is the order with respect to A and b is the order with respect to B. The first order rate law is one in which the rate is proportional to the concentration of A raised to the power 1. First order rates constants have units of time^{-1}.

$$r = k_{1st}\,[A]^1 \qquad\qquad \textbf{Equation 8}$$

A second order reaction has the concentration raised to the power of 2. The units are conc^{-1} and time^{-1}.

$$r = k_{2nd}[A]^2 \qquad\qquad \textbf{Equation 9}$$

First order reactions have their rate dependent on only one reactant species, i.e.

$$A \rightarrow \text{Products}$$

$$\text{Rate at which A converts to products} \quad = -\frac{\delta A}{\delta t} = k[A]$$

$$k\delta t = -\frac{\delta[A]}{[A]} \qquad\qquad \textbf{Equation 10}$$

If $[A]_0$ is the concentration when $t = 0$ (t_0) and $[A]'$ is the concentration at t' then

$$\int_{t_0}^{t'} k\,dt = -\int_{[A]_0}^{[A]'} d\,([A]'/[A]_0) \qquad \textbf{Equation 11}$$

Then

$$kt = \ln \frac{[A]_0}{[A]'}$$

$$-kt = \ln \frac{[A]'}{[A]_0}$$

$$e^{(-kt)} = \frac{[A]'}{[A]_0}$$

$$[A]' = [A]_0 e^{-kt}$$

$$\ln[A] = -kt + \ln[A]_0 \qquad \textbf{Equation 12}$$

This equation is equivalent to the general form y = mx + c, i.e. a straight line with a gradient equal to the negative of the rate constant, k. Calorimetric outputs yield a plot of power (Φ) with time (t). For a standard calorimetric analysis the output observed at any time point during the experiment is proportional to the quantity of material available to react (n) and the change in enthalpy for the process (ΔH) i.e. number of moles reacted multiplied by the enthalpy per mole. This assumes over the concentration range studied the mechanism for the process remains constant. A general calorimetric relationship can therefore be written as

$$\text{Calorimetric output} = \Phi \propto n \, . \, \Delta H \qquad \textbf{Equation 13}$$

Therefore, the calorimetric output is proportional to the quantity of reactable material, i.e. $\Phi \, \alpha \, n$. This allows calorimetric power outputs to be analysed using standard first order mathematical models as outlined previously, i.e.

$$\ln \Phi = -kt + \ln\Phi_0 \qquad \textbf{Equation 14}$$

Therefore, assuming the reaction to be first order leads to a linear plot of ln (power) with time, thus establishing the associated rate constant, k. In addition, the change in enthalpy can also be determined from identifying the linear intercept (Φ_0), and applying Equation

$$\Delta H = \frac{\Phi_o \times 10^{-6}}{-k \times A^n} \qquad \textbf{Equation 15}$$

Equation 15 was used to determine ΔH. Where Φ_o (dq/dt) is the intercept, -k is the slope, A the number of moles and n the order of reaction.
Equation 15 was derived from **Equation 16**.[10]

$$\left(\frac{dq}{dt}\right) = kHA^n \qquad \textbf{Equation 16}$$

This theory can only be applied to experimental data based on two assumptions, firstly, the reaction is first order (confirmed by the linearity of the resultant logarithmic graph) and secondly the total power output is a true reflection of the total enthalpy change.

Graphs were plotted using Microcal Origin 7.0.

1. Data was imported from Digitam™ which is connected to the calorimeter.
2. The data is imported as a single ASCII file into Microcal origin.
3. Columns A and B were copied into a new spreadsheet.
4. Column values were set (A) col(A) + (time s). It is important to note that the equilibration time plus time of mixing was included. The time it took to mix

the solutions and lower them into the calorimeter was recorded and added to the equilibration time.

5. Column values were set for (B), ln (col(B)) (first order) or 1/(col(B)) (second order)

6. Columns A and B were highlighted and a line graph was plotted. Data was selected after 3600s. This is the time taken for the calorimeter to settle. When ampoules are lowered the initial thermal disruption interferes with the calorimetric signal and this time interference is not included in the analysis.

7. The double arrow option was selected to highlight the area of analysis.

Error values were calculated using the T- test statistics analytical method. The table below is used to calculate errors using the T-test.

Degrees of freedom (n-1)	T Value Confidence Interval	
	90 %	95%
1	6.314	12.706
2	2.920	4.303
3	2.353	3.182
4	2.132	2.776
5	2.015	2.571
10	1.812	2.228
15	1.753	2.132
20	1.725	2.086
30	1.697	2.042
60	1.671	2.000
Infinite	1.645	1.960

Table 3: T-test method

The t-table value depends on the sample size you have used to estimate the standard deviation. n-1 refers to the degrees of freedom.[9] A 95% confidence limit was used in this thesis.

Results and Discussion

3.3 Test and reference reaction: Imidazole catalysed hydrolysis of triacetin.
The imidazole catalysed hydrolysis of triacetin is a test reaction for isothermal heat conduction calorimeters. Calorimetric data was obtained and analysed using MicroCal origin. The following method was used to analyse the data. The data was imported and a line graph plotted, using power (μW) against time (s). A non linear curved fit was plotted.

$$\frac{dq}{dt} = -\Delta HVk \left(\frac{[A_0]}{1 + [A_0]\, kt} \right)^2 \qquad \textbf{Equation 17}$$

$\frac{dq}{dt}$ = thermal power

k = reaction rate constant

ΔH = reaction enthalpy change

$\left[A_0 \right]$ = initial concentration of triacetin

t = time

V = volume of solution placed into ampoule

2 = in the fitting procedure the order is fixed as two.

The equation is part of the MicoCal origin data software package. A typical calorimetric output is shown in **Figure 35**.
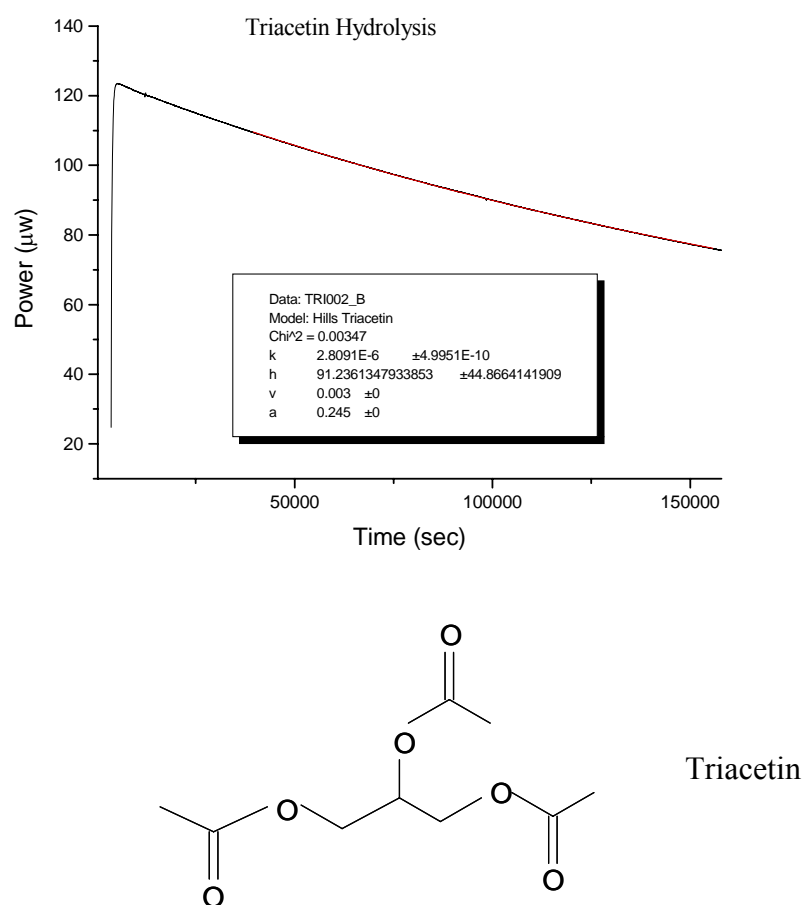
Figure 35: An example of a typical calorimetric output for the imidazole catalysed hydrolysis of triacetin (see structure above) at 298K .

The imidazole catalysed hydrolysis of triacetin is second order. **Figure 35** shows a calorimetric output where **Equation 17** was fitted too. All parameters derived from the Microcal Origin package are in line with those results published.[2] For example S. Gaisford, R.A. Lane and G. Buckton (London School of pharmacy) published the following results.

	$\begin{bmatrix} A_0 \end{bmatrix}$ (mol dm^{-3})	V (dm^3)	ΔH° (kJ mol^{-1})	k (dm^3 mol^{-1} s^{-1})
London School of Pharmacy	0.245 0.245 0.245	0.0030 0.0030 0.0030	-89.39 -96.20 -91.40	2.98 x 10^{-6} 2.61 x 10^{-6} 2.83 x 10^{-6}
University of Greenwich (Summia)	0.245	0.0030	-91.23	2.80 x 10^{-6}

Table 4: Imidazole catalysed hydrolysis of triacetin compared to results obtained at the London School of Pharmacy.

3.3.1 Solid state studies at 298K, 310K and 323K, for β-sultams A-D.

Solid state experiments were conducted at 298K, 310K and 323K; rate constants and enthalpies are reported in **Table 5** and **Table 6**. Results were inconclusive for compound C and D at 298K, D at 310K and B, C and D at 323K, which will be discussed later.

Data were analysed after 5000 seconds, the data before this reflects the disruption caused to the power output upon lowering the ampoules. Data analysis ceased after the reaction had reached completion, the calorimetric output had reached zero or when the signal was too close to the base line. All experiments discussed in this section are first order degradation reactions.

298K solid state	A	B
$t_{1/2}$ (s)	25600	8250
Rate constant (s^{-1})	2.64×10^{-5}	8.20×10^{-5}
	2.53×10^{-5}	8.88×10^{-5}
	2.97×10^{-5}	8.36×10^{-5}
	2.73×10^{-5}	8.01×10^{-5}
Average	2.7×10^{-5} ($\pm 0.6 \times 10^{-5}$)	8.4×10^{-5} ($\pm 1.2 \times 10^{-5}$)
$\Delta H°$ (298K) (kJmol^{-1})	-4.23	- 6.19
	-4.02	- 8.33
	-3.78	- 8.97
	-3.56	- 9.81
Average	-3.9 ($\pm$ 0.9)	- 8.3 ($\pm$ 4.9)

Table 5: A summary of the data obtained for compounds A and B at 298K.

| 310K solid state	A	B	C
$t_{1/2}$ (s)	40760	4330	5330
Rate constant (s^{-1})	1.76×10^{-5}	1.75×10^{-4}	1.25×10^{-4}
	1.68×10^{-5}	1.53×10^{-4}	1.29×10^{-4}
	1.70×10^{-5}	1.50×10^{-4}	1.28×10^{-4}
	1.55×10^{-5}	1.43×10^{-4}	1.29×10^{-4}
Average	1.7×10^{-5} ($\pm 0.3 \times 10^{-5}$)	1.6×10^{-4} ($\pm 0.4 \times 10^{-4}$)	1.3×10^{-4} ($\pm 0.06 \times 10^{-4}$)
$\Delta H°$(310K)(kJmol^{-1})	- 1.91	- 11.44	- 4.38
	- 2.60	- 12.69	- 4.56
	- 1.93	- 12.56	- 5.19
	- 3.47	- 14.51	- 6.03
Average	- 2.5 ($\pm$ 2.3)	- 12.8 ($\pm$ 4.0)	- 5.0 ($\pm$ 2.4)

Table 6: A summary of the data obtained for compounds A, B, and C in their solid state at temperature 310K.

β-sultam A was investigated at a third temperature see **Table 7**.

323K solid state	A
$t_{1/2}$ (s)	17770
Rate constant (s^{-1})	4.06×10^{-5}
	3.86×10^{-5}
	3.61×10^{-5}
	3.89×10^{-5}
Average	3.9×10^{-5} ($\pm$ 0.6×10^{-5})
$\Delta H°$ (323K)(kJmol^{-1})	- 24.63
	- 21.63
	- 27.88
	- 21.41
Average	- 23.9 ($\pm$ 9.6)

Table 7: Compound A in the solid state at 323K.

Example graphs will now follow for compound A at 298K, 310K and 323K. β-sultam B at 298K and 310K and compound C at 310K, followed by a discussion of the data. Exothermic signals were observed and a typical example is shown in **Figure 36** where the natural logarithm of the power output (μW) was plotted against time (s).
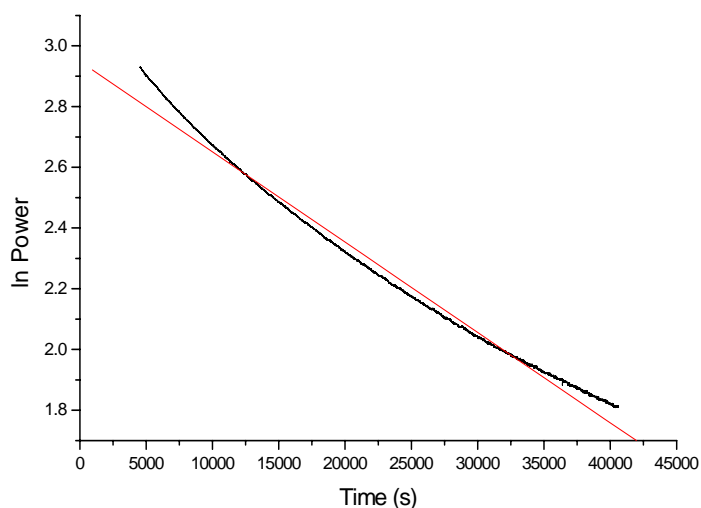
Slope = -2.97 x 10^{-5}, intercept = 2.94, R^2 = 0.994.

Figure 36: An example of a typical calorimetric output at 298K for β-sultam A in the solid state.
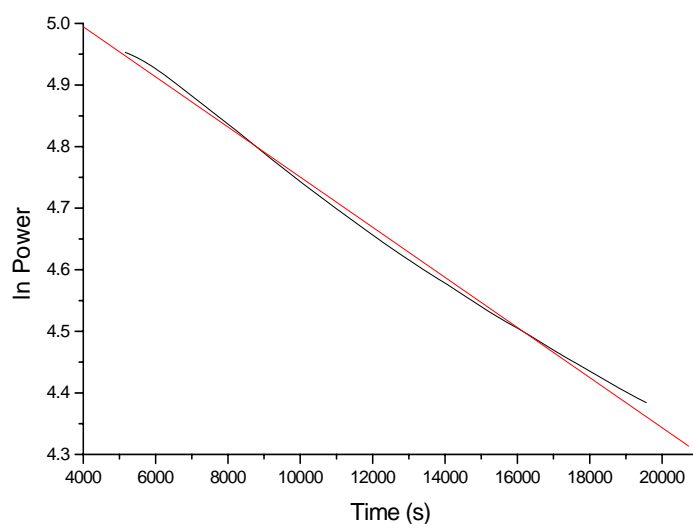
The data was analysed from 5000s – 40000s and over 1.5 half lives. For the best linear fit, the rate constant was 2.97 x $10^{-5}s^{-1}$ and ΔH was -3.78 kJmol^{-1}. β-sultam A was also analysed at 310K, as shown in **Figure 37**.
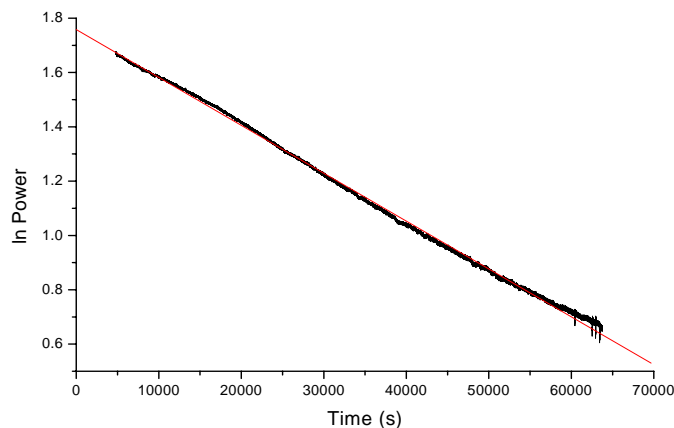
Slope = -1.76 x 10^{-5}, intercept = 1.75, R^2 = 0.999.

Figure 37: An example of a typical calorimetric output at 310K for β-sultam A in the solid state.

The data was analysed from 5000s – 63000s and over 1.5 half lives. The rate constant was 1.76 x $10^{-5}s^{-1}$ and ΔH was -1.91 kJmol^{-1} for this experiment. β-sultam A was also analysed at 323K, as shown in **Figure 38**.

Slope = -4.06 x 10^{-5}, intercept = 5.15, R^2 = 0.998.

Figure 38: An example of a typical calorimetric output at 323K for β-sultam A in the solid state.

The data was analysed from 5000s – 19000s over 1.5 half lives. The rate constant for this example was 4.06 x $10^{-5}s^{-1}$ and ΔH was -24.63 kJmol^{-1}.

For β-sultam B at 298K and 310K exothermic signals were observed (**Figures 39 and 40**) and the natural logarithm of power output (μW) was plotted against time (s) to determine the associated rate constant and enthalpy change.
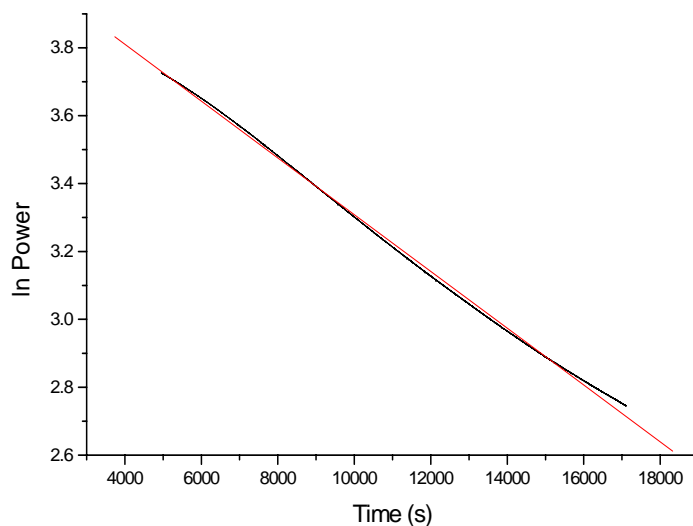
Slope = -8.36 x 10^{-5}, intercept = 4.14, R^2 = 0.999.

Figure 39: An example of a typical calorimetric output at 298K for β-sultam B in the solid state.

It can be seen from the example in **Figure 39** that the relationship between the natural logarithm of the power output and time is linear. The data was analysed from 5000s – 17000s and over 2 half lives. The rate constant of hydrolysis was 8.36 x $10^{-5}s^{-1}$ and ΔH was -8.97 kJmol^{-1}. As show in **Figure 40** β-sultam B was also studied at 310K.
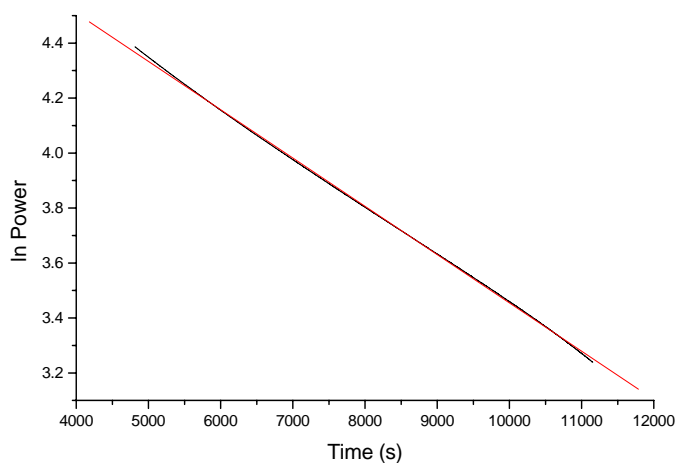
Slope = -1.75 x 10^{-4}, intercept = 5.21, R^2 = 0.999.

Figure 40: An example of a typical calorimetric output at 310K for β-sultam B in the solid state.

The data at 310K (**Figure 40**) was analysed from 5000s – 11000s and over 2.5 half life. The rate constant was 1.75 x $10^{-4}s^{-1}$ and ΔH was -11.44 kJmol^{-1}. For β-sultam C at 310K an exothermic signal was observed (**Figure 41**). The natural logarithm of power (μW) was plotted against time (s).
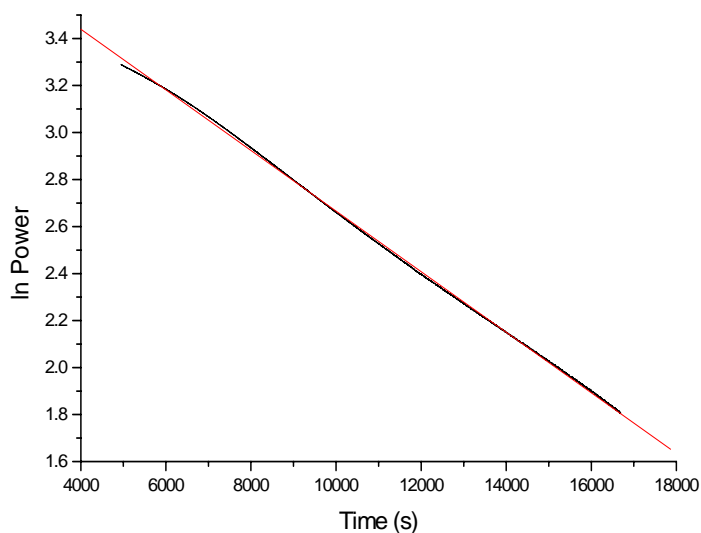
Slope = -1.28 x 10^{-4}, intercept = 3.95, R^2 = 0.999.

Figure 41: An example of a typical calorimetric output at 310K for β-sultam C in the solid state.

The data was analysed from 5000s – 16000s and over 3 half life. The rate constant of degradation was 1.28 x $10^{-4}s^{-1}$ and ΔH was -5.19 kJmol^{-1}.

3.3.2 Discussion of solid state studies at 298K, 310K, and 323K.

Table 5 and **Table 6** demonstrate that a change in substituents affects the rate constant and enthalpy. Although full solid state data sets are not reported, rates of hydrolysis were observed in the solid state. At 298K β-sultam A hydrolysed slower than β-sultam B. At 310K the general trend in rate of reaction witnessed is as follows; A> C > B. β-Sultam C has a chlorine substituent attached to the phenyl ring which has an electron withdrawing effect, removing electron density from the aromatic system. β-Sultam B rates of hydrolysis were compared to β-sultam C and were similar. The unsubstituted β-sultam A hydrolysed the slowest when compared to the substituted β-sultams B and C, the stability of β-sultam A allowed further experiments to be conducted at 323K. No calorimetric outputs were observed when β-sultam D was subjected to these experiments.

The rate constants for both the benzoyl and chlorobenzoyl compounds (B and C) display a ten-fold increase when compared to the unsubstituted β-sultam (compound A). For the methoxybenzoyl substituent (D), it was not possible to establish reproducible data. With respect to the associated change in enthalpy, β-sultam A provided the smallest enthalpy change, followed by a two-fold increase for β-sultam C and a more significant increase of approximately 10 kJmol^{-1} for β-sultam B. Again, β-sultam D did not provide reproducible data thus no enthalpic results can be reported. Although full data sets are not reported hydrolysis was observed. There was no real correlation between rates of hydrolysis and the electronic effect of the substituent. The solid state experiments provided a platform for further calorimetric studies, which are discussed later in this chapter.

The β-sultams are heat and moisture sensitive, during synthesis they were kept dry under nitrogen, and after synthesis they were stored under nitrogen at 273K to prevent hydrolysis. The conditions the β-sultams were exposed to in the calorimeter were atmospheric conditions, under which they are known to degrade.

The calorimetric outputs for β-sultam D and C at 298K, D at 310K and B, C and D at 323K were too complex to analyse. The relationship between the natural logarithm of the power output and time did not give a linear fit and the signal observed was endothermic followed by exothermic. **Figure 42** shows a typical complex calorimetric example output.
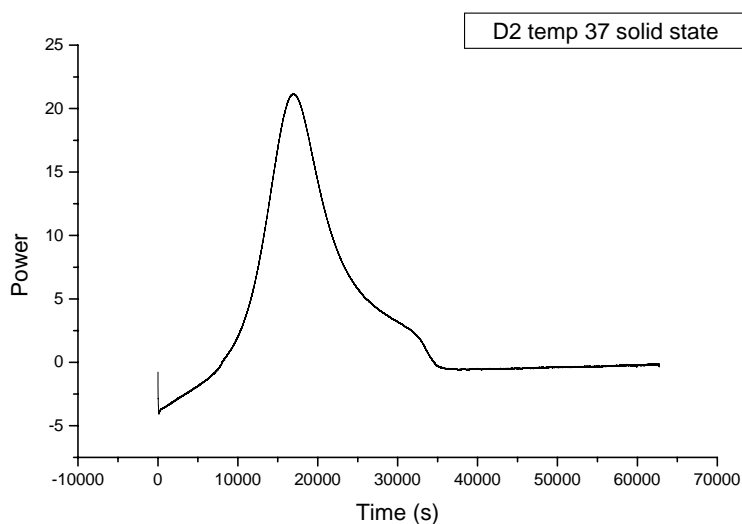

Figure 42: An example of a typical calorimetric output for β-sultam D at 310K in the solid state.

Solid state calorimetry, as discussed previously, can be extremely useful within the pharmaceutical industry, for example, to determine physical and chemical stability. However, there are advantages and disadvantages associated with solid state isothermal microcalorimetry (IMC). The typical calorimetric outputs that can be seen for β-sultam C and D at 298K involve more than one step, and there are several different reasons why more than one process was occurring. This may seem to be a disadvantage but is in fact one of the advantages of using IMC in that it is sensitive enough to monitor more than one process. The possible processes and advantages using this technique have been highlighted previously.

Previous IMC solid state studies conducted have shown that more than one process may be occurring with several factors contributing to the complex calorimetric outputs observed. For example, during the oxidation of ascorbic

acid by Angberg *et al*., a mechanistic change was observed after only 1.5 hours.[11] Although the mechanism was considered to be first order, the rate constant changed by almost two orders of magnitude. The rate change would have been missed using conventional methods; however the sensitivity of the calorimeter observed this.

Other previous research reported observing similar phenomena during the pharmaceutical processing of crystalline drugs. The ability to detect and quantify the amount of amorphous material within a highly crystalline drug is important when considering a solid dosage form. Processing operations such as milling,[12] spray drying,[13] mixing[14] and lypophilization[15] can cause disruption or activation to the crystal structure, leading to various degrees of disorder. Briggner *et al*.[16] used isothermal microcalorimetry to study changes in the crystallinity of spray dried and micronized lactose monohydrate. This study used a humidity chamber, where the sample was placed in an ampoule under conditions that allow the transition to the thermodynamically stable crystalline state to occur. Saturated salt solutions were used to generate humidities between 53% and 85% RH. The absorbed water behaved as a plasticizer to lower the glass transition temperature of the amorphous lactose below the experimental temperature (298K), at which point recrystallisation occurred. The response is shown in **Figure 43**.
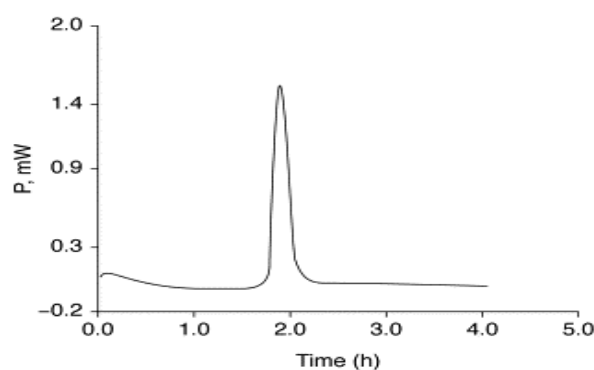

Figure 43: Typical microcalorimetric output for spray-dried lactose (20 mg powder, 85% RH, 25°C).[17]

The initial response is thought to be caused by a slight imbalance in the generation of water vapour or the amorphous material undergoing structural collapse followed by absorption of water (endothermic). At hour two there is a

sharp response from the recrystallisation process or sorption of water vapour onto the powder (exothermic).[17] The calorimetric output for the compounds that were too complex to analyse may have been a result of a combination of these factors as well as hydrolysis.

3.3.3 ^{1}H NMR of solid state study

In order to verify that the calorimetric observations were a reflection of hydrolysis, samples were analysed prior to and immediately after TAM experimentation. Thin Layer Chromatography (TLC) was conducted throughout the synthesis, before and after calorimetric studies. Samples analysed prior to calorimetric investigations provided evidence for intact β-sultam and after experimentation showed the classic β-amino sulfonic product of hydrolysis.

To further validate hydrolysis, ^{1}H NMR experiments were conducted. The β-sultam structure used for ^{1}H NMR analysis is shown in **Figure 44**. Examples of ^{1}H NMR spectra for β-sultam B are shown before and after hydrolysis in the solid state. **Figures 45** and **46** show ^{1}H NMR for the intact β-sultam and hydrolysed β-sultam.
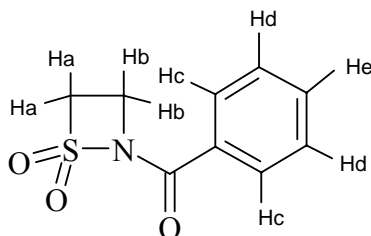

Figure 44: β-sultam structure used for ^{1}HNMR analysis.

Chemical shift ppm
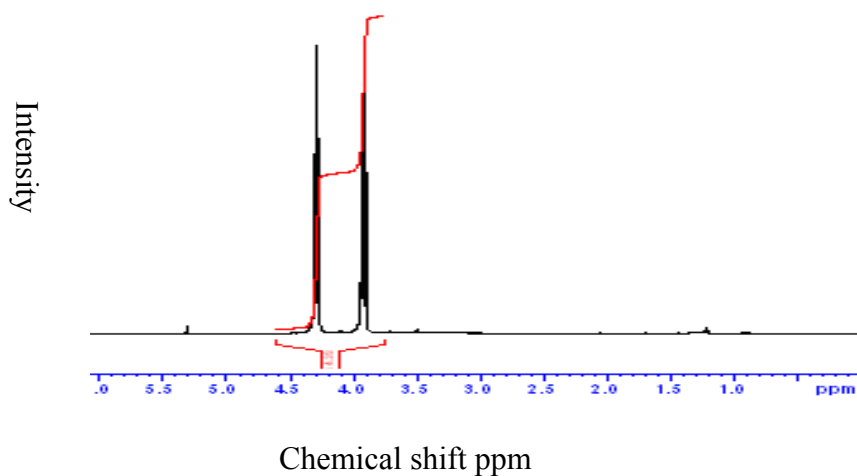
Figure 45: ^{1}H NMR spectrum before hydrolysis experiment at 298K for β-sultam B.
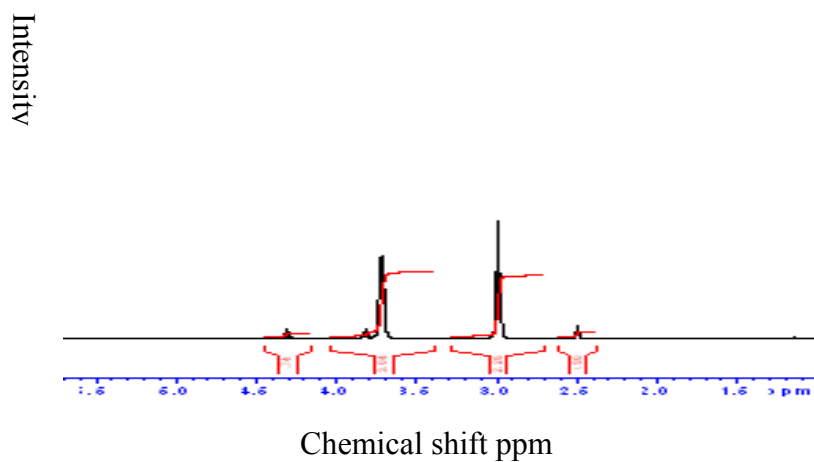

Chemical shift ppm

Figure 46: ^{1}H NMR spectrum after hydrolysis experiment at 298K for β-sultam B.

The ^{1}H NMR for intact β-sultam B shows that the Ha/Hb hydrogens resonate as triplets at CH_2-SO_2 3.90 ppm and CH_2-NR 4.30 ppm. The Hc/Hd hydrogens resonate further down field, and the Hc hydrogens are closest to the

electronegative carbonyl group which moves the chemical shift for these hydrogens furthest down field.

A broad N-H peak for the hydrolysed β-sultam was also seen at 8.20 ppm, indicating hydrolysis. In addition there are multiple peaks within the phenyl region corresponding to the phenyl hydrogens in the hydrolysed β-sultam spectra. The CH$_2$ peaks for the intact β-sultam, shown in **Figure 46**, resonate at 3.80 ppm and 4.40 ppm and move to 3.00 ppm and 3.70 ppm in the hydrolysed β-sultam.

The TAM does not provide specific molecular information and therefore ^{1}H NMR was a useful way of determining specific products of hydrolysis or to show if hydrolysis has even occurred. Although the TAM results for β-sultam D at 298K and 310K and C at 298K were not analysable the post TAM ^{1}H NMR clearly showed hydrolysis had occurred. ^{1}H NMR spectroscopy was used routinely to confirm that hydrolysis events were being observed.

The data provided from the ^{1}H NMR can also be used to determine whether hydrolysis occurs via S-N fission or via C-N fission (**Figure 47**). It has been established previously that S-N fission is the preferred mode of reaction, and this is related in the results shown which show no evidence for the formation of the ethane β-sultam C-N fission product.
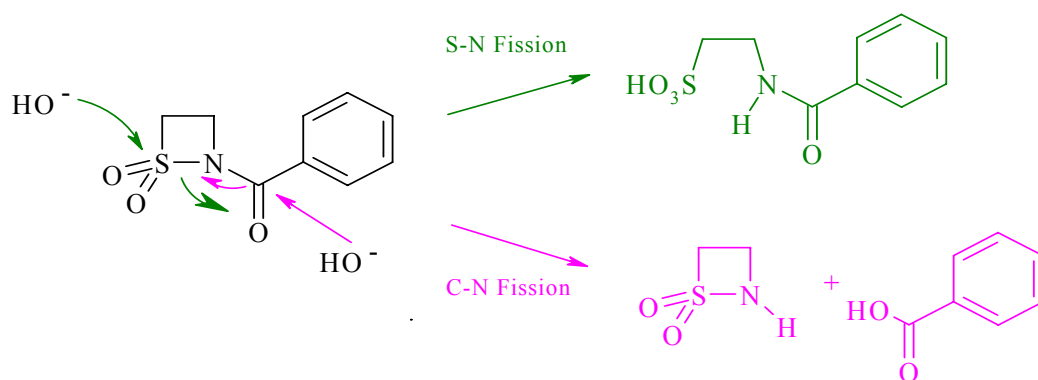

Figure 47: Hydroxide ion attack via S-N fission and C-N fission.

3.3.4 Relative humidity experiments

Up to this point the conditions used were atmospheric. To understand further the possible various processes occurring, experiments were conducted under controlled humidities. Several relative humidity (RH) experiments were conducted using the hygrostat method. Hygrostats are small glass inserts; they were filled with saturated solutions of NaCl (sodium chloride) and NaOH (sodium hydroxide) with water.

The results were not reproducible, possibly caused by the non uniformity of the solid state particles. Although hydrolysis was observed within the solid state, the results observed varying the RH were difficult and too complex to analyse.

Solution state IMC has proved to be useful and less complex with regards to studying hydrolysis, and in light of the difficulties observed with solid state studies it was decided to pursue solution phase studies.

Preliminary solution state experiments were conducted in water and solvent at pH 7, varying the volumes of water, solvent and compound mass. Gratifyingly, hydrolysis was observed. The method was then modified to control the ionic strength and pH. It is important to note although the imidazole catalysed hydrolysis of triacetin was conducted as a test reference reaction these tests were created in addition in order to find a method suitable for the *β*-sultams and TAM.

Initial experiments were carried out using a 0.02M solution of *β*-sultam followed by a concentration of 0.008M. Smaller amounts of compound were used for the lower concentration and thus more time was dedicated to the calorimetric experiments rather than to re-synthesise.

3.4 Solution state studies at 298K, 0.02M, pH 4, *β*-sultams A-D

Data was analysed after 10000s, the data before this reflects the disruption caused to the power output upon lowering the ampoules. Data analysis ceased after the reaction had reached completion, the calorimetric output had reached

zero or when the signal was too close to the base line. All experiments discussed were first order hydrolysis reactions. An example of each compound is shown in the following graphs (**Figures 48 – 51**) and results are summarised in **Table 8**. The results are discussed in later sections of the thesis. A summary of the results obtained at 298K, pH 4 and 0.02M is shown below.

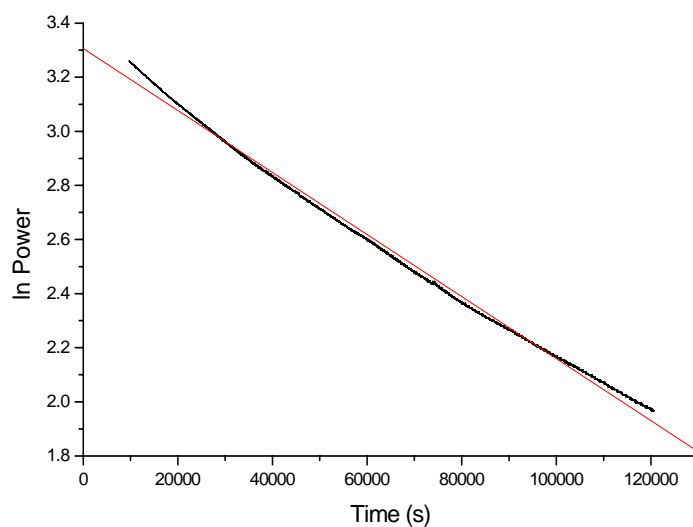| 298K 0.02M	A	B	C	D
$t_{1/2}$ (s)	7700	63000	23900	115500
Rate constant (s^{-1})	1.03×10^{-4}	1.15×10^{-5}	3.00×10^{-5}	6.18×10^{-6}
	8.67×10^{-5}	1.15×10^{-5}	3.06×10^{-5}	6.26×10^{-6}
	8.84×10^{-5}	1.11×10^{-5}	3.09×10^{-5}	5.49×10^{-6}
	8.59×10^{-5}	1.12×10^{-5}	2.62×10^{-5}	5.44×10^{-6}
	8.57×10^{-5}	1.04×10^{-5}	2.60×10^{-5}	6.90×10^{-6}
Average	9.0×10^{-5} $(\pm 9.5 \times 10^{-5})$	1.1×10^{-5} $(\pm 0.1 \times 10^{-5})$	2.9×10^{-5} $(\pm 0.6 \times 10^{-5})$	6.0×10^{-6} $(\pm 1.6 \times 10^{-6})$
$\Delta H°(298K)$ $(kJmol^{-1})$	- 40.29	- 25.35	- 39.56	- 14.86
	- 39.62	- 25.86	- 35.43	- 15.59
	- 38.85	- 26.07	- 34.31	- 16.39
	- 39.56	- 25.57	- 35.65	- 16.57
	- 39.27	- 24.67	- 35.82	- 14.40
Average	- 39.5 (± 1.4)	- 25.5 (± 1.5)	- 36.2 (± 5.5)	- 15.7 (± 2.6)

Table 8: Results for the hydrolysis of β-sultams A-D at 298K, 0.02M, pH 4.
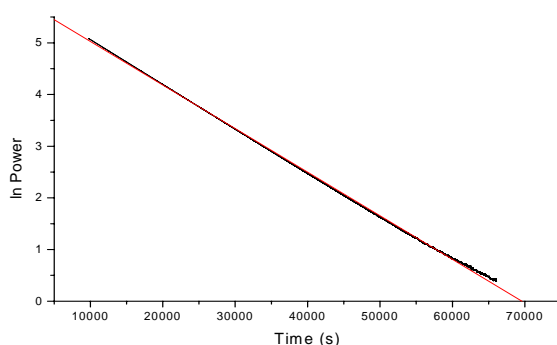
Slope = -8.43 x 10^{-5}, intercept = 5.87, R^2 = - 0.999.

Figure 48: An example of a typical calorimetric output for β-sultam A in solution at 298K, 0.02M and pH 4.
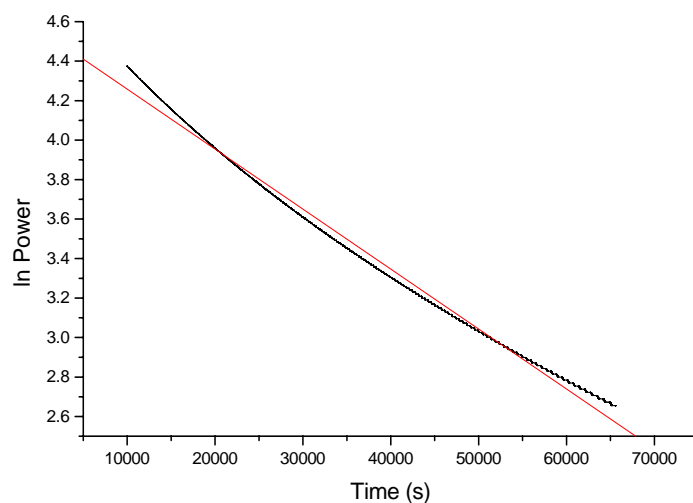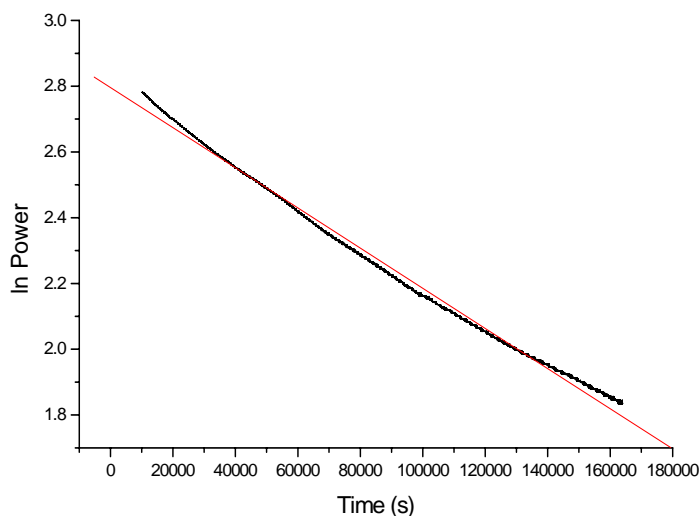
The data was analysed from 10000s – 66000s and over 8 half lives. The rate constant was $8.43 \times 10^{-5} \text{s}^{-1}$ and ΔH was $-22.70 \text{ kJmol}^{-1}$.

Slope $= -1.14 \times 10^{-5}$, intercept $= 3.30$, $R^2 = -0.998$.

Figure 49: An example of a typical calorimetric output for β-sultam B in solution at 298K, 0.02M and pH 4.

The data was analysed from 10000s – 120000s and over 2 half lives. The rate constant was $1.14 \times 10^{-5} \text{s}^{-1}$ and ΔH was $-25.33 \text{ kJmol}^{-1}$.
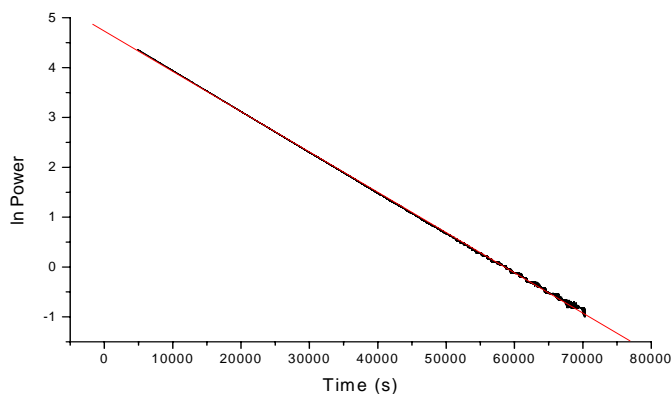

Slope $= -3.03 \times 10^{-5}$, intercept $= 4.56$, $R^2 = -0.996$.

Figure 50: An example of a typical calorimetric output for β-sultam C in solution at 298K, 0.02M and pH 4.

The data was analysed from 10000s – 65000s and over 3 half lives. The rate constant was 3.03 x $10^{-5}s^{-1}$ and ΔH was -38.66 kJmol^{-1}.

Slope = -6.10 x 10^{-6}, intercept = 2.79, R^2 = - 0.997.

Figure 51: An example of a typical calorimetric output for β-sultam D in solution at 298K, 0.02M, and pH 4.

The data was analysed from 10000s – 164000s and over 2.2 half lives. The rate constant was 6.10 x $10^{-6}s^{-1}$ and ΔH was -14.40 kJmol^{-1}.

3.5 Solution state studies at 298K, 0.008M, pH 4, β-sultams A-D

To improve the quality of results and determine the validity, a full set of experiments at 0.008M were conducted. The experiments were conducted at three different temperatures (also see sections **3.5.1** and **3.5.2**).

Data was analysed after 5000s, the data before this reflects the disruption caused to the power output upon lowering the ampoules. Data analysis stopped after the reaction had reached completion, the calorimetric output had reached zero or when the signal was close to the base line. All experiments discussed are first order degradation. An example of each compound is shown in the graphs that follow (**Figures 52 – 55**) and results are summarised in **Table 9**.

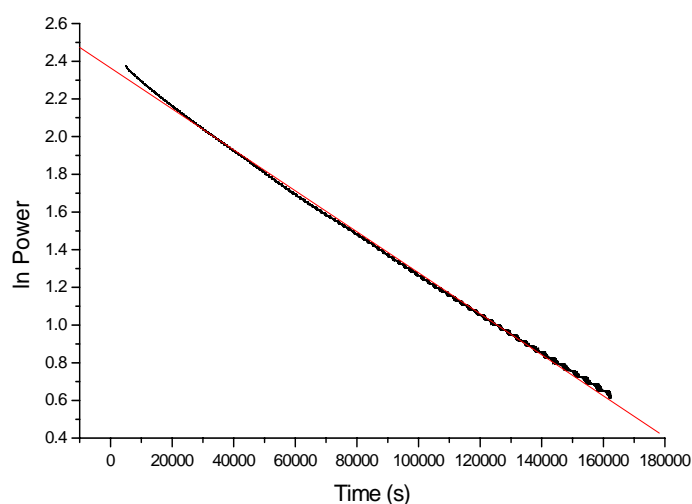| 298K 0.008M	A	B	C	D
t $_{\frac{1}{2}}$ (s)	8550	63000	21000	117460
Rate constant (s^{-1})	8.07x10^{-5}	1.11x10^{-5}	3.35x10^{-5}	6.23x10^{-6}
	7.90x10^{-5}	1.11x10^{-5}	3.47x10^{-5}	6.20x10^{-6}
	8.36x10^{-5}	1.14x10^{-5}	3.28x10^{-5}	6.29x10^{-6}
	8.01x10^{-5}	1.05x10^{-5}	3.22x10^{-5}	5.51x10^{-6}
	8.08x10^{-5}	1.09x10^{-5}	3.27x10^{-5}	5.45x10^{-6}
Average	**8.1x10^{-5}** **(± 0.5x10^{-5})**	**1.1x10^{-5}** **(± 0.09x10^{-5})**	**3.3x10^{-5}** **(± 0.26x10^{-5})**	**5.9x10^{-6}** **(± 1.1x10^{-6})**
ΔH° (298K) (kJmol^{-1})	- 13.88	- 23.65	- 28.57	- 32.06
	- 14.33	- 21.61	- 28.11	- 29.72
	- 14.37	- 21.28	- 29.51	- 31.07
	- 15.29	- 21.55	- 29.66	- 33.02
	- 15.02	- 20.76	- 28.35	- 33.15
Average	**- 14.6 (± 1.5)**	**- 21.8 (± 3.1)**	**- 28.9 (± 1.9)**	**- 31.8 (± 3.9)**

Table 9: Results for the hydrolysis of β-sultams A-D at 298K, 0.008M and pH4.

Slope = -8.08 x 10^{-5}, intercept = 4.73, R^2 = - 0.999.

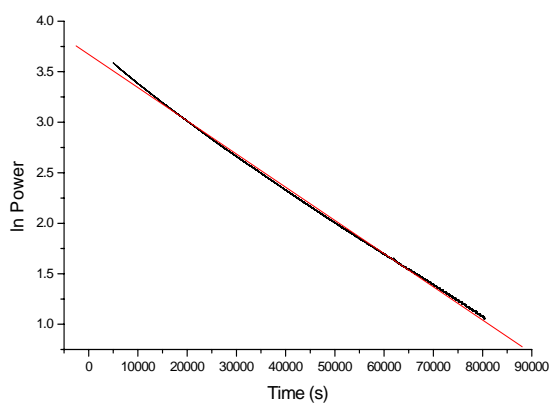**Figure 52: An example of a typical calorimetric output for β-sultam A in solution at 298K, 0.008M and pH 4.**
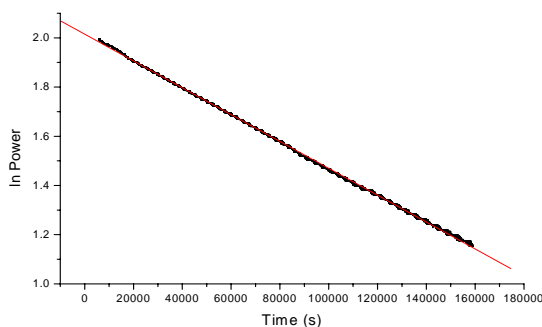
The data was analysed from 5000s – 70000s and over 8 half lives. The rate constant was 8.08 x 10^{-5}s^{-1} and ΔH was -15.02 kJmol^{-1}.

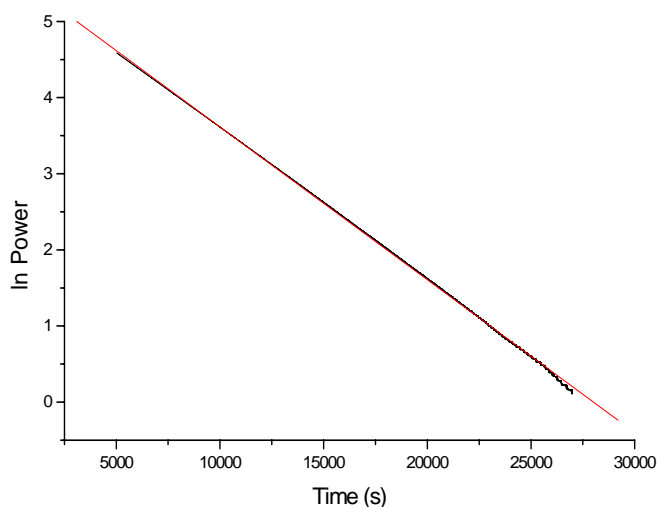Slope = -1.08 x 10^{-5}, intercept = 2.36, R^2 = - 0.999.

Figure 53: An example of a typical calorimetric output for β-sultam B in solution at 298K, 0.008M and pH 4.

The data was analysed from 5000s – 160000s and over 2.5 half lives. The rate constant was 1.08 x 10^{-5}s^{-1} and ΔH was - 20.76 kJmol^{-1}.

Slope = -3.28 x 10^{-5}, intercept = 3.67, R^2 = - 0.999.

Figure 54: An example of a typical calorimetric output for β-sultam C in solution at 298K, 0.008M and pH4.

The data was analysed from 5000s – 80000s and over 3.5 half lives. The rate constant was 3.28 x 10^{-5}s^{-1} and ΔH was - 29.51 kJmol^{-1}.

Slope = -5.45 x 10^{-6}, intercept = 2.01, R^2 = - 0.999.

Figure 55: An example of a typical calorimetric output for β-sultam D in solution at 298K, 0.008M and pH4.

The data was analysed from 5000s – 160000s and over 1.5 half lives. The rate constant was 5.45 x 10^{-6}s^{-1} and ΔH was - 33.15 kJmol^{-1}.

3.5.1 Solution state studies at 310K, 0.008M, pH 4, β-sultams A-D

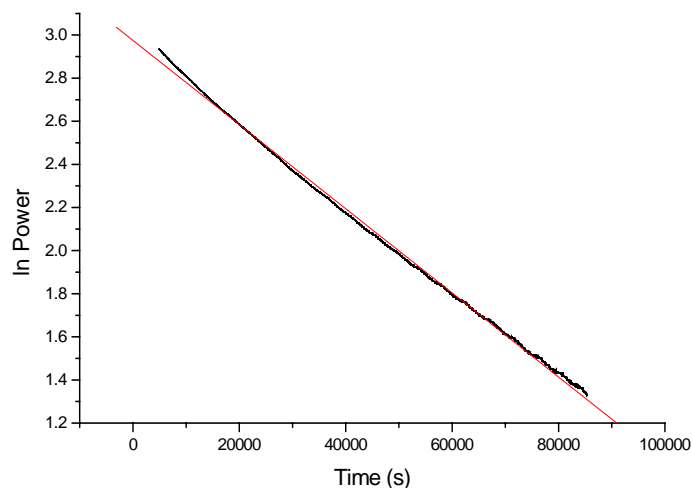| 310K 0.008M	A	B	C	D
t $_{½}$ (s)	3465	34650	14140	69300
Rate constant (s^{-1})	2.00x10^{-4}	1.95x10^{-5}	4.87x10^{-5}	1.10x10^{-5}
	2.07x10^{-4}	1.96x10^{-5}	5.10x10^{-5}	1.03x10^{-5}
	2.07x10^{-4}	1.94x10^{-5}	5.00x10^{-5}	1.09x10^{-5}
	1.96x10^{-4}	1.94x10^{-5}	4.79x10^{-5}	1.09x10^{-5}
	2.03x10^{-4}	1.99x10^{-5}	4.83x10^{-5}	1.09x10^{-5}
Average	**2.0x10^{-4} (± 0.1x10^{-4})**	**2.0x10^{-5} (± 0.05x10^{-5})**	**4.9x10^{-5} (± 4.5x10^{-5})**	**1.0x10^{-5} (± 0.08x10^{-5})**
$\Delta H°$ (310K) (kJmol^{-1})	- 14.83	- 21.13	- 29.86	- 25.97
	- 15.64	- 23.70	- 30.80	- 28.59
	- 15.64	- 23.24	- 31.40	- 27.53
	- 17.34	- 21.46	- 27.99	- 25.94
	- 17.12	- 20.71	- 27.43	- 27.00
Average	**- 16.1 (± 2.9)**	**- 22.0 (± 3.7)**	**- 29.5 (± 4.8)**	**- 27.0 (± 3.1)**

Table 10: Results to show the hydrolysis of β-sultams A-D at 310K, 0.008M and pH 4.

Slope = -2.00 x 10^{-4}, intercept = 5.62, R^2 = - 0.999.

Figure 56 An example of a typical calorimetric output for β-sultam A in solution at 310K, 0.008M and pH 4.
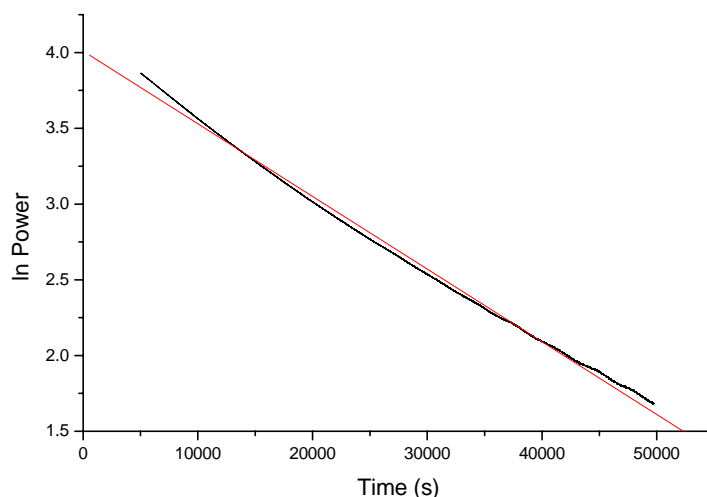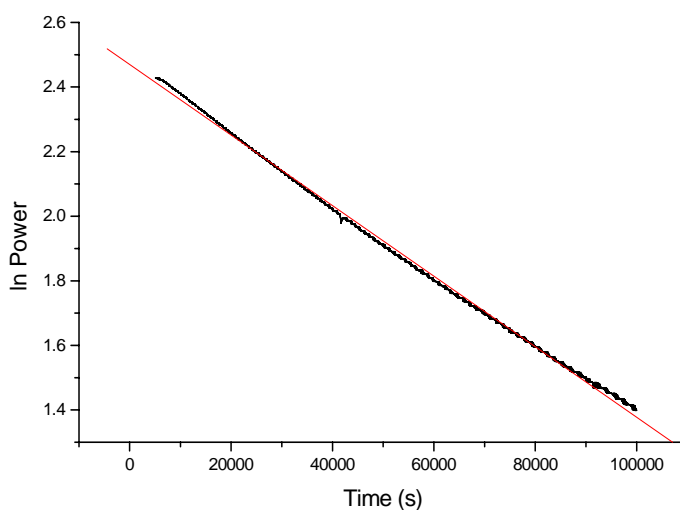
The data was analysed from 5000s – 27000s and over 8 half lives. The rate constant was 2.00 x 10^{-4}s^{-1} and ΔH was - 14.83 kJmol^{-1}.

Slope = -1.95 x 10^{-5}, intercept = 2.97, R^2 = - 0.999.

Figure 57: An example of a typical calorimetric output for β-sultam B in solution at 310K, 0.008M and pH 4.

The data was analysed from 5000s – 85000s and over 2.5 half lives. The rate constant was 1.95 x 10^{-5}s^{-1} and ΔH was - 21.13 kJmol^{-1}.

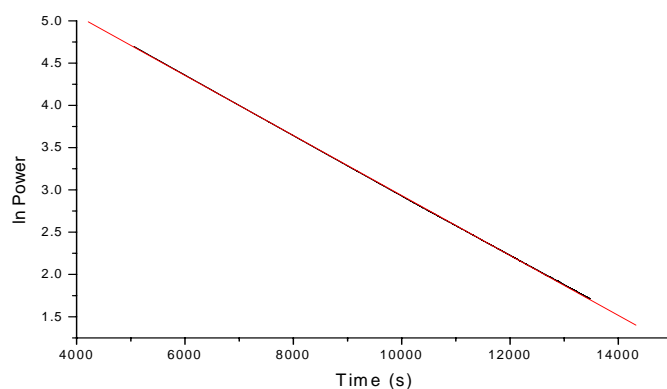Slope = -4.79 x 10^{-5}, intercept = 4.00, R^2 = - 0.998.

Figure 58: An example of a typical calorimetric output for β-sultam C in solution at 310K, 0.008M and pH 4.

The data was analysed from 5000s – 50000s and over 3.5 half lives. The rate constant was 4.79 x 10^{-5}s^{-1} and ΔH was - 27.99 kJmol^{-1}.

Slope = -1.09 x 10^{-5}, intercept = 2.46, R^2 = - 0.999.

Figure 59: An example of a typical calorimetric output for β-sultam D in solution at 310K, 0.008M and pH 4.

The data was analysed from 5000s – 100000s and over 1.5 half lives. The rate constant was 1.09 x 10^{-5}s^{-1} and ΔH was - 25.94 kJmol^{-1}.

3.5.2 Solution state studies at 323K, 0.008M, pH 4, β-sultams A-D

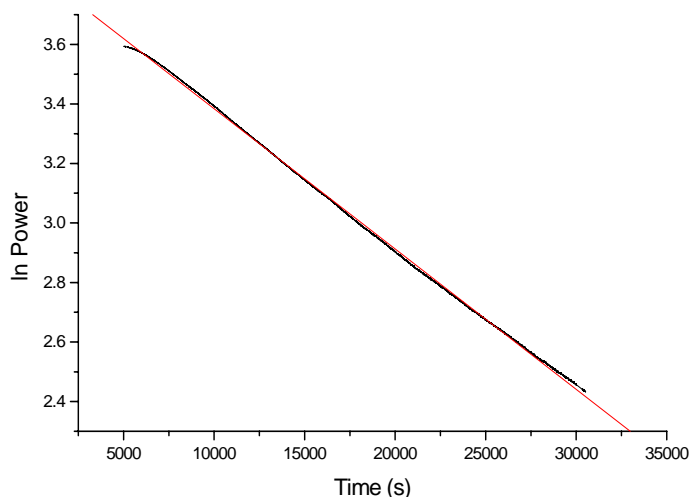| 323K 0.008M	A	B	C	D
t $_{1/2}$ (s)	1820	14400	5330	16500
Rate constant (s^{-1})	3.54x10^{-4}	4.81x10^{-5}	1.16x10^{-4}	4.51x10^{-5}
	3.56x10^{-4}	4.75x10^{-5}	1.11x10^{-4}	4.18x10^{-5}
	3.70x10^{-4}	4.92x10^{-5}	1.52x10^{-4}	4.07x10^{-5}
	4.02x10^{-4}	4.71x10^{-5}	1.51x10^{-4}	4.12x10^{-5}
	4.00x10^{-4}	4.66x10^{-5}	1.34x10^{-4}	4.13x10^{-5}
Average	**3.8x10^{-4}** **(± 0.6x10^{-4})**	**4.8x10^{-5}** **(± 0.8x10^{-5})**	**1.3x10^{-4}** **(± 0.5x10^{-4})**	**4.2x10^{-5}** **(± 0.5x10^{-5})**
ΔH° (323K) (kJmol^{-1})	- 19.75	- 22.20	- 29.84	- 30.24
	- 17.41	- 21.83	- 30.92	- 32.52
	- 19.27	- 22.60	- 30.73	- 32.49
	- 18.64	- 21.16	- 30.93	- 33.75
	- 20.30	- 20.72	- 30.04	- 32.43
Average	**- 19.1 (± 3.1)**	**- 21.7 (± 2.1)**	**- 30.5 (± 1.4)**	**- 32.3 (± 3.5)**

Table 11: Results to show the hydrolysis of β-sultams A-D at 323K, 0.008M and pH 4.

Slope = -3.54 x 10^{-4}, intercept = 6.48, R^2 = - 0.999.

Figure 60: An example of a typical calorimetric output for β-sultam A in solution at 323K, 0.008M and pH4.
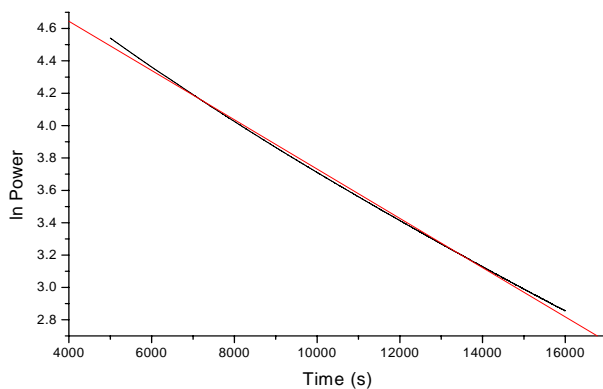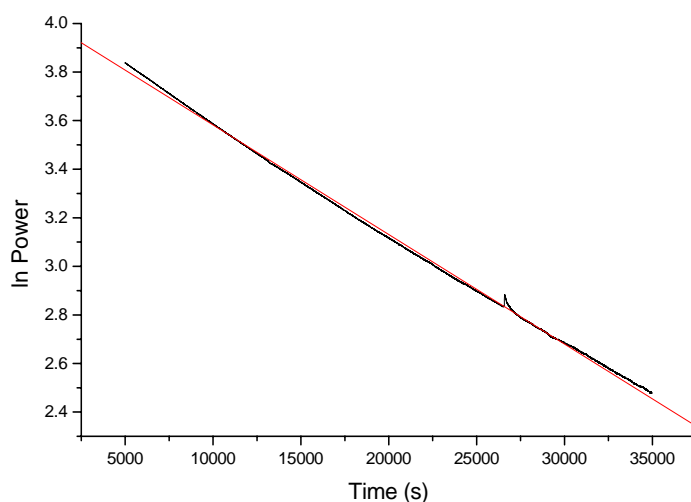
The data was analysed from 5000s – 13000s and over 7 half lives. The rate constant was 3.54 x 10^{-4}s^{-1} and ΔH was - 19.75 kJmol^{-1}.

Slope = -4.71 x 10^{-5}, intercept = 3.85, R^2 = - 0.999.

Figure 61: An example of a typical calorimetric output for β-sultam B in solution at 323K, 0.008M and pH4.

The data was analysed from 5000s – 30000s and over 2 half lives. The rate constant was 4.71 x $10^{-5}s^{-1}$ and ΔH was - 21.16 kJmol^{-1}.

Slope = -1.52 x 10^{-4}, intercept = 5.25, R^2 = - 0.999.

Figure 62: An example of a typical calorimetric output for β-sultam C in solution at 323K, 0.008M and pH 4.

The data was analysed from 5000s – 16000s and over 3 half lives. The rate constant was 1.52 x $10^{-4}s^{-1}$ and ΔH was - 30.73 kJmol^{-1}.

Slope = -4.51 x 10^{-5}, intercept = 4.03, R^2 = - 0.999.

Figure 63: An example of a typical calorimetric output for β-sultam D in solution at 323K, 0.008M and pH 4.

The data was analysed from 5000s – 35000s and over 2 half lives. The rate constant was 4.51 x $10^{-5} s^{-1}$ and ΔH was - 30.24 kJmol^{-1}.

3.6 Discussion of results at pH 4

Initial solution state hydrolysis experiments were conducted at pH 4 using a buffer and a solvent, namely acetonitrile. For *N*-aroylated β-sultams the TAM results (see **Tables 8**, **9**, **10** and **11**) show a common trend with respect to substituent effect and show similar trends when compared to previous kinetic results obtained by other means.[18] It is apparent that substituents greatly affect the stability of the β-sultams. The proposed mechanism for the hydrolytic degradation is shown in **Figure 64**.
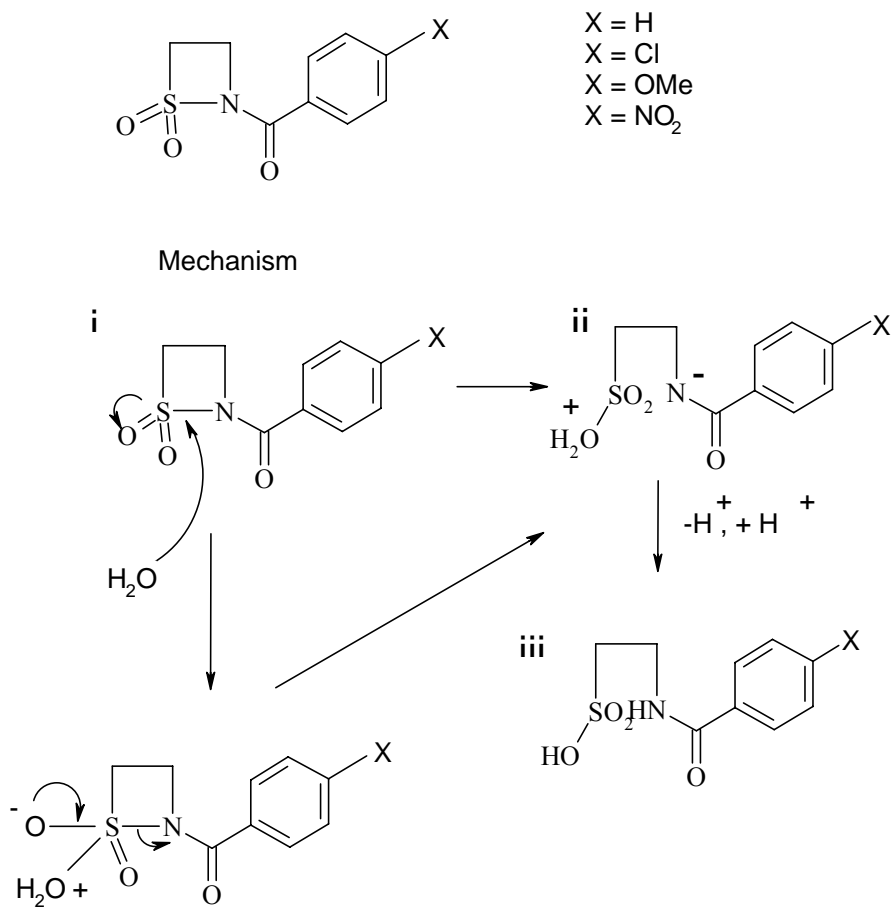
N-Aroylated Beta -sultams

X = H
X = Cl
X = OMe
X = NO$_2$

Mechanism

Figure 64: Hydrolysis mechanism of *N*-aroylated β-sultams.

As suggested in the mechanism a fifth compound was synthesised. Unfortunately the attempted synthesis for the *N*-substituted β-sultam containing the nitro group was unsuccessful. When considering β-sultams A-D in all cases (see **Tables 8**, **9**, **10** and **11**) it can be seen that under these conditions the unsubstituted β-sultam (A) is the most susceptible to hydrolyse in solution followed by C (X=Cl), B (X=H) and D (X=OMe).

When considering the mechanism for β-sultams A-D it is proposed that the β-sultam ring undergoes S-N bond fission (see **Figure 64**). The intermediate (ii) is formed as a result. The difference in stability arises from the effect the substituents (X) have on the stability of the nitrogen leaving group and phenyl

ring. Certain atoms or groups can add or withdraw electron density to a system. Electron withdrawing groups and electron donating groups affect the stability of the intermediate. For example, the methoxy group is electron donating and would destabilise and disfavour the intermediate (ii) and hence contribute to the slower rate of hydrolysis of *β*-sultam D. This destabilisation is a result of the carbonyl group being less available to stabilise the N⁻ leaving group in such a system.

β-Sultam C has a chlorine attached to the phenyl ring which has an electron withdrawing effect. Electron density is removed from the aromatic system by the inductive effect, allowing the charge on the nitrogen to delocalise onto the carbonyl and hence stabilise the hydrolysis intermediate and therefore increase the rate of hydrolysis of C.

Comparisons can also be made between *β*-sultam B and *β*-sultam C. *β*-sultam B appears to be slightly more stable than *β*-sultam C when considering the half life and rate constants. *β*-Sultam B has no substituents on the phenyl ring, meaning that its rate of hydrolysis lies between that of the electron donating D and the electron deficient C.

It is relevant to note that the nitro *N*-aroylated *β*-sultam could not be prepared because it underwent rapid hydrolysis. Presumably the very electron withdrawing NO_2 group allows such high stabilisation of the intermediate (ii) that hydrolysis is facile and prevents isolation of the intact *β*-sultam.

Hydrolysis experiments conducted using IMC (TAM), provided data that gave key kinetic information. To obtain molecular information and clarify the nature of the process being observed, ^{1}H NMR studies were conducted and a selection of results for each *β*-sultam studied is shown. The conditions that were used for the ^{1}H NMR experiments were those used for the calorimetric studies, i.e. buffer (potassium chloride and potassium acetate) at pH 4 and the *β*-sultam dissolved in acetonitrile. The water peak was suppressed to allow a clear and true representation of the *β*-sultam; most of the peaks that represent the *β*-

sultam are clearly identified. It can be noted that in some of the spectra the CH_2-SO_2, CH_2-NH/R peaks are very close to the signal-noise ratio and the CH_2-SO_2 peak for the hydrolysed sultam is embedded in the acetonitrile peak but can be seen for the intact sultam. However the ^{1}H NMR spectra show clear hydrolysis for β-sultams A-D and hence confirm this as the process under observation. **Figure 65** shows the substituted β-sultam used for NMR analysis. The NMR results are discussed.

N-Aroylated β-sultams
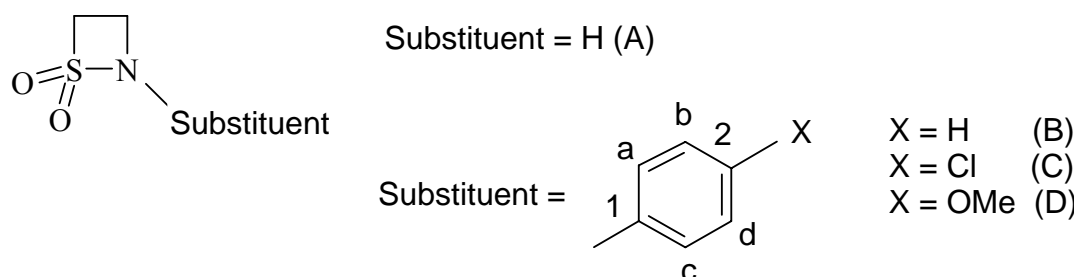
Figure 65: β-sultam structures used for ^{1}H NMR analysis.

β-Sultam A

During the first hour of analysis (**Figure 66**) there are peaks at 3.60 ppm and 2.98 ppm for the two β-sultam CH_2s. Hour 3 (**Figure 67**) shows the same peaks starting to disappear together with the appearance of hydrolysis products. The appearance of a CH_2 for the hydrolysed β-sultam (at 3.3 ppm) can be seen progressing from hour 1 and 3. At hour 20 (**Figure 68**) the peak for the hydrolysed β-sultam (3.3 ppm) is more prevalent. The CH_2-SO_2 and CH_2-NH peaks of the sultam have reduced significantly, showing significant hydrolysis.

The fact that after 20 hours significant hydrolysis has occurred corresponds well with the TAM data, where analysis was stopped after 18-19 hours. An important point to note is that there is a general shift of peaks to the right for the hydrolysed β-sultams, with relief of ring strain contributing to this general shift.
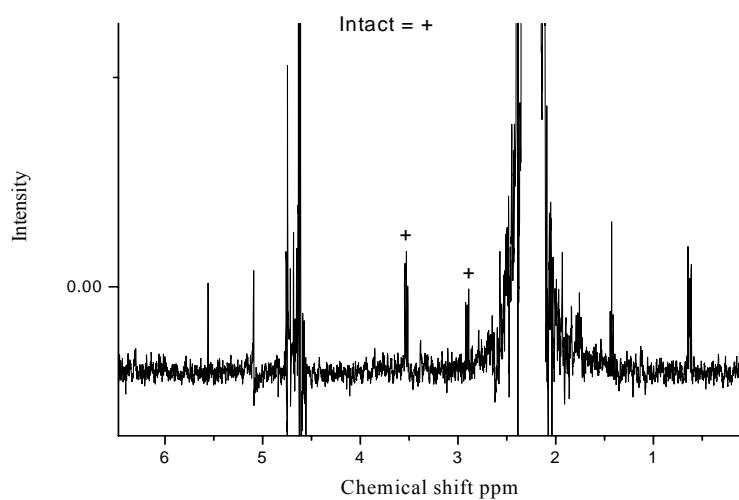
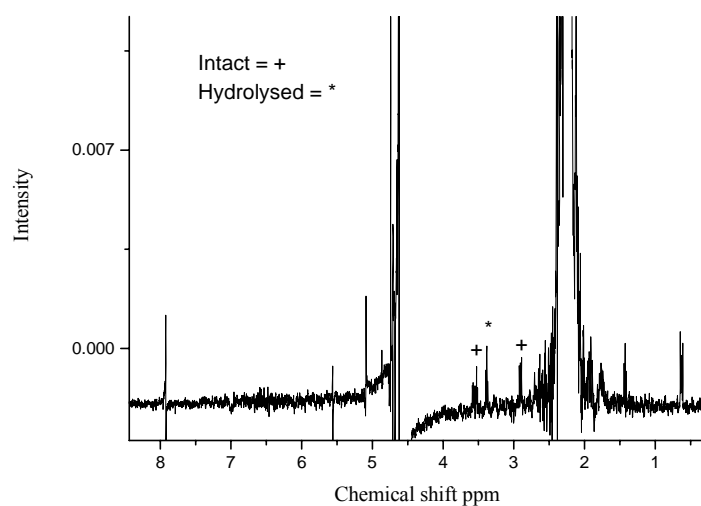**Figure 66: Hydrolysis ^{1}H NMR for β-sultam A at hour 1, 298K.**

Figure 67: Hydrolysis ^{1}H NMR for β-sultam A at hour 3, 298K.
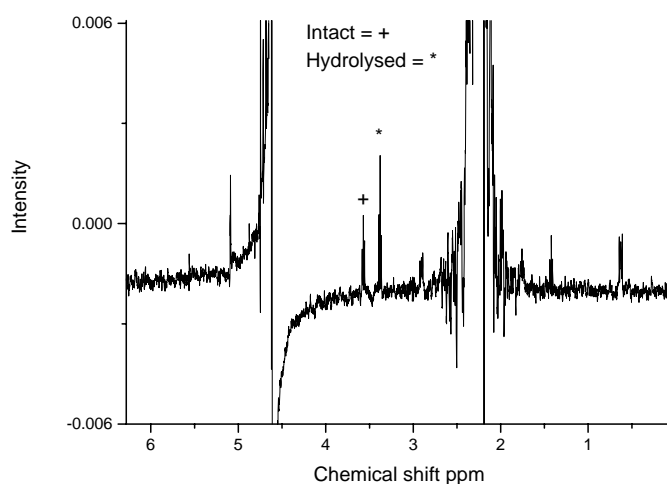
Figure 68: Hydrolysis ^{1}H NMR for β-sultam A at hour 20, 298K.

β-Sultam B

During the first hour (**Figure 69**) of analysis it is clear from the presence of two sets of peaks in the phenyl region that there is already a combination of intact and hydrolysed β-sultam. At hour 20 the distinct CH_2-NR peak at 3.30 ppm for the hydrolysed β-sultam can be seen. In addition when looking at the phenyl region and comparing hour 1 and hour 20 it can clearly be seen that the peaks corresponding to the intact β-sultam have been reduced. An important point to note is the appearance of the N-H peak which is a clear indication of hydrolysis.
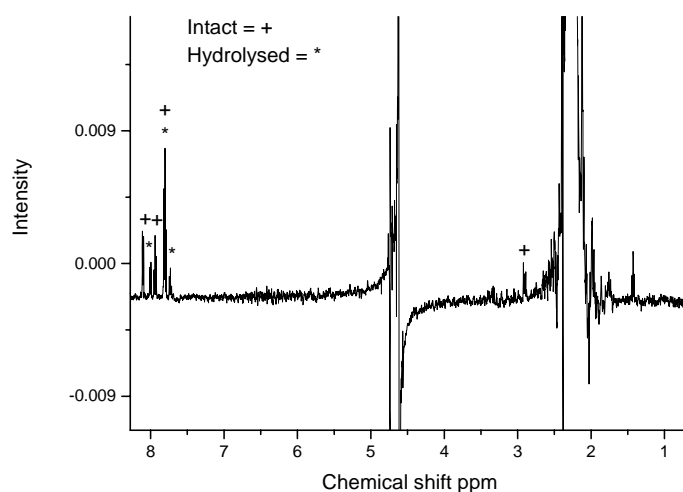

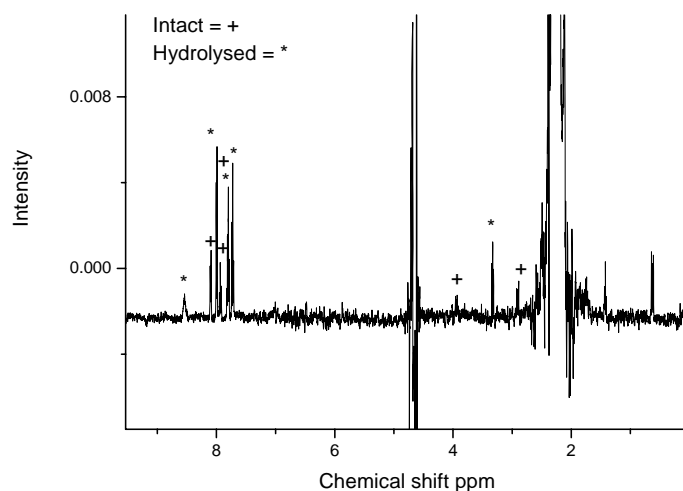**Figure 69: Hydrolysis ^{1}H NMR for β-sultam B at hour 1, 298K.**

Figure 70: Hydrolysis ^{1}H NMR for β-sultam B at hour 18, 298K.
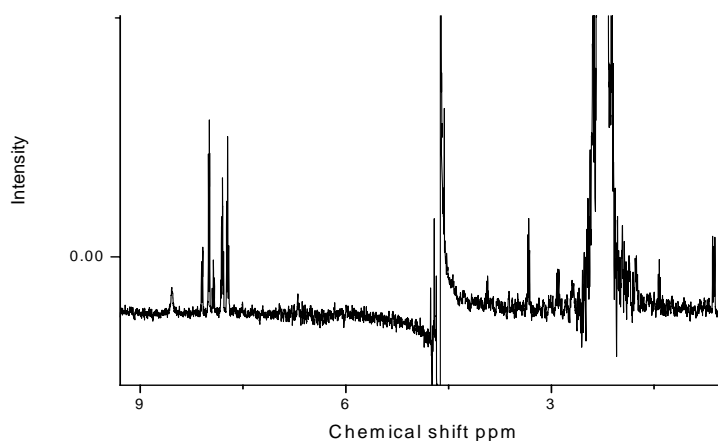

Figure 71: Hydrolysis ^{1}H NMR for β-sultam B at hour 20, 298K.

Sultam C

Sultam C at hour 1 (**Figure 72**) shows a small amount of hydrolysis. There are two distinct sets of peaks in the phenyl region with Ha/c at 8.25 ppm and Hb/d at 7.80 ppm with the corresponding peaks for the hydrolysed sultam shifted slightly to the right. At hour 3 (**Figure 73**) the N-H peak is very clear and more hydrolysed product is apparent. At hour 20 (**Figure 74**) further hydrolysis can be seen. The two peaks that correspond to the Ha/c and Hb/d region for the intact sultam are smaller and the same peaks for the hydrolysed sultam are now

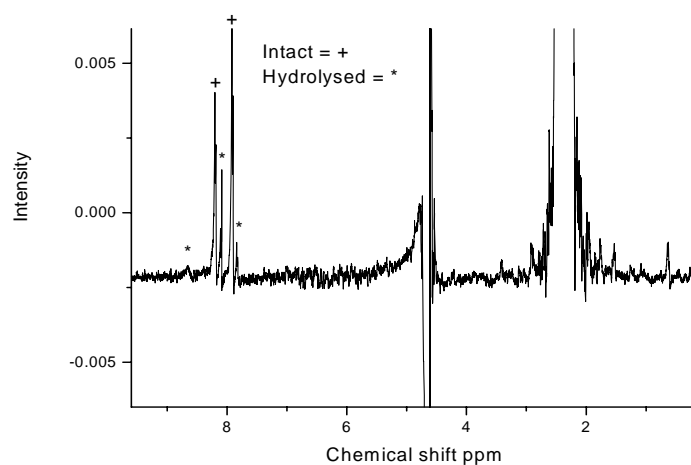more significant. The N-H peak at hour 20 is more distinct, and a new CH_2 signal has appeared at 3.31 ppm.

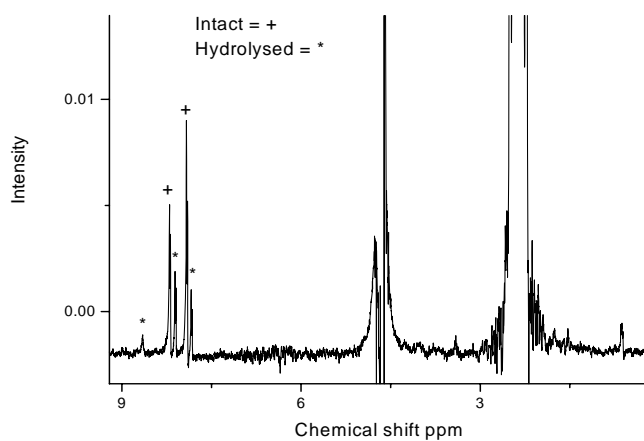**Figure 72: Hydrolysis ^{1}H NMR for β-sultam C at hour 1, 298K.**

Figure 73: Hydrolysis ^{1}H NMR for β-sultam C at hour 3, 298K.
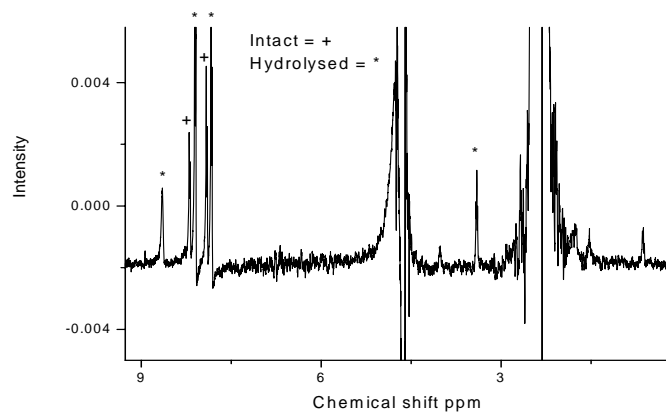
Figure 74: Hydrolysis ^{1}H NMR for β-sultam C at hour 20, 298K.

β-Sultam D

The TAM studies conducted showed that β-sultam D appears to be the most stable. NMR experimental analysis for this β-sultam was conducted over a longer period of time, indicating greater stability, a fact reflected already in the TAM studies. The ^{1}H NMR spectra at hour 1 (**Figure 75**) showed complete intact sultam with Ha/c at 8.10 ppm and Hb/d at 7.30 ppm. At hour 3 (**Figure 76**) there is little change with only a small amount of hydrolysis apparent. However at hour 20 (**Figure 77**) it is apparent that the β-sultam has undergone noticeable hydrolysis. When looking at the phenyl region there are the characteristic Ha/c and Hb/d peaks for the hydrolysed β-sultam, together with a small NH peak at 8.50 ppm.

When considering the TAM and ^{1}H NMR data, the TAM analysis showed that it took 44-45 hours for β-sultam D to hydrolyse and the ^{1}H NMR shows that after 20 hours, less than half the compound had hydrolysed. The ^{1}H NMR data thus reinforces that seen in the TAM measurements.
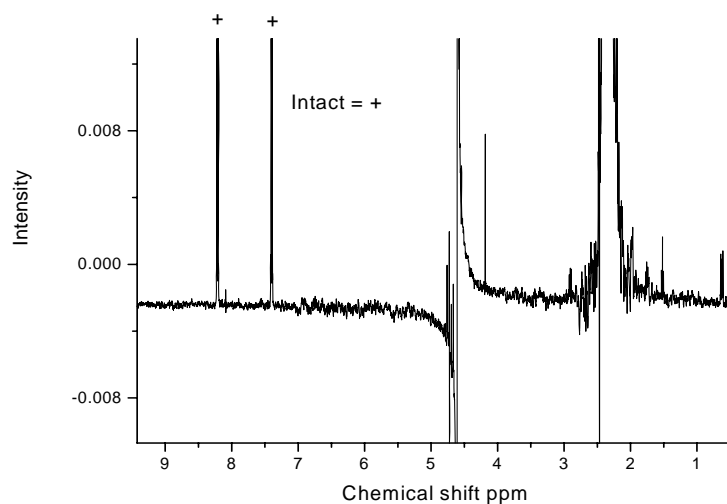

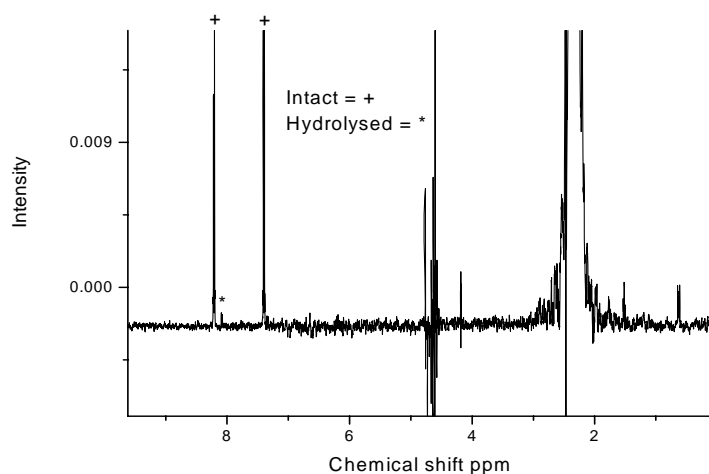**Figure 75: Hydrolysis ^{1}H NMR for β-sultam D at hour 1, 298K.**

Figure 76: Hydrolysis ^{1}H NMR for β-sultam D at hour 3, 298K.
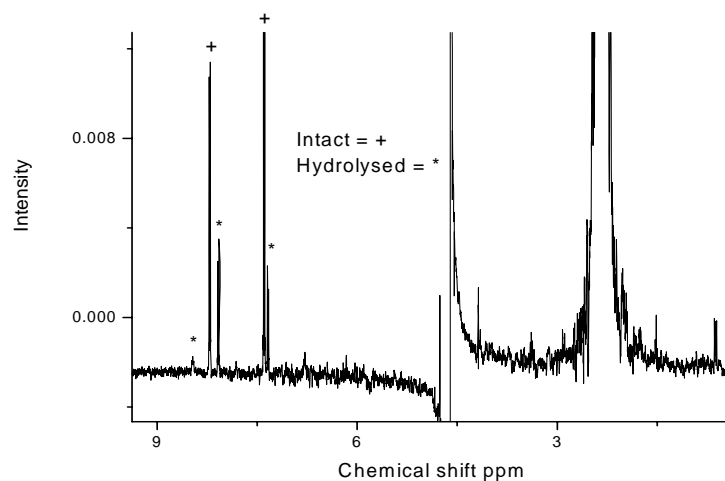
Figure 77: Hydrolysis ^{1}H NMR for β-sultam D at hour 20, 298K.

When comparing all four sets of ^{1}H NMR spectra it is apparent that the same trend is observed using either NMR or IMC. β-sultam A appears to be the least stable, β-sultam D appears to be the most stable and β-sultams B and C appear to be similar with respect to stability, with β-sultam B slightly more stable than C. This also correlates well when looking at the role of the different substituents and how they affect the stability of the intermediates during the hydrolysis process as discussed previously.

For the solid state results, it can also be seen that the nature of the substituents present affects both the rate constant and the change in enthalpy for the hydrolytic process. As expected, there is a steady increase in rate constant for all four compounds with an increase in temperature across the three temperatures (298K, 310K and 323K) studied.

Applying the Arrhenius equation to the kinetic data permits calculation of the activation energy (E_a) for the hydrolysis of the four compounds. For each compound a plot of ln$k$ against 1/T provided a linear relationship (R^2 ranged from 0.81 to 0.99). All experiments for each reaction were exothermic. For exothermic reactions the lower the activation energy the faster the reaction.

The E_a values for A is +42.2 kJmol^{-1}, +38.5 kJmol^{-1} for B, +34.9 kJmol^{-1} for C and 49.9 kJmol^{-1} respectively. There was not much difference in the activation energies calculated.
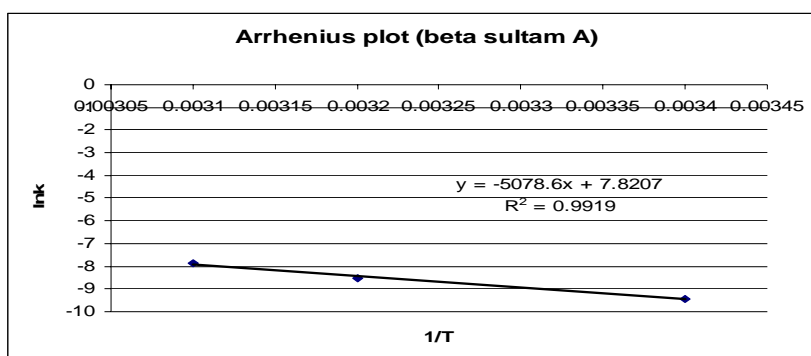
Slope = -Ea/R = -(-5078.6)*8.314/1000 = +42.2 kJmol^{-1}

Figure 78: β-sultam A Arrhenius plot
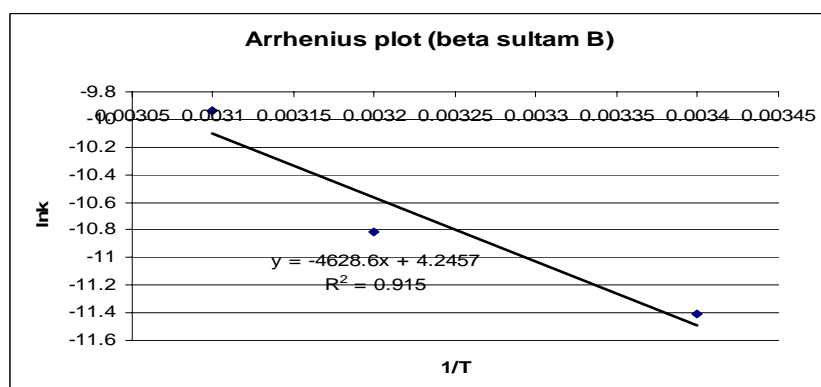
Slope = -Ea/R = -(4628.6)*8.314/1000 = +38.5 kJmol^{-1}

Figure 79: *β*-sultam B Arrhenius plot
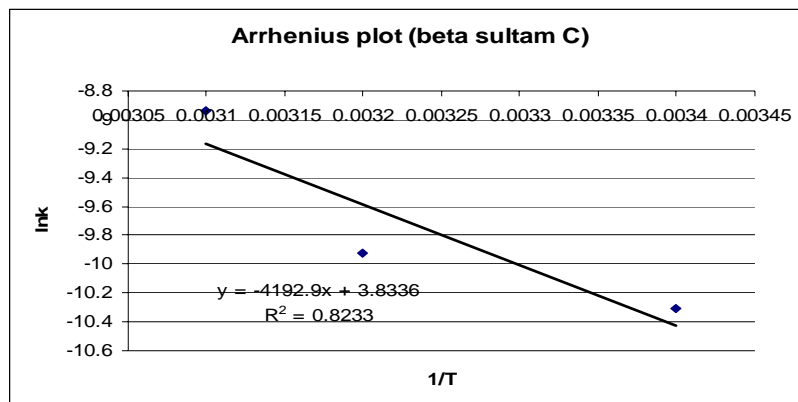
Slope = -Ea/R = -(4192.9)*8.314/1000 = +34.9 kJmol^{-1}

Figure 80: *β*-sultam C Arrhenius plot
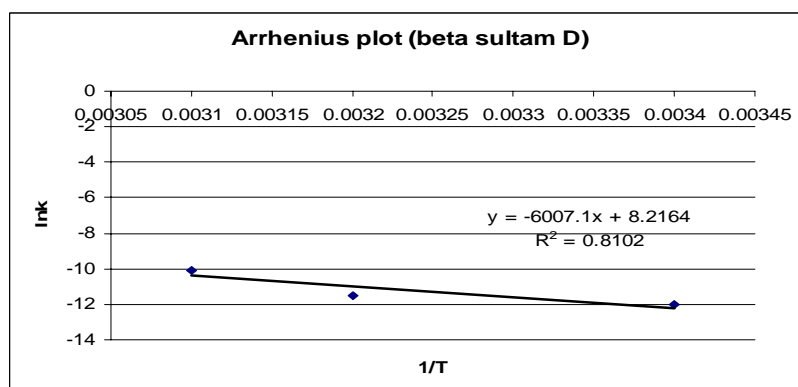
Slope = -Ea/R = -(6007.1)*8.314/1000 = +49.9 kJmol^{-1}

Figure 81: *β*-sultam D Arrhenius plot

Enthalpic data presented confirmed that for each of the four compounds there is no significant change in enthalpy over the temperature range.

At 0.008M the substituted *β*-sultams (B, C and D) compared to the unsubstituted *β*-sultam (A) displayed more negative changes in enthalpy at all temperatures. This is believed to be a reflection of the stabilising effect exerted by the substituents on the S-N bond thus resulting in a more negative change in enthalpy associated with the hydrolytic process.

The enthalpy for β-sultam A and D at 0.02M were inconsistent. This inconsistency could have been related to the different batches used.

Calorimetric studies were also conducted at 0.008M at pH8 to investigate the hydrolysis further and compare how a change in pH and concentration affects the reaction.

3.7 Solution state studies of β-sultams A-D at 298K, pH 8, 0.008M

The following experiments were conducted at pH 8. Data was analysed after 3600s. The data before this reflects the disruption caused to the power output upon lowering the ampoules. Data analysis ceased after the reaction had reached completion, the calorimetric output had reached zero or when the signal was close to the base line. All experiments discussed were first order degradation. An example of each β-sultam is shown in the graphs that follow (**Figures 82 – 84**) and results are summarised in **Table 12**.

298K 0.008M	A	B	C	D
$t_{1/2}$ (s)	8482	435	-	525
Rate constant (s^{-1})	4.32×10^{-5}	0.00156	-	0.00135
	7.14×10^{-5}	0.0016	-	0.00139
	8.25×10^{-5}	0.0016	-	0.00128
	1.30×10^{-4}	0.00163	-	0.00129
Average	8.2×10^{-5} ($\pm 9.8 \times 10^{-5}$)	1.6×10^{-3} ($\pm 0.09 \times 10^{-3}$)	-	1.3×10^{-3} ($\pm 0.2 \times 10^{-3}$)
$\Delta H°$ (298K)	- 1.22	- 47.40	-	- 78.90

(kJmol^{-1})				
	- 0.68	- 55.95	-	- 80.49
	- 0.47	- 57.65	-	- 62.90
	- 0.57	- 45.43	-	- 61.08
Average	**- 0.7 (± 1.04)**	**- 51.6 (± 19.3)**	**-**	**- 70.8 (± 32.6)**

Table 12: Results for the hydrolysis of β-sultams A-D at 298K, 0.008M and pH 8.
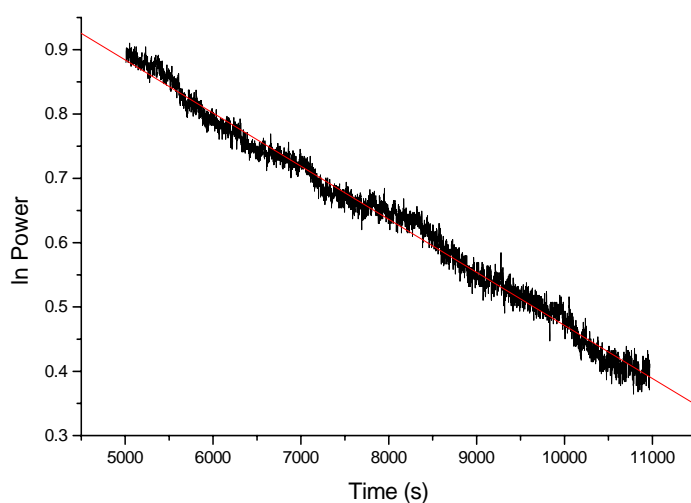
Slope = -8.25 x 10^{-5}, intercept = 1.29, R^2 = - 0.994.

Figure 82: An example of a typical calorimetric output for β-sultam A in solution at 298K, 0.008M and pH 8.

The data was analysed from 5000s – 11000s and over 1.5 half lives. The rate constant was 8.25 x 10^{-5}s^{-1} and ΔH was -0.47 kJmol^{-1}.
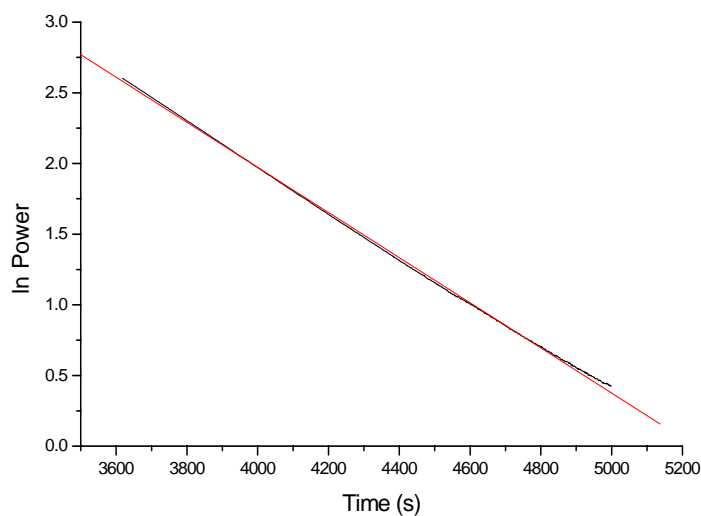
Slope = -0.0016, intercept = 8.35, R^2 = - 0.999.

Figure 83: An example of a typical calorimetric output for β-sultam B in solution at 298K, 0.008M and pH8.

The data was analysed from 3600s – 5000s and over 1 half life. The rate constant was 0.0016 s^{-1} and ΔH was -55.95 kJmol^{-1}.

Slope = -0.0012, intercept = 8.11, R^2 = - 0.997.

Figure 84: An example of a typical calorimetric output for β-sultam D in solution at 298K, 0.008M and pH8.
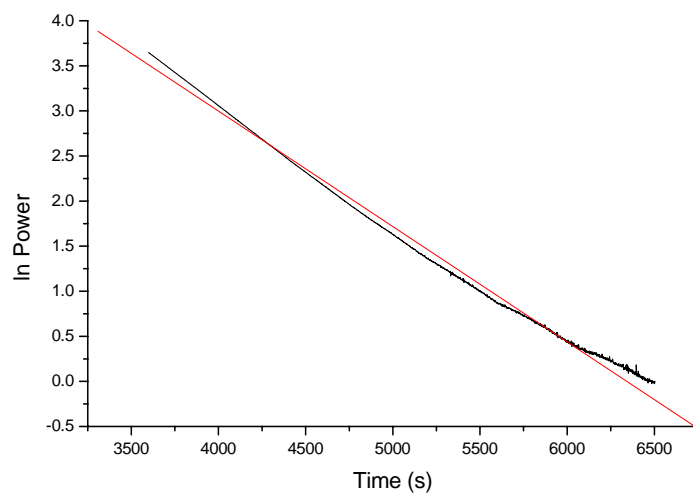
The data was analysed from 3600s – 6500s and over 1 half life. The rate constant was 0.0012 s^{-1} and ΔH was -62.90 kJmol^{-1}.

3.7.1 Discussion, β-sultams at 298K, pH 8 in solution at 0.008M

It can be noted that experiments were also attempted at 310K and 323K however under these conditions the β-sultam underwent complete hydrolysis at the higher temperatures.

To obtain molecular information and confirm the hydrolysis of the β-sultams over the calorimetric study time frame ^{1}H NMR studies were conducted. The same conditions that were used for the ^{1}H NMR experiments were used for the calorimetric studies i.e. a buffer (potassium chloride and sodium hydrogen phosphate) at pH 8. The compound was dissolved in acetonitrile when conducting the calorimetric experiments; the same was repeated for the ^{1}H NMR experiments. For the ^{1}H NMR experiments the water peak was suppressed to allow a clear and true representation of the β-sultam, most peaks that represent the β-sultam are clear. The ^{1}H NMR spectra showed clear hydrolysis for each of the β-sultams A, B and D. In addition and more importantly, the hydrolysis experiments conducted were extremely quick in comparison with previous experiments discussed, reflecting the calorimetric measurements shown in **Table 12**.

The ^{1}H NMR of β-sultam D, for example, shows the progress of hydrolysis which can be analysed by looking within the phenyl region. At 20 minutes (**Figure 85**), there are clearly two species present in the aromatic region, there appears to be a mixture of hydrolysed and non hydrolysed material. By 40 minutes (**Figure 86**) the reaction is essentially complete with only minor amounts of non-hydrolysed product present. **Figure 87** (one hour into the reaction) confirms the reaction to be complete by ^{1}H NMR.
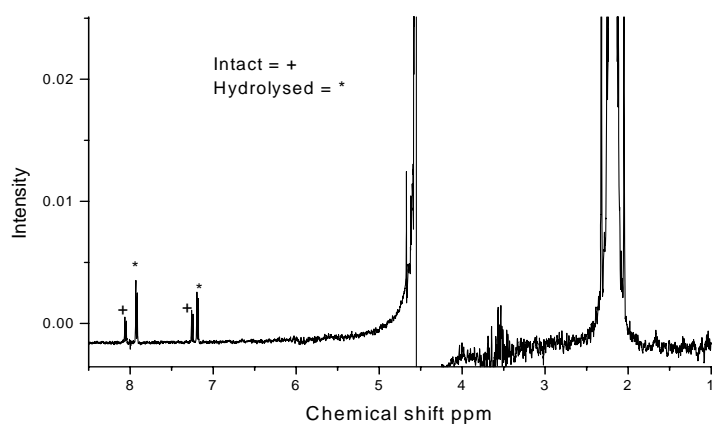
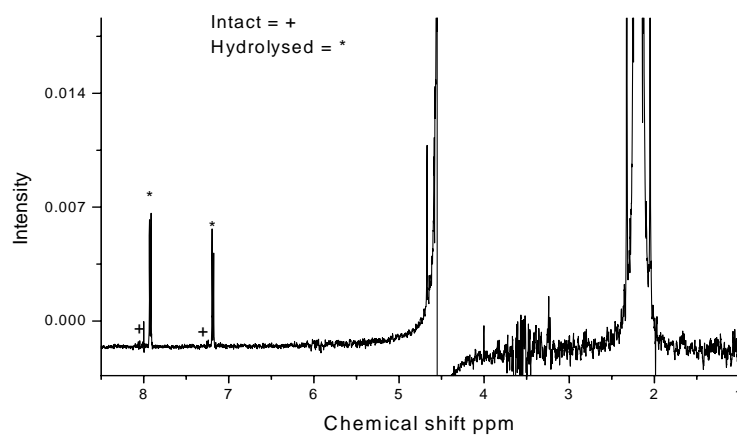**Figure 85: Hydrolysis ^{1}H NMR for *β*-sultam D at 20 minutes, 298K.**

Figure 86: Hydrolysis ^{1}H NMR for *β*-sultam D at 40 minutes, 298K.
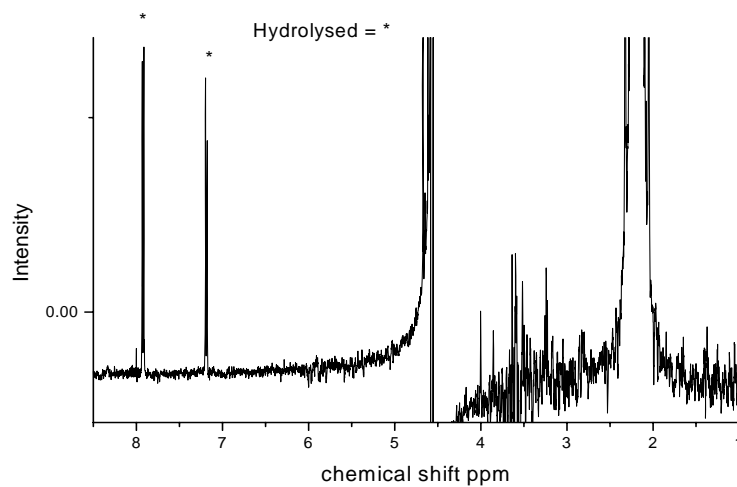

Figure 87: Hydrolysis ^{1}H NMR for *β*-sultam D at hour 1, 298K.

It is noteworthy that compound C underwent hydrolysis too quickly to allow measurement using the TAM. Experiments conducted at pH 4 and pH 8 showed similar trends with respect to the effect of substituents on hydrolysis, with compound C being more reactive than B and D, where D was the least reactive. The substituted β-sultams are more reactive to hydrolysis at pH 8 than at pH 4. β-Sultam A showed the same reactivity at both pHs, hence becoming the least reactive towards hydrolysis at pH 8 but most reactive at pH 4, the rate for A remained the same at both pHs whereas the rate changed for the substituted β-sultams at the different pHs. The change in enthalpy for β-Sultam A at pH 8 is close to zero indicating a slower rate of hydrolysis. The small change in enthalpy could be a result of fewer bonds breaking and as a result less heat released.

3.8 Solution state studies of β-sultam F at 298K, pH 4 and pH 8, 0.008M

As part of a collaborative programme of work, the *N*-acyl β-sultam (**Figure 88**) was synthesised by Arnaud Pitard at the University of Huddersfield as an anti-inflammatory agent with potential activity as a taurine pro-drug for the development of new drugs active against Alzheimer's disease. The lack of a chromophore made this compound unsuitable for U.V. detector kinetic studies, but ideal for the TAM method developed in this thesis. With an electron donating methyl group on the carbonyl, it was predicted that this new β-sultam (F) should have a similar reactivity to that of the electron donating methoxy substituted β-sultam (D) and be less reactive than the electron withdrawing chlorobenzoyl β-sultam (C).
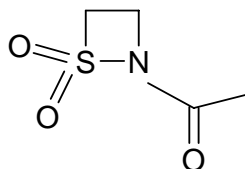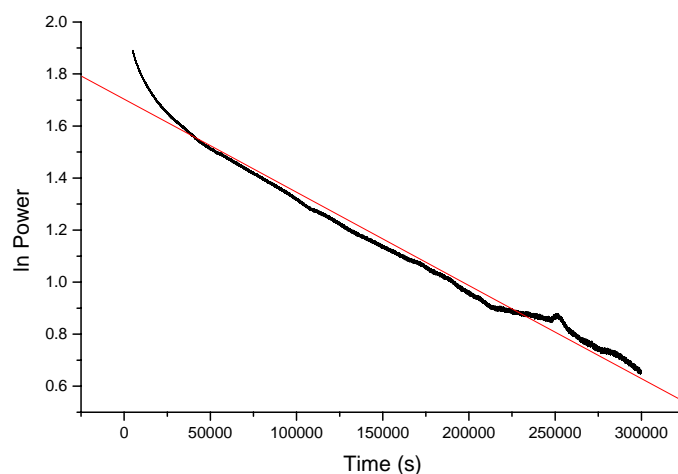

Figure 88: β-sultam F

Solution state hydrolysis experiments were conducted at pH 4 and pH 8 (**Figure 89** and **90**). Data was analysed after 5000s, the data before this reflects the

disruption caused to the power output upon lowering the ampoules. Data analysis ceased after the reaction had reached completion, the calorimetric output had reached zero or when the signal was close to the base line. All experiments discussed were first order degradation. Results are summarised in **Table 13** and the hydrolytic mechanism can be seen in **Figure 91**.

| 298K 0.008M	pH4	pH8
t $_{1/2}$ (s)	191000	3107
Rate constant (s-¹)	3.64×10^{-6}	2.04×10^{-4}
	3.55×10^{-6}	1.78×10^{-4}
	3.71×10^{-6}	2.49×10^{-4}
	3.58×10^{-6}	2.64×10^{-4}
Average	**3.6×10^{-6} ($\pm 0.2 \times 10^{-6}$)**	**2.2×10^{-4} ($\pm 1.2 \times 10^{-4}$)**
ΔH° (298K) (kJmol^{-1})	- 23.31	- 0.30
	- 18.82	- 0.30
	- 18.22	- 0.20
	- 22.79	- 0.21
Average	**- 20.8 (± 8.4)**	**- 0.3 (± 0.2)**

Table 13: Results for the hydrolysis of β-sultam F at 298K, 0.008M, pH4 and pH8.

Slope = -3.58×10^{-6}, intercept = 1.70, R^2 = - 0.992.

Figure 89: An example of a typical calorimetric output for β-sultam F in solution at 298K, 0.008M and pH 4.

The data was analysed from 5000s – 300000s and over 1.5 half lives. The rate constant was $3.58 \times 10^{-6} s^{-1}$ and ΔH was -22.79 kJmol^{-1}.
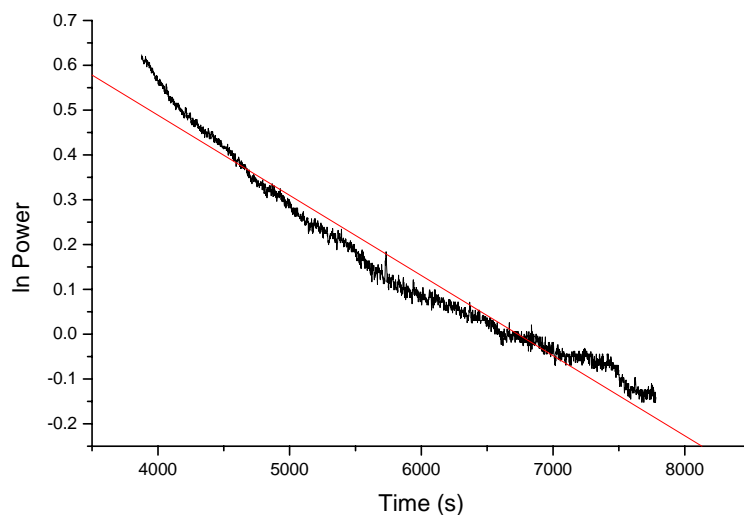
Slope = -1.78×10^{-4}, intercept = 1.20, R^2 = - 0.981.

Figure 90: An example of a typical calorimetric output for β-sultam F in solution at 298K, 0.008M and pH 8.

The data was analysed from 5000s – 8000s and over 2.5 half lives. The rate constant was $1.78 \times 10^{-4} s^{-1}$ and ΔH was -0.30 kJmol^{-1}.

3.8.1 Discussion, β-sultam F at 298K, pH 4 and pH 8 in solution at 0.008M

The hydrolytic experiments conducted on β-sultam F confirmed the ability of the TAM to monitor compounds without a chromophore with low reactivity. At both pHs the *N*-acyl compound F was shown to be the least reactive species when comparing rates of hydrolysis to all other substituted β-sultams discussed. In particular when comparing reactivity to β-sultam D at pH 4 and pH 8 β-sultam F is lower in reactivity. However at pH 8 β-sultam A is the least reactive when comparing β-sultams A-F.

^{1}H NMR studies confirmed that hydrolysis was observed. The intact *N*-acyl β-sultam CH$_2$ peaks resonate at 4.23 ppm and 3.71 ppm and Me at 2.27 ppm. The

hydrolysed β-sultam showed the corresponding peaks at 4.00 ppm and 3.72 ppm respectively.

Mechanism
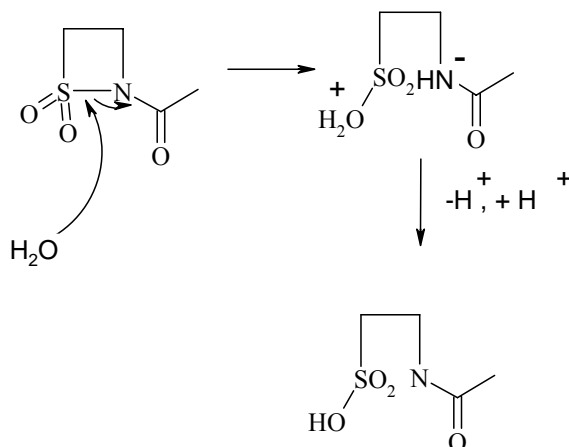
Figure 91: Mechanism to show hydrolysis for β-sultam F.

Figure 91 shows the mechanism of hydrolysis. The mechanistic nature is the same as those β-sultams discussed previously. However it is the effect the substituent has on stabilising or destabilising the intermediate. In all cases β-sultam F appeared to be the most stable.

3.9 Discussion (overall)

The hydrolytic degradation was investigated using Isothermal microcalorimetry to determine kinetic and enthalpic data.

Solid state studies were conducted on compounds A-D, there was a significant substituent stabilising and destabilising effect observed. All four compounds were analysed for hydrolytic degradation in the solution phase. Experiments were conducted at pH 4 and pH 8 at varying temperatures, 298K, 310K and 323K. The substituents affected the change in enthalpy and rate constants. There was a steady increase in the rate constant for all four compounds with an increase in temperature. [19]

First order calorimetric outputs were observed for all calorimetric experiments. Rates of hydrolysis for the β-sultams at pH 4, 0.02M and 0.008M at the three different temperatures, 298K, 310K and 323K were consistent (**Table 14** and **15**).

Temperature and concentration	Rates of hydrolysis – Rate constant (s⁻¹)			
	A	B	C	D
298K 0.02M	9.0×10^{-5} ($\pm 9.5 \times 10^{-5}$)	1.1×10^{-5} ($\pm 0.1 \times 10^{-5}$)	2.9×10^{-5} ($\pm 0.7 \times 10^{-5}$)	6.0×10^{-6} ($\pm 1.6 \times 10^{-6}$)

Table 14: Table to show β-sultam rates of hydrolysis at temperature 298K and 0.02M

Temperature and concentration	Rates of hydrolysis – Rate constant (s⁻¹)			
	A	B	C	D
298K 0.008M	8.1×10^{-5} ($\pm 0.5 \times 10^{-5}$)	1.1×10^{-5} ($\pm 0.09 \times 10^{-5}$)	3.3×10^{-5} ($\pm 0.3 \times 10^{-5}$)	5.9×10^{-6} ($\pm 1.1 \times 10^{-6}$)
310K 0.008M	2.0×10^{-4} ($\pm 0.1 \times 10^{-4}$)	2.0×10^{-5} ($\pm 0.06 \times 10^{-5}$)	4.9×10^{-5} ($\pm 4.5 \times 10^{-5}$)	1.0×10^{-5} ($\pm 0.08 \times 10^{-5}$)
323K 0.008M	3.8×10^{-4} ($\pm 0.6 \times 10^{-4}$)	4.8×10^{-5} ($\pm 0.8 \times 10^{-5}$)	1.3×10^{-4} ($\pm 0.5 \times 10^{-4}$)	4.2×10^{-5} ($\pm 0.5 \times 10^{-5}$)

Table 15: Table to show β-sultam rates of hydrolysis at temperature 298K, 310K, 323K and 0.008M

When comparing the change in enthalpy, at 0.008M and 0.02M the results are consistent and lie within the error range (**Table 16** and **17**)
.

Temperature and concentration	Change in Enthalpy - $\Delta H°$ (298K) (kJmol⁻¹)			
	A	B	C	D
298K 0.02M	- 39.5 (± 1.4)	- 25.5 (± 1.5)	- 36.2 (± 5.5)	- 15.7 (± 2.6)

Table 16: Table to show β-sultam change enthalpy values at temperature 298K and 0.02M

Temperature and concentration	Change in Enthalpy - ΔH (kJmol^{-1})			
	A	B	C	D
298K 0.008M	- 14.6 (± 1.6)	- 21.8 (± 3.1)	- 28.9 (± 1.9)	- 31.8 (± 3.9)
310K 0.008M	- 16.1 (± 2.9)	- 22.0 (± 3.7)	- 29.5 (± 4.8)	- 27.0 (± 3.1)
323K 0.008M	- 19.1 (± 3.1)	- 21.7 (± 2.1)	- 30.5 (± 1.4)	- 32.3 (± 3.5)

Table 17: Table to show β-sultam change in enthalpy values at temperature 298K, 310K and 323K and 0.008M

The change in enthalpy for A and D is inconsistent with all other data shown. This may have been a result of hydrolysis prior to experimentation or possibly the use of different batches.

First order calorimetric outputs were observed for all the β-sultams and hydrolysis was confirmed by ^{1}H NMR. The order for the rate of hydrolysis for the substituted β-sultams is as follows $C_6H_4Cl > C_6H_5 > C_6H_7OMe > N$-acyl. The rate for C is greater than B then D, and then F. Hydrolysis studies conducted on the unsubstituted β-sultam at pH 4 and pH 8 showed no rate change at 298K. It is noteworthy that the unsubstituted β-sultam is the least reactive of all at pH 8 but the most reactive of all at pH 4. This clearly implies that the N-aroyl and N-acyl β-sultams are reacting via different mechanisms at these two pHs, whilst the unsubstituted β-sultam seems to react in the same manner, suggested mechanisms are shown in **Figure 92 a/b**
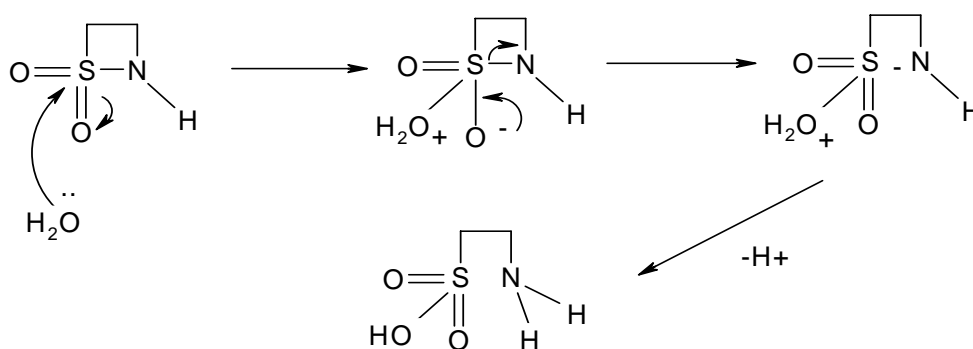

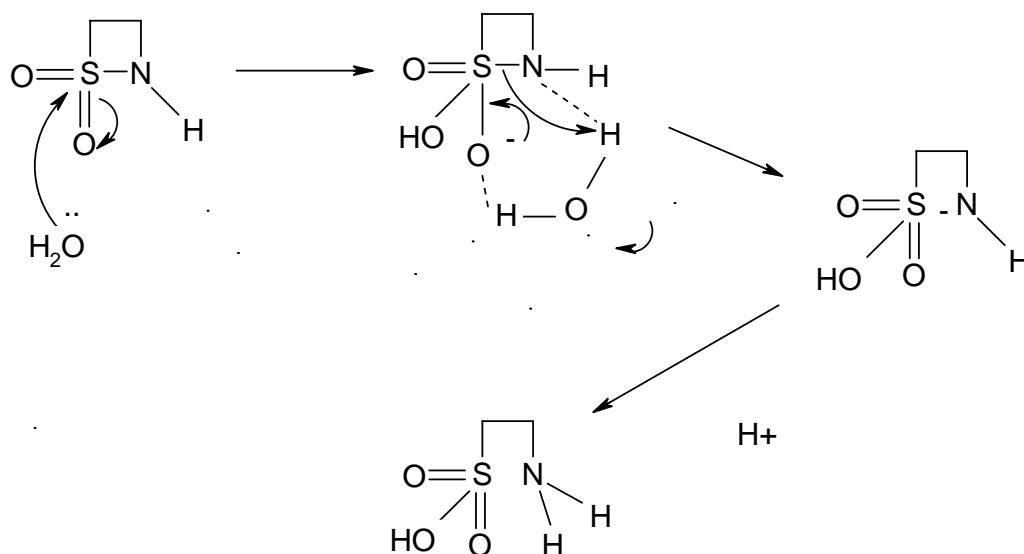**Figure 92a: Unsubstituted β-sultam A hydrolysis mechanism.**

Figure 92b: Unsubstituted β-sultam A hydrolysis mechanism.

However for the *N*-acyl and *N*-aroyl β-sultams a significant change in rate is observed when comparing rates of hydrolysis at pH 4 and pH 8. Therefore implying a change in mechanism. Possible mechanisms for pH 4 are shown in **Figures 93** and **94**, but are linked by the common need for acid catalysis. **Figure 93** shows an acid catalysed hydrolysis with a bimolecular rate determining step, with **Figure 94** showing the unimolecular version.
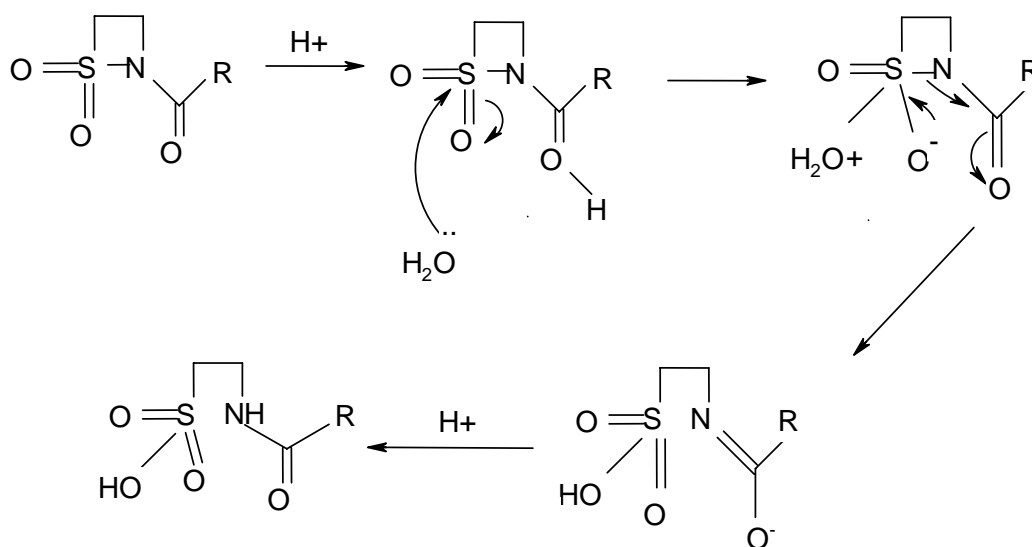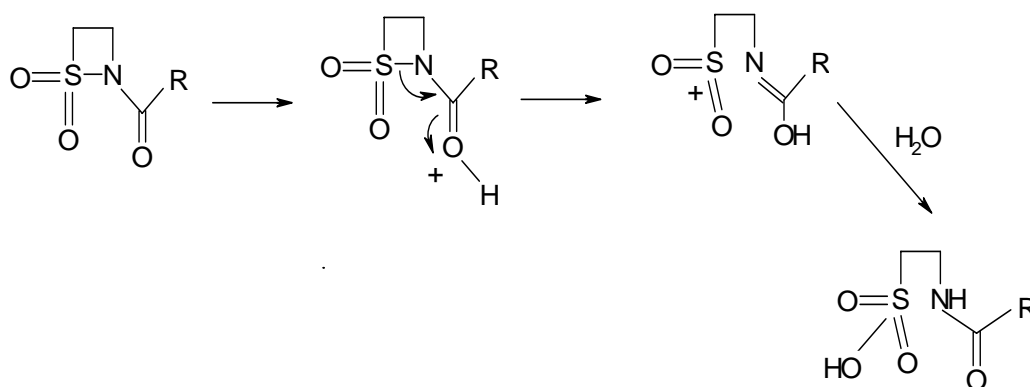

Figure 93: Hydrolysis at pH4.

Figure 94: Hydrolysis at pH4.

The mechanism at pH 8 changes in response to the non-availability of acid catalysis and a likely mechanism, to that used for the unsubstituted system shown in **Figure 95**.
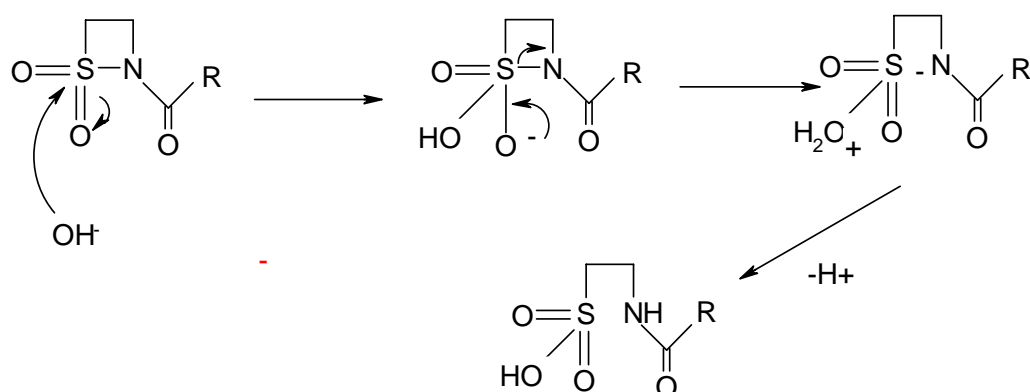

Figure 95: Hydrolysis at pH8.

3.10 Conclusion

Solid state IMC on β-sultams has never been conducted previously. The solid state calorimetric experiments in these studies show that substituents effect stability, revealing that electron donating aromatic rings stabilise *N*-aroyl systems. In addition calorimetric experiments provided information on rates and enthalpies for β-sultam A (ethane sultam) at three different temperatures, 298K, 310K and 323K.

Further calorimetric experiments were conducted at different relative humidities and in solution at pH 7 (water/acetonitrile). The calorimetric outputs observed for the experiments conducted at different relative humidities showed variable

results too complex to analyse. The outputs were possibly a combination of different mechanisms: generation of water vapour, absorption of water, recrystallisation or sorption of water vapour onto the powder. The experiments conducted at pH 7 using different volumes of water, acetonitrile and β-sultam did not produce significant calorimetric outputs to allow analysis.

The solution state experiments were first conducted at pH 4 using a 0.02M solution of β-sultam. The first significant point is that β-sultam A appears to be the least stable in comparison to the substituted β-sultams. The rate at which the β-sultams hydrolyse from most reactive to least reactive are as follows: A>C>B>D. When comparing the substituted β-sultams the rate at which they hydrolyse relates classically to aromatic substituent effects. In addition the enthalpy correlates well with the different rates of hydrolysis. For example β-sultam A appears to be the least stable, the rate constant shows a quicker rate of hydrolysis and the change in enthalpy is greater.

In the *N*-aroyl series, it was found that an electron donating group (OMe) increased the stability of the β-sultam ring towards hydrolysis whereas the electron withdrawing chlorine substituent decreased the stability of the β-sultam ring towards hydrolysis and rendered this molecule the most easily hydrolysed of the *N*-substituted systems. In all cases ^{1}H NMR spectroscopy was used to verify that the process under observation was indeed hydrolysis.

Calorimetric experiments were also conducted at pH 4 at 0.008M concentration at three different temperatures, 298K, 310K and 323K. The results obtained showed the exact same trend and there was no real change in half life.

The experiments conducted at pH 8 showed rapid hydrolysis for the substituted β-sultams in comparison to experiments conducted at pH 4 and in the solid state. A clear difference witnessed at pH 8 is that β-sultam A appears to be the most stable rather than the least. The *N*-aroyl substituted β-sultams show the same order of reactivity at both pHs with β-sultam C too reactive to analyse at

pH 8. Although the *N*-aroyl β-sultams were more reactive at pH 8 than pH 4, the unsubstituted β-sultam showed no such change in reactivity, implying different mechanisms for the *N*-aroyl systems at the two pHs.

Another major advantage of the IMC (TAM) technique is that small amounts of compound can be used, with only 10 mg used for most experiments. This was advantageous in reducing the amount of time spent on synthesis.

Finally it was found that *N*-acyl β-sultam F could be analysed using this technique, allowing kinetic data to be obtained without recourse to U.V. techniques. This is the first time IMC (TAM) has been used to study β-sultams and has been shown to be a reliable technique for obtaining kinetic and thermodynamic data for the hydrolysis of β-sultams.

References

1. M.A.A. O'Neill, PhD Thesis, University Of Greenwich, **2002**, 16.

2. A.E. Beezer, A.K. Hills, M.A.A. O'Neill, A.C. Morris, K.T.E. Kierstan, R.M. Deal, L.J. Waters, J. Hadgraft, J.C. Mitchell, J.A. Connor, J.E. Orchard, R.J. Willson, T.C. Hofelich, J. Beaudin, G. Wolf, F. Baitalow, S. Gaisford, R.A. Lane, G. Buckton, M.A. Phipps, R.A. Winneke, E.A. Schmitt, L.D. Hansen, D. O'Sullivan, M.K. Parmer, The imidazole catalysed hydrolysis of triacetin: an inter- and intra-laboratory development of a test reaction for isothermal heat conduction microcalorimeters used for determination of both thermodynamic and kinetic parameters, *Thermochimica Acta*, 380, (1), **2001**, 13-17.

3. M.G. Nordmark, J. Laynez, A. Schön, J. Suurkuusk, I. Wadso, Design and testing of a new microcalorimetric vessel for use with living cellular systems and in titration experiments, *Journal of Biochemical and Biophysical Methods*, 10, (3-4), **1984**, 187-202.

4. M. Angberg, C. Nyström, S. Castensson, Evaluation of heat-conduction microcalorimetry in pharmaceutical stability studies (II) methods to evaluate the microcalorimetric response, *International Journal of Pharmaceutics,* 61, (1-2), **1990**, 67-77.

5. M.J. Pikal, K.M. Dellerman, Stability testing of pharmaceuticals by high-sensitivity isothermal calorimetry at 25°C: cephalosporins in the solid and aqueous solution states, *International Journal of Pharmaceutics*, 50, (3), **1989**, 233-252.

6. A.G.S. Prado, C. Airoldi, Microcalorimetry of the degradation of the herbicide 2,4-D via the microbial population on a typical Brazilian red Latosol soil , *Thermochimica Acta*, 371, (1-2), **2001**, 169-174.

7. E.A. Schmitt, K. Peck, Y. Sun, J-M. Geoffroy, Rapid, practical and predictive excipient compatibility screening using isothermal microcalorimetry, *Thermochimica Acta*, 380, (2), **2001**, 175-183.

8. S. Conti, S. Gaisford, G. Buckton, U. Conte, Solution calorimetry to monitor swelling and dissolution of polymers and polymer blends, *Thermochimica Acta*, 450, (1-2), **2006**, 56-60.

9. J. Bell, *The statistics for practical people series*, 1988.

10. A.E.Beezer, An outline of new calculation methods for the determination of both thermodynamic and kinetic parameters from isothermal heat conduction microcalorimetry, *Thermochimica Acta*, 380, **2001**, 205-208.

11. L.J. Waters, PhD Thesis, University Of Greenwich **2003**, 50.

12. J.F. Kirsch, W.P. Jencks, Base catalysis of imidazole catalysis of ester hydrolysis, *Journal of the American Society*, 86, (5), **1964**, 833-837.

13. M. Angberg, C. Nyström, S. Castensson, Evaluation of heat-conduction microcalorimetry in pharmaceutical stability studies. VII. Oxidation of ascorbic acid in aqueous solution, *International Journal of Pharmaceutics,* 90, (1), **1993**, 19–33.

14. J. Waltersson, P. Lundgren, The effect of mechanical communition on drug stability, *Acta Pharmaceutica Suecica*, 22, (5), **1985**, 291–300.

15. M. Mumenthaler, H. Leuenberger, Atmospheric spray-freeze drying: a suitable alternative in freeze-drying technology, *International Journal of Pharmaceutics,* 72, (2), **1991**, 97–110.

16. T. Konno, Physical and chemical changes of medicinals in mixtures with adsorbents in the solid state IV. Reduced-pressure mixing for practical use of amorphous mixtures of flufenamic acid, *Chemical and Pharmaceutical Bulletin,* 38, (7), **1990**, 2003.

17. M.J. Pikal, A.L. Lukes, J.E. Lang, K. Gaines. Quantitative crystallinity determinations for *β*-lactam antibiotics by solution calorimetry, *Journal of Pharmaceutical Sciences,* 67, **1978**, 767–772.

18. L-E. Briggner, G.Buckton, K. Byström, P. Darcy, The use of isothermal microcalorimetry in the study of changes in crystallinity induced during the processing of powders, *International journal of Pharmaceutics*, 105, (2), **1994**, 125–135.

19. L. J. Waters, S. Naz, K. Hemming, Calorimetric investigations of the hydrolytic degradation for a series of *β*-sultams, *Journal of Thermal Analysis and Calorimetry*, 93, 2, **2008**, 339-342.

4. Calorimetric studies of β-lactams

4.0 Introduction

β-Lactams are four membered cyclic amides.[1] β-lactams are highly strained, whereby the reduced bond angle is responsible for angle strain and the rigid four membered ring is responsible for increased torsional strain. The β-lactam ring is part of the structure of several antibiotic families, for example, penicillins and cephalosporins. These antibiotics primarily work by inhibiting bacterial cell wall synthesis; however these antibiotics are no longer as effective due to the build up of resistance. The primary reason is the bacterial production of β-lactamases which bind to the β-lactam ring in an irreversible manner, rendering it ineffective, as discussed in the introduction.

In order to provide a relevant comparison between the β-sultams studied previously in this thesis and a series of β-lactams, it was necessary to work with the identical series of *N*-aroyl analogues.

The *N*-aroyl β-lactams used in this work contain both endocyclic and exocyclic centres which are potential sites for nucleophilic attack. Hydrolysis could occur via two potential routes, attack at the exocyclic carbonyl (route 1) and endocyclic carbonyl (route 2) to give a ring opened product (**Figure 96**). Further hydrolysis in each case could then lead to a β-amino acid and benzoic acid.
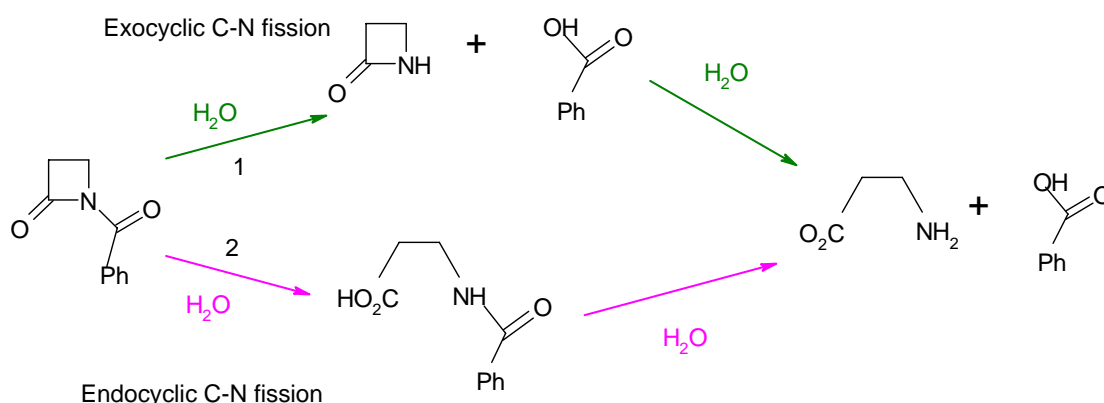

Figure 96: *N*-benzoyl β-lactam endocyclic and exocyclic hydrolysis.

Previous non-calorimetric kinetic studies have been conducted on the *N*-benzoyl β-lactams. These studies showed that alkaline hydrolysis occurred via competing exocyclic (19%) and endocyclic (81%) C-N bond fission. The pH-independent studies showed competing exocyclic (<3%) and endocyclic (>97%) C-N bond fission. The acid catalysed hydrolysis showed competing exocyclic (<4%) and endocyclic (96%) C-N bond fission.[2] β-Lactams are also known to be much less susceptible to hydrolysis than the corresponding β-sultams.

In order to establish if isothermal microcalorimetry (IMC) could be used to detect reactivity at these relatively low levels, it was decided to examine the β-lactams A-D and compare their reactivity to the β-sultams. Hydrolysis studies using the same calorimetric methods discussed in Chapter 3 were conducted at the University of Greenwich. β-Lactams (**Figure 97**) were synthesised at the University of Huddersfield from the unusubstitued β-lactam (A), which was purchased from Aldrich.
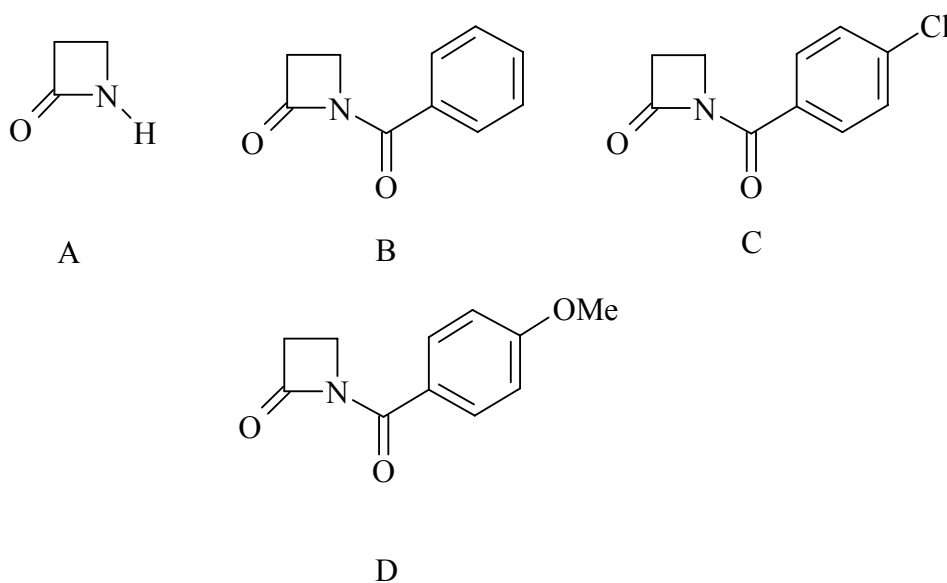

Figure 97: β-lactams used to conduct hydrolysis experiments.

4.1 TAM experimental

Experiments were conducted at the University of Greenwich. TAM 2277 was the isothermal microcalorimeter (IMC) used to conduct the hydrolysis studies. MicroCal origin was used to analyse the TAM data and **Equation 18** to

calculate the ΔH, where $\Phi_o\,(\mathrm{d}q/\mathrm{d}t)$ is the intercept, -k is the slope, A the number of moles and n the order of reaction. **Equation 18** was derived from **Equation 19**.[3]

$$\Delta H = \frac{\Phi_o \times 10^{-6}}{-k \times A^n} \qquad\qquad \textbf{Equation 18}$$

$$\left(\frac{\mathrm{d}q}{\mathrm{d}t}\right) = k\mathrm{HA}^n \qquad\qquad \textbf{Equation 19}$$

4.1.1 Hydrolysis of β-lactams A, B, C and D at 298K and 323K in aqueous solution (controlled ionic strength, pH 8 at 0.008M).

Reactions were conducted at pH 8 and 323K. A buffer solution consisting of 0.60 g sodium dihydrogen phosphate and 2.26 g potassium chloride was added to 50 mL distilled water and the mixture was shaken vigorously to ensure thorough mixing. HCl was added to obtain pH 8 using a pH meter. The β-lactam was mixed with acetonitrile to make a 0.008M solution. The reference ampoule was filled with 2 mL buffer, 1 mL acetonitrile and hermetically crimp-sealed. The reaction ampoule was filled with 2 mL buffer and 1 mL of the β-lactam solution and hermetically crimp-sealed. Both ampoules were lowered into the calorimeter and left to thermally equilibrate for 40 minutes in the load position prior to being lowered over a one minute period to the measurement position, at which point data recording began. The same protocol was used for experiments at 298K. These experiments were repeated several times to ensure accuracy, validity and reliability was achieved.

4.1.2 Hydrolysis of β-lactams A, B, C and D at 298K and 323K in aqueous solution (controlled ionic strength, pH 4 at 0.008M).

The reaction was conducted at pH 4. A buffer solution consisting of 0.49 g potassium acetate and 3.35 g potassium chloride was added to 50 mL distilled water and shaken vigorously to ensure thorough mixing. HCl was added to obtain pH 4.0 using a pH meter. The β-lactam was mixed with acetonitrile to make a 0.008M solution. The reference ampoule was filled with 2 mL buffer, 1 mL solvent and hermetically crimp-sealed. The reaction ampoule was filled with 2 mL buffer, 1 mL of the β-lactam solution and hermetically crimp-sealed. Both ampoules were lowered into the calorimeter and left to thermally equilibrate for 40 minutes in the load position prior to being lowered over a one minute period to the measurement position, at which point data recording began. These experiments were repeated several times to ensure accuracy, validity and reliability was achieved.

4.2 Results for the hydrolysis of β-lactams A, B, C and D at 323K in aqueous solution (controlled ionic strength, pH 8 at 0.008M)

Data were analysed after 5000s, the data before this reflects the disruption caused to the power output upon lowering the ampoules. Data analysis ceased after the reaction had reached completion, the calorimetric output had reached zero or when the signal was too close to the base line. All experiments discussed are first order hydrolysis reactions. Results are summarised in **Table 18**, and some typical calorimetric outputs follow. β-lactam A showed no significant calorimetric output under these conditions.

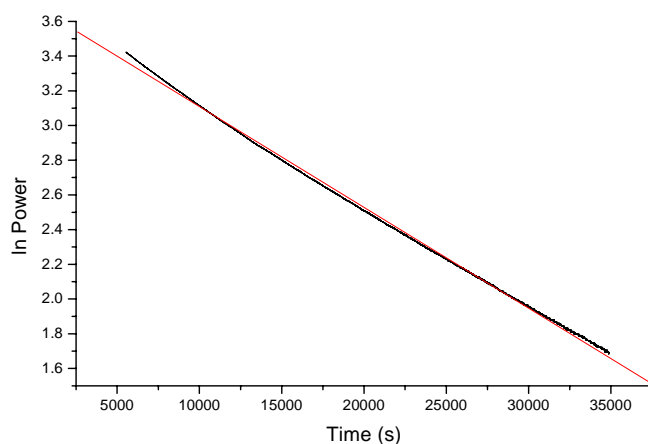| 323K 0.008M	A	B	C	D
t $_{1/2}$ (s)	-	15503	11454	28285
Rate constant (s^{-1})	-	4.23 x10^{-5}	5.80 x10^{-5}	2.07 x10^{-5}
	-	4.63 x10^{-5}	5.00 x10^{-5}	3.02 x10^{-5}
	-	4.77 x10^{-5}	6.59 x10^{-5}	2.36 x10^{-5}
	-	4.69 x10^{-5}	6.86 x10^{-5}	2.76 x10^{-5}
	-	4.04 x10^{-5}	6.04 x10^{-5}	2.06 x10^{-5}
Average	-	**4.5 x10^{-5} (± 0.9 x10^{-5})**	**6.0 x10^{-5} (± 2.0 x10^{-5})**	**2.5 x10^{-5} (± 1.2 x10^{-5})**
ΔH°(323K) (kJmol^{-1})	-	-15.28	- 16.79	- 21.65
	-	- 16.36	- 19.62	- 15.59
	-	- 15.01	- 16.69	- 20.55
	-	- 14.25	- 18.24	- 14.85
	-	-16.00	- 19.10	- 21.53
Average	-	**- 15.4 (± 2.3)**	**- 18.1 (± 3.7)**	**-18.8 (± 9.3)**

Table 18: A summary of the data obtained for compounds A, B, C and D in solution at 323K.
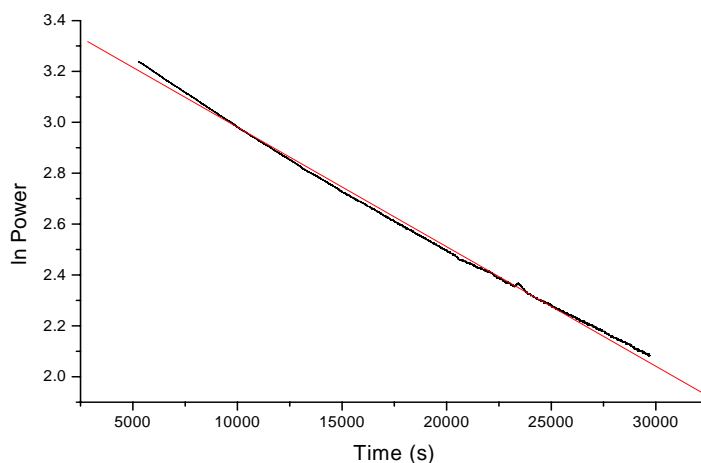
Slope = -4.69 x 10^{-5}, intercept = 3.45, R^2 = - 0.998

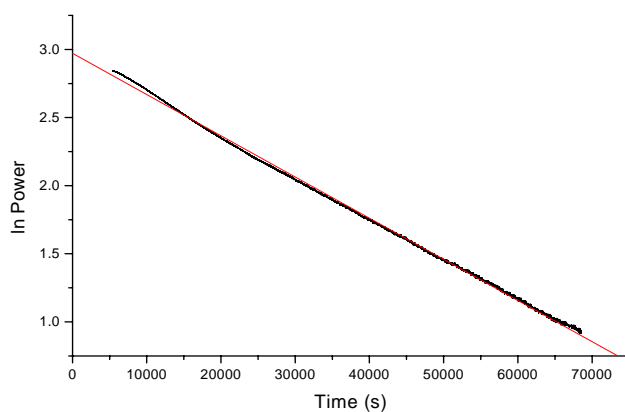**Figure 98: An example of a typical calorimetric output for β-lactam B at 323K, 0.008M and pH 8.**

The data was analysed from 5000s – 30000s and over 2 half lives. The rate constant was 4.69 x 10^{-5}s^{-1} and ΔH was - 14.25 kJmol^{-1}.

Slope = -5.80 x 10^{-5}, intercept = 3.68, R^2 = - 0.999

Figure 99: An example of a typical calorimetric output for β-lactam C at 323K, 0.008M and pH 8.

The data was analysed from 5000s – 35000s and over 3 half lives. The rate constant was 5.80 x 10^{-5}s^{-1} and ΔH was - 16.79 kJmol^{-1}.

Slope = -3.02 x 10^{-5}, intercept = 2.97, R^2 = - 0.999

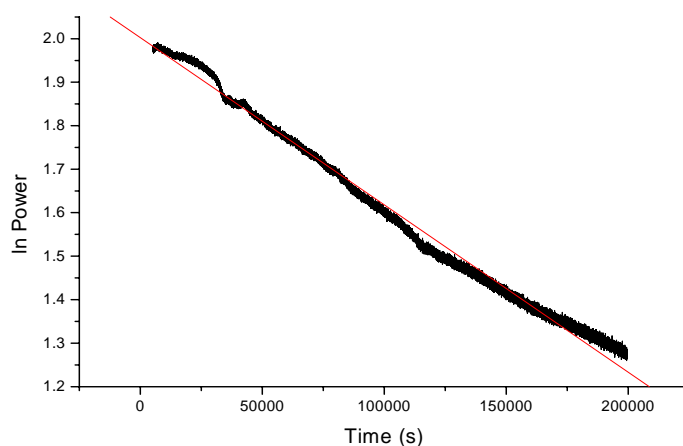**Figure 100: An example of a typical calorimetric output for β-lactam D at 323K, 0.008M and pH 8.**

The data was analysed from 5000s – 68000s and over 2.5 half lives. The rate constant was 3.02 x 10^{-5}s^{-1} and ΔH was - 15.59 kJmol^{-1}.

4.2.1 Results for the hydrolysis of β-lactams A, B, C and D at 298K in aqueous solution (controlled ionic strength, pH 8 at 0.008M)

Data were analysed after 5000s, the data before this reflects the disruption caused to the power output upon lowering the ampoules. Data analysis ceased after the reaction had reached completion, the calorimetric output had reached zero or when the signal was too close to the base line. All experiments discussed were first order hydrolysis reactions. Results are summarised in **Table 19**, it should be noted that β-lactam A and D were unreactive under the experimental conditions.

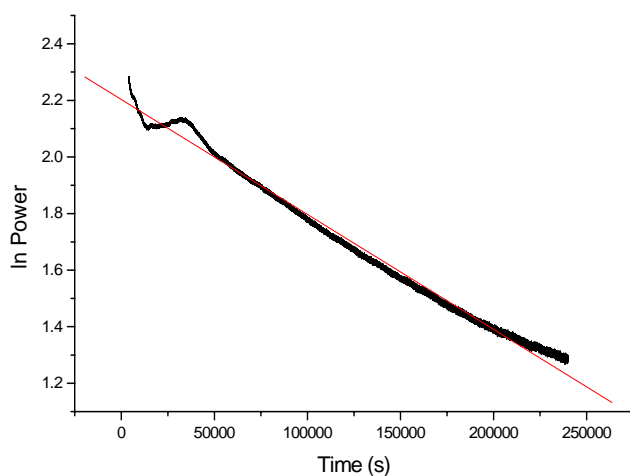| 298K 0.008M	A	B	C	D
t $_{1/2}$ (s)	-	18,1800	15,7500	-
Rate constant (s^{-1})	-	3.49×10^{-6}	5.45×10^{-6}	-
	-	3.84×10^{-6}	3.86×10^{-6}	-
	-	3.84×10^{-6}	4.06×10^{-6}	-
	-	4.08×10^{-6}	4.24×10^{-6}	-
Average	**-**	**3.8×10^{-6} ($\pm 0.8 \times 10^{-6}$)**	**4.4×10^{-6} ($\pm 2.3 \times 10^{-6}$)**	**-**
$\Delta H°(298K)$ (kJmol^{-1})	-	- 43.87	-50.63	-
	-	- 41.21	-53.05	-
	-	- 40.77	-54.66	-
	-	-38.85	-49.88	-
Average	**-**	**-41.2 (± 6.6)**	**52.1 (± 7.0)**	**-**

Table 19: A summary of the data obtained for compounds B and C in solution at 298K at pH 8.

Slope = -3.84 x 10^{-6}, intercept = 2.00, R^2 = - 0.996

Figure 101: An example of a typical calorimetric output for β-lactam B at 298K, 0.008M and pH 8.

The data was analysed from 5000s – 200000s and over 1 half life. The rate constant was 3.84 x 10^{-6}s^{-1} and ΔH was – 40.77 kJmol^{-1}.

Slope = 4.06 x 10^{-6}, intercept = 2.20, R^2 = - 0.995

Figure 102: An example of a typical calorimetric output for β-lactam C at 298K, 0.008M and pH 8.

The data was analysed from 4000s – 240000s and over 1.5 half lives. The rate constant was 4.06 x 10^{-6}s^{-1} and ΔH was - 54.66mol^{-1}.

4.3 Discussion

Initial experiments were conducted at 323K pH8. β-Lactams are more stable than β-sultams therefore the highest temperature was used to make initial comparisons and to see if the method was compatible with the TAM. No reaction was observed for any of the β-lactams studied at pH 4.

No significant calorimetric output was observed for β-lactam A at temperatures 323K, 298K, pH 4 and pH 8. Results for B and C at 298K and B, C and D at 323K showed that a change in substituent affects the hydrolysis. The electron donating substituents have a stabilising effect whereas electron withdrawing substituents remove electron density from the system contributing to its instability. At 323K β-lactam C when compared to β-lactams B and D appears to be the most reactive. At 298K the rate of hydrolysis for β-lactam C is very close to that of β-lactam B. No significant calorimetric output was observed for β-lactam D at 298K. As discussed previously, the methoxy substituent has a stabilising effect therefore at 298K β-lactam D is not reactive. At 323K β-lactam D showed a significant calorimetric output, but was still the least reactive of the three systems studied.

To clarify hydrolysis had occurred ^{1}H NMR studies were conducted at 323K for all four β-lactams. The results for β-lactam A, which IMC (TAM) indicated was not reactive, are shown in **Figures 103**, **104**, **105**, **106** and **107**. The CH$_2$-NR at 3.40 ppm and CH$_2$CO at 3.80 ppm peaks are clearly present.
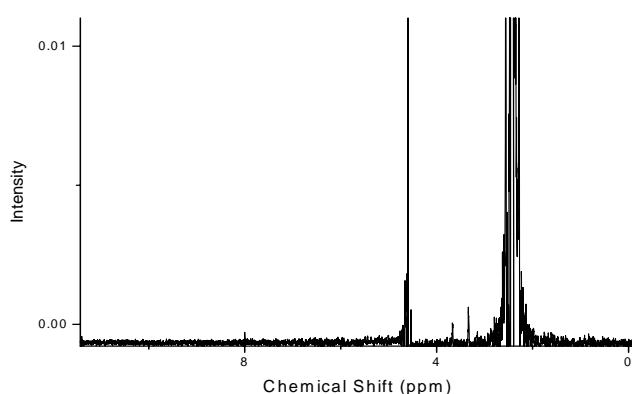
β-Lactam A

Figure 103: Hydrolysis ^{1}H NMR for β-lactam A at hour 1, 323K.
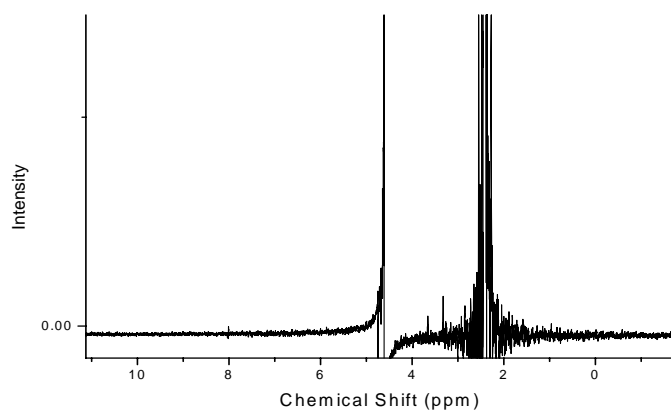
Figure 104: Hydrolysis ^{1}H NMR for β-lactam A at hour 5, 323K.
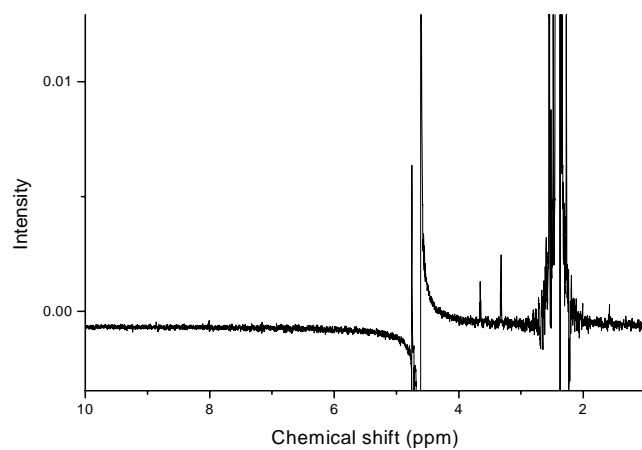
Figure 105: Hydrolysis ^{1}H NMR for β-lactam A at hour 10, 323K.
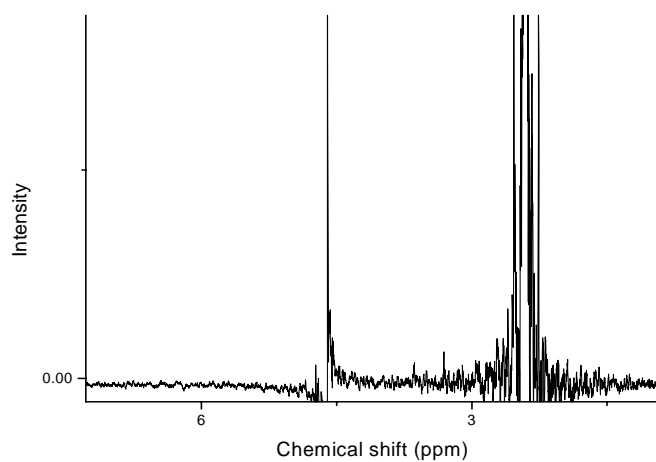
Figure 106: Hydrolysis ^{1}H NMR for β-lactam A at hour 15, 323K.
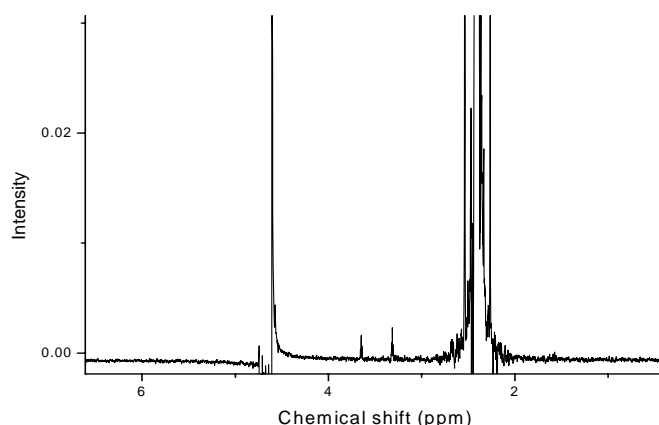
Figure 107: Hydrolysis ^{1}H NMR for β-lactam A at hour 20, 323K.

^{1}H NMR analysis confirmed that no reaction had taken place. **Figures 103, 104, 105**, **106** and **107** display the intact β-lactam A, starting at hour one and ending at hour 20 (**Figure 107**). There are two clear peaks in all spectra corresponding to the intact β-lactam (CH$_2$-NR at 3.40 ppm and CH$_2$CO at 3.80 ppm). The 3 *N*-aroyl β-lactams B, C and D were reactive at 323K and the ^{1}H NMR results for these systems are discussed below. **Figure 108** shows the atom labels that are used in the subsequent discussion for β-lactam B.
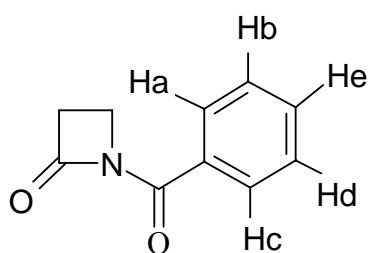

Figure 108: Atom labels used for ^{1}H NMR analysis.

β-Lactam B

β-Lactam B hydrolysis was observable using the TAM (**Table 18** and **19**) but was also studied using ^{1}H NMR in order to verify that a chemical process was being observed. There is no hydrolysis at hour one (see **Figure 109**) where the following peaks correspond to the intact β-lactam: Ha/Hc 8.01 ppm, He 7.80

ppm, Hb/Hd 7.45 ppm. The CH$_2$NR peak is at 3.50 ppm and the CH$_2$CO resonates at 2.95 ppm. **Figure 110** shows there is hydrolysis at hour 5. The intact β-lactam peaks resonate at 8.01 ppm for Ha/Hc, 7.80 ppm for He and 7.45 ppm for Hb/Hd. Peaks corresponding to the hydrolysed β-lactam B are slightly to the right of the intact β-lactam peaks at 8.00 ppm, 7.77 ppm and 7.44 ppm. The original CH$_2$NR and CH$_2$CO peaks can still be seen in addition to the corresponding hydrolysed CH$_2$NR and CH$_2$CO peaks at 3.00 ppm and 2.70 ppm which have shifted slightly to the right. **Figure 111** shows hydrolysis at hour 10 and reveals the original signals to be significantly diminished whilst the new signals ascribed to the hydrolysis product are enhanced.
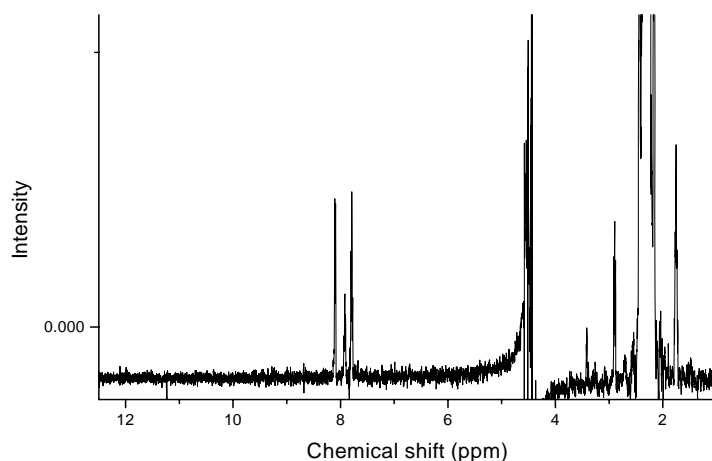

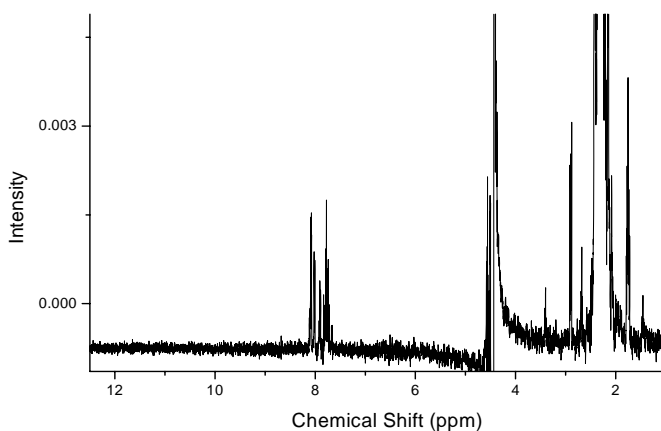**Figure 109: Hydrolysis ^{1}H NMR for β-lactam B at hour 1, 323K**

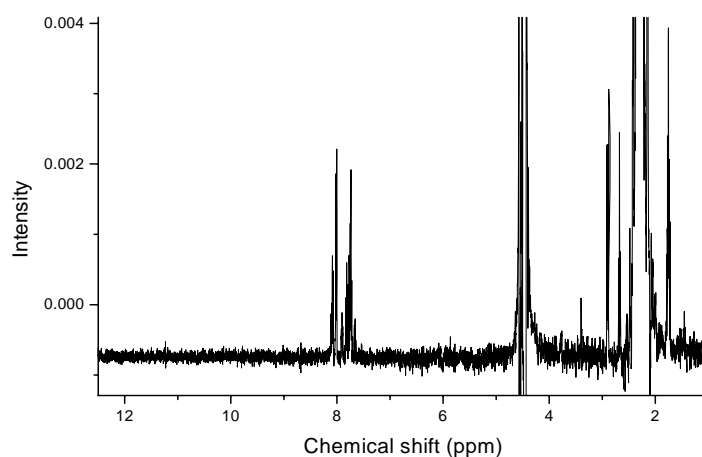**Figure 110: Hydrolysis ^{1}H NMR for β-lactam B at hour 5, 323K.**

Figure 111: Hydrolysis ^{1}H NMR for β-lactam B at hour 10, 323K.
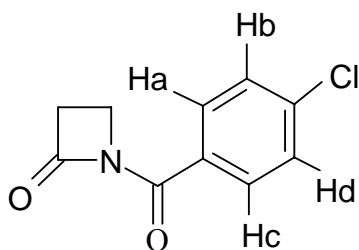
β-Lactam C

Figure 112: Atom labels used for ^{1}H NMR analysis.

Figure 112 was used to analyse the ^{1}HNMR for β-lactam C. **Figure 113** shows no hydrolysis for β-lactam C at hour 1. Within the aromatic region, 2 distinct peaks can be seen corresponding to Ha/Hc at 8.01 ppm and Hb/Hd at 7.70 ppm with the CH$_2$CO peak just visible at 2.98 ppm. **Figure 114** displays extra peaks due to the hydrolysis product within the aromatic region at hour 5. There are multiple peaks corresponding to possible competitive endocyclic and exocyclic C-N fission.
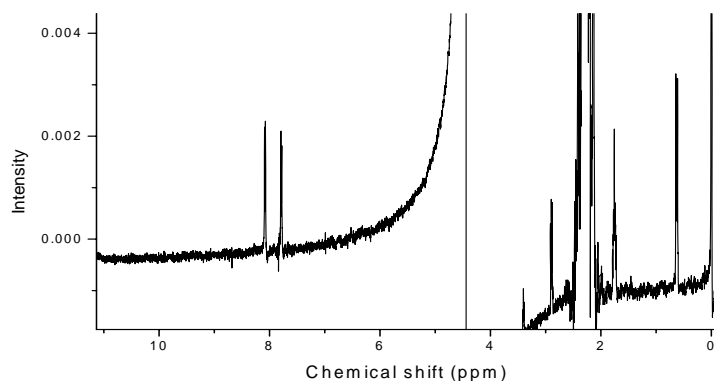
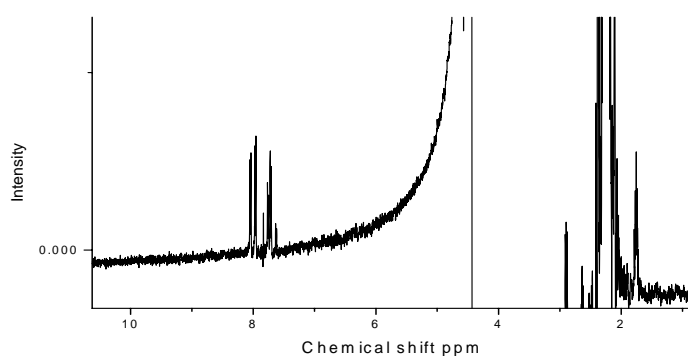**Figure 113: Hydrolysis ¹H NMR for β-lactam C at hour 1, 323K**

Figure 114: Hydrolysis ¹H NMR for β-lactam C at hour 5, 323K.
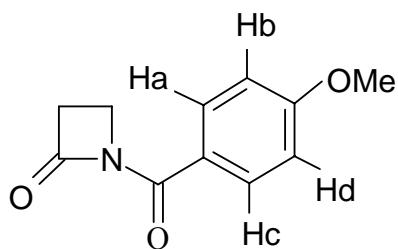
β-Lactam D

Figure 115: Atom labels used for ¹H NMR analysis.

Figure 115 shows the atom labels used for ¹H NMR analysis. **Figure 116** shows no hydrolysis for β-lactam D at hour 1. There are two peaks within the phenyl region corresponding to Ha/Hc resonating at 8.20 ppm and Hb/Hd at 7.20 ppm. The methoxy peak (OCH₃) cannot be seen and is embedded into the MeCN signal. The CH₂N and CH₂CO signals cannot be recognised and are embedded into the noise. **Figure 117** shows hydrolysis of β-lactam D at hour 5 and this is indicated by the presence of new peaks at 7.95 ppm and at 7.18 ppm.

By hour 10 (**Figure 118**) further peaks have appeared again indicating that competing endocyclic and exocyclic amide hydrolysis might be occurring.
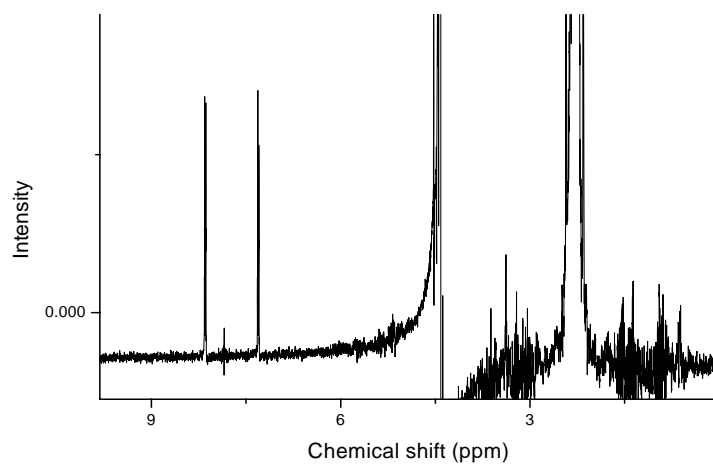

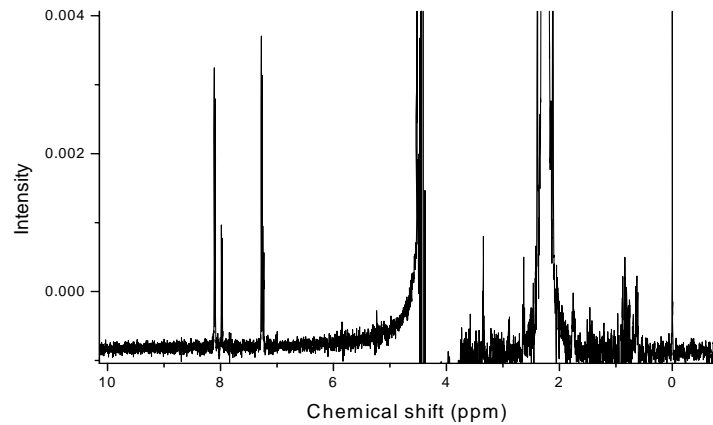**Figure 116: Hydrolysis ¹H NMR for β-lactam D at hour 1, 323K.**

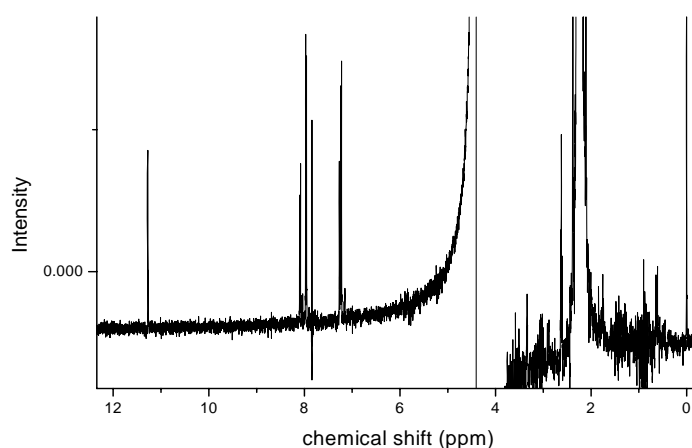**Figure 117: Hydrolysis ¹H NMR for β-lactam D at hour 5, 323K.**

Figure 118: Hydrolysis ^{1}H NMR for β-lactam D at hour 10, 323K.

4.4 Conclusion

β-Lactams were shown to have a lower reactivity than β-sultams as expected. Calorimetric studies were conducted to compare stability to hydrolysis with respect to benzene ring substituent effect and the results reflected those of the β-sultams with para-OMe > H > para-Cl >. Like the β-sultams pH 4 generated conditions in which the β-lactams were more stable, so much so that no thermal output was observed. Again it may be that different mechanisms are operating at the two pHs and at pH 4 the reaction is too slow to observe over the time frame used.

At 323K and 298K no output for the unsubstituted β-lactam was observed. ^{1}H NMR studies were conducted and showed no hydrolysis confirming that the system is indeed unreactive. No output was observed for β-lactam D at 298K, reflecting the stability of this system.

4.5 Calorimetric β-sultam and β-lactam comparative study

Synthesising and conducting calorimetric experiments to study the hydrolysis of *N*-aroyl-β-lactams and *N*-aroyl-β-sultams is of great importance. Previous research showed that the β-sultams are about 10^3 fold more reactive than the corresponding β-lactams.[4] Calorimetric studies conducted also showed that β-sultams were more reactive than the corresponding β-lactams in all cases. The

greater reactivity of the *β*-sultams can be explained by comparing the different intermediates involved during the hydrolysis. **Figure 119** and **120** display the relevant hydrolysis mechanisms.
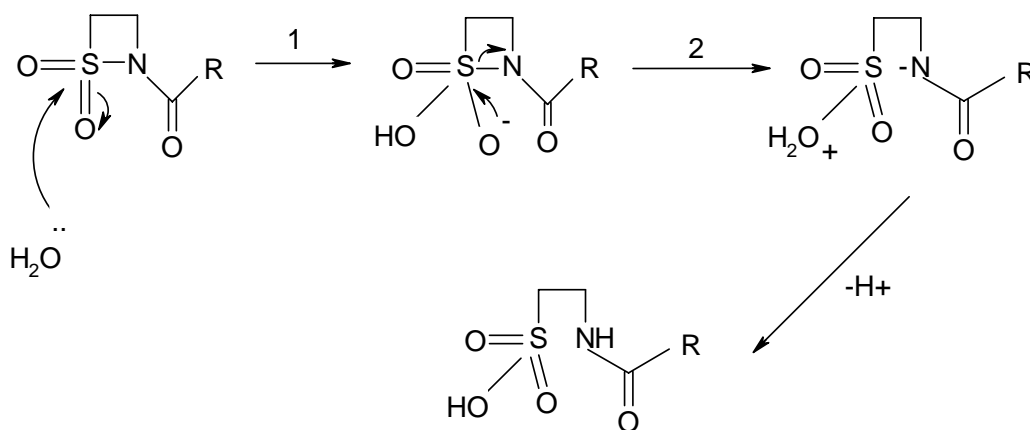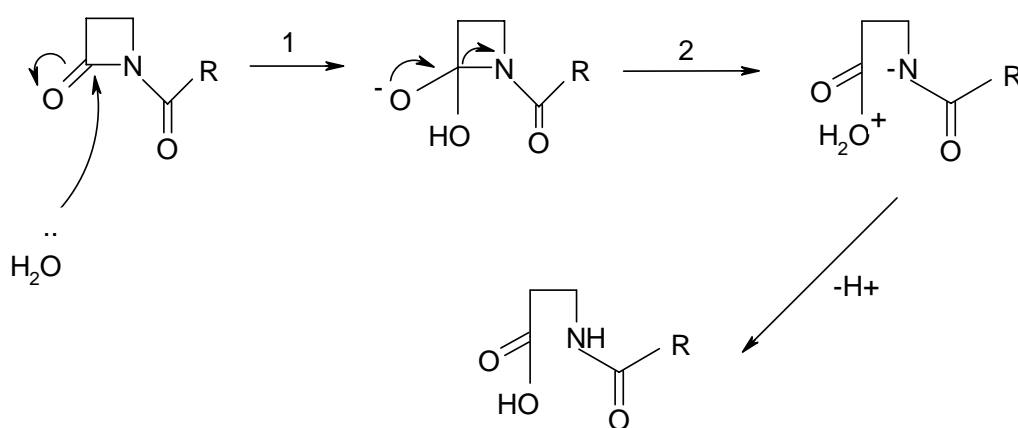

Figure 119: *β*-sultam mechanism.

Figure 120: *β*-lactam mechanism.

When comparing step 1 of the initial hydrolysis for the *β*-sultams to step 1 of the *β*-lactam, step 1 for the *β*-sultams is more favoured as a result of greater relief in ring strain. **Figure 121** compares the intact *β*-sultam and *β*-lactam.
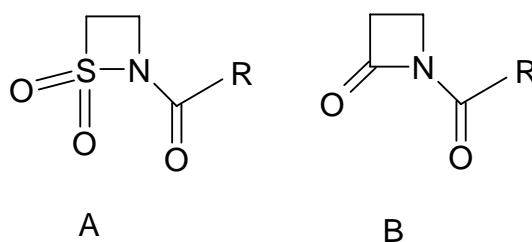
Figure 121: β-sultam (A) and β-lactam (B) structures.

The β-sultam sulphur in A is sp^3 tetrahedral. The ideal tetrahedral angle is 109°. The β-lactam C=O bond angle is sp^2 planar, for which 120° is the ideal bond angle. After step 1 the intermediates formed shown in **Figure 122** can be compared again and the effect bond angle has on ring strain can be seen.
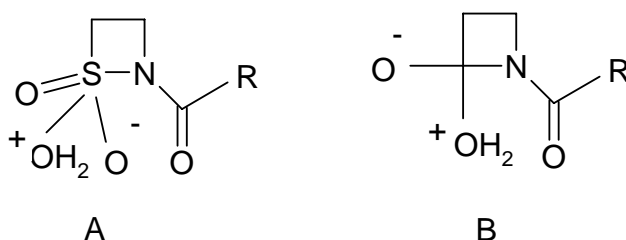
Figure 122: β-sultam (A) and β-lactam (B) structures.

Figure 122 shows the β-sultam intermediate (A) which is now sp^{3}d trigonal bypyramidal and therefore there is increased relief of ring strain as such systems can easily accommodate bond angles of 90°. However for the β-lactam intermediate the bond angle is at 109° (tetrahedral) and is therefore still strained compared with the desired bond angle in a four membered ring (90°).

Usually sulfonamides are less reactive than amides towards hydrolysis. In this case the β-sultam ring is unique and, as discussed more reactive than the β-lactam ring.

References

1. A. Fleming, On the antibacterial action of cultures of a penicillium with special reference to their use in the isolation of B. *influenzae*, *British Journal of Experimental Pathology*, 10, **1929**, 226-236.

2. W.Y. Tsang, PhD Thesis, University of Huddersfield, **2005**.

3. A.E.Beezer, An outline of new calculation methods for the determination of both thermodynamic and kinetic parameters from isothermal heat conduction microcalorimetry, *Thermochimica Acta*, 380, **2001**, 205-208.

4. N.J. Baxter, L.J.M Rigoreau, A.P. Laws, M.I. Page, Reactivity and mechanism in the hydolysis of β-sultams, *Journal of the American Chemical Society*, 122, (14), **2000**, 3375-3385.

5. Conclusions and future work

5.0 Conclusions

The aim of this research was to conduct calorimetric experiments on *β*-sultams and *β*-lactams. Solid and solution state hydrolysis studies were conducted using a Thermal Activity Monitor (TAM 2277) in the batch mode. Calorimetry is an analytical technique widely used to characterise new chemical entities.

Previous studies conducted at the University of Huddersfield using *β*-sultams and *β*-lactams showed a relationship between hydrolysis and *N*-substituents. However, these results were limited to compounds in solution and compounds with a chromophore. Extensive *β*-sultam solid and solution state hydrolysis studies discussed in **Chapter 3** were conducted varying pH, RH, concentration and temperature. To fully understand the hydrolytic process, calorimetric studies were conducted on *β*-lactams under some of the same conditions that the *β*-sultams were studied under. **Table 20** shows a summary of some of the solution state results reported in this thesis for the *β*-sultams. **Figure 123** shows the *β*-sultam structures.
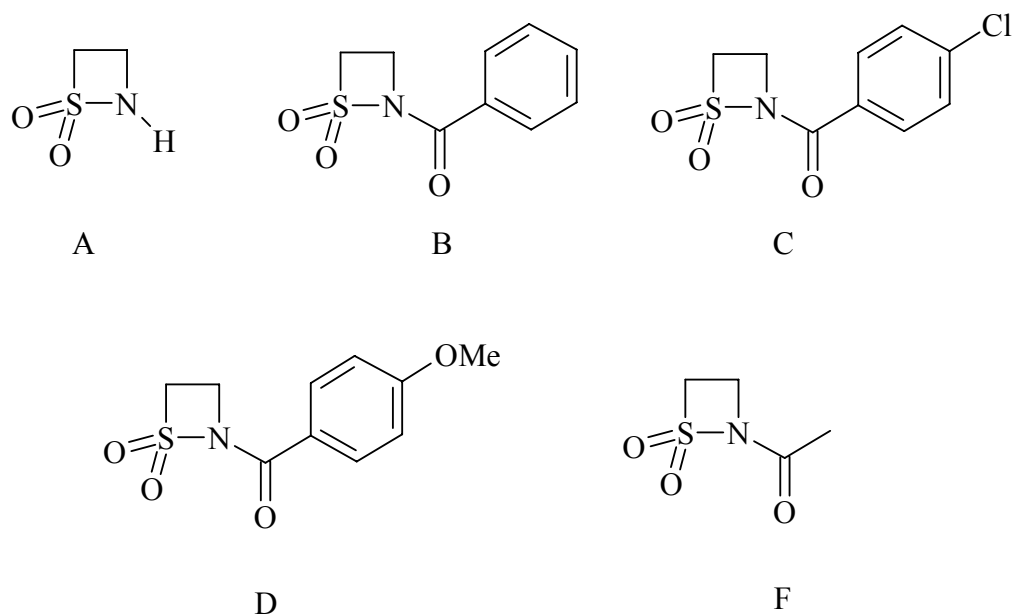

Figure 123: *β*-sultam structures.

Slow Hydrolysis --------------------------------→ Fast Hydrolysis

β-sultam (pH4, 298K) Rate constant (s^{-1})	F 3.6x10^{-6}	D 5.9x10^{-6}	B 1.1x10^{-5}	C 3.3x10^{-5}	A 8.1x10^{-5}
β-sultam (pH8, 298K) Rate constant (s^{-1})	A 8.2x10^{-5}	F 2.2 x10^{-4}	D 1.3 x10^{-3}	B 1.6 x 10^{-3}	C Too fast to measure.

Table 20: Summary of solution state hydrolysis results at 298K pH 4 and pH 8.

With reference to **Table 20** it was found that rates of hydrolysis were slower at pH 4 in comparison to rates at pH 8. The slower reacting β-sultams have electron donating substituents on the nitrogen carbonyl substituent. The para chloro benzoyl substituted β-sultam C is electron withdrawing and the least stable of the substituted systems in all cases. β-Sultam A appears to be the least stable at pH 4 but the most stable at pH 8 although the rate at which it hydrolyses does not change (discussed in **Chapter 3**).

β-Sultam F was synthesised at the University of Huddersfield by Arnaud Pitard. β-Sultam F is an anti-inflammatory agent with potential activity as a taurine pro-drug for the development of a new drug active against Alzheimer's disease. The lack of a chromophore made β-sultam F unsuitable for U.V. detector kinetic studies but ideal for the TAM method developed within this thesis. With an electron releasing methyl group it was predicted that the new β-sultam should have a similar reactivity to that of the methoxy benzoyl compound (D). Results showed that β-sultam F hydrolysed slower than all of the other substituted β-sultams discussed.

A series of analogous β-lactams were also studied calorimetrically. As expected these β-lactams underwent hydrolysis at a slower rate than the analogous β-sultams. The same trend was witnessed with respect to N-substituents. With

respect to the two unsubstituted systems, the β-sultam was reactive whereas the β-lactam was found to be stable to hydrolysis. ^{1}H NMR studies were conducted to clarify that hydrolysis had occurred, and confirmed that hydrolytic processes were being observed, with the exception of the unsubstituted β-lactam A, which was shown to be stable.

To summarise the results and findings of this work each research objective shall now be discussed separately.

5.1 Achievement of research objectives

1. **To synthesise a series of β-sultams and β-lactams using conventional synthetic techniques.**

The first aim of this research was the synthesis of the β-sultams and β-lactams needed for the calorimetric experiments. Traditional organic synthetic techniques were used and are discussed in detail in Chapter 2. Once synthesis was complete, column chromatography (sometimes repeatedly) was used to purify the compounds. TLC was used to monitor the reactions and to confirm the purity of the final compounds. Traditional analytical techniques (IR and ^{1}H NMR) were used to analyse the pure compounds.

2. **To conduct solid state calorimetric experiments to determine the stability of four β-sultams (A-D).**

Initial solid state experiments were conducted on β-sultams A-D. Experiments were conducted at three different temperatures 298K, 310K and 323K. IMC batch experiments were conducted using TAM 2277 under atmospheric conditions. 20 mg sample mass was sufficient to observe a significant calorimetric output. Several such experiments were inconclusive which was a result of various phenomena occurring at the same time.

3. To conduct calorimetric relative humidity experiments on the four *β*-sultams investigated in objective 2.

Calorimetric studies were conducted in the batch mode, solid state, 310K, under atmospheric conditions at varying RH, 7% RH (NaOH) and 75% RH (NaCl). RH was varied in order to control the atmospheric conditions in the calorimetric ampoules. Results proved to be inconclusive.

4. To conduct solution state calorimetric experiments using the same four *β*-sultams investigated in objective 2 at both pH 4 and pH 8 at 298K, 310K and 323K.

Hydrolysis of *β*-sultams A, B, C and D was observed first at 298K in aqueous solution (controlled ionic strength, pH 4 at 0.02M). First order calorimetric outputs were observed. There was a good correlation with respect to substituent effect and hydrolysis, more importantly hydrolysis was observed for *β*-sultam A. The *N*-(methoxybenzoyl) substituted compound proved to be the least reactive *N*-substituted *β*-sultam, whereas the *N*-(chlorobenzoyl) substituted compound showed the highest rate of hydrolysis. The next sets of experiments were conducted at pH 4, 3 different temperatures and at a lower concentration of 0.008M. Small yields were obtained after synthesis and the lower concentration had the advantage of requiring a smaller mass of compound. Excellent first order calorimetric outputs were observed at all three temperatures. Results showed *N*-substituents affect the stability of the *β*-sultams, when comparing rates of hydrolysis. Change in enthalpy also showed the same trend at all three different temperatures. To clarify that hydrolysis had occurred ^{1}H NMR experiments were conducted, and provided excellent correlation when compared to the TAM results.

Further calorimetric studies were conducted at pH 8 to investigate how pH changes the rate of hydrolysis. Rates of hydrolysis for substituted *β*-sultams were significantly quicker when compared to hydrolysis at pH 4. The unsubstituted *β*-sultam A showed no rate change at these two pHs.

5. **Using the information obtained from objectives 2-4 to predict and test the calorimetric method on a *β*-sultam without a chromophore (F).**

The *N*-acyl *β*-sultam has no chromophore and therefore was unsuitable for U.V. detector kinetic studies, but was shown to be ideally suited to the TAM method developed in this thesis. A good agreement was found between the theoretical prediction of the rate of hydrolysis for F and the experimental value

6. **To conduct solution state calorimetric experiments for a series of four *β*-lactams at both pH 4 and pH 8 at 298K and 323K.**

Initial studies were conducted at pH 8 and at the higher temperature of 323K due to *β*-lactams hydrolysing more slowly than *β*-sultams. *β*-Lactams were studied under the same conditions that were used for the *β*-sultams. Results showed that *N*-substituents affected the rate of hydrolysis in the same manner as for the *β*-sultams. Experiments were also conducted at 298K although the data set was not complete due to their low reactivity. ^{1}H NMR experiments were conducted under the same conditions and at temperature 323K to clarify hydrolysis had occurred. Results at pH 4 were inconclusive.

7. **To compare and contrast *β*-sultam and *β*-lactam data with respect to hydrolysis and substituent effect based on the data obtained in objectives 2-6.**

Experimental results showed that *β*-sultams hydrolyse faster than *β*-lactams. The effect of the *N*-substituents upon hydrolysis was found to be the same in both series of compounds. The unsubstituted *β*-lactam A was unreactive under the conditions studied, whereas the unsubstituted *β*-sultam was to undergo hydrolysis at both pHs.

5.2 Future work

There are many avenues for potential future work, the main ones are:

1) Continue to investigate the hydrolysis of *N*-acyl-β-sultams and *N*-acyl-β-lactams calorimetrically

2) The TAM 2277 also has an Isothermal Titration Calorimetry unit (ITC) which can be used to conduct enzyme inhibition studies using enzymes such as β-lactamase. Hydrolysis studies conducted in this research showed that water reacts with the ring system in the same way that the β-lactamase enzyme could potentially attack.

3) To investigate and further characterise the β-sultams and β-lactams, dispersive Raman spectroscopy is to be conducted on the β-sultams and β-lactams (A-D). Structural information which is based upon vibrational modes can be determined. In addition, ab initio calculations can be determined and compared to the experimental results. From these results potential energy distribution values can be determined and vibrational bands can be assigned. The experimental work and *ab initio* calculations are to be conducted by Saima Jabeen at the University of Greenwich. A LabRam Raman spectrometer shown in **Figure 124** is to be used to conduct the experimental work.

Figure 124: LabRam Raman spectrometer at the University of Greenwich used to conduct Raman experiments.